Scoping of a commercial micro reformer for the production of hydrogen

By

Waldo Koorts 211195863

Submitted in fulfilment/partial fulfilment of the requirements for the degree of MTech Chemistry to be awarded at the Nelson Mandela Metropolitan University

April 2016

Supervisor: Dr Gary Dugmore

Co-Supervisor: Mr Stephen Roberts

Declaration

I, Waldo Pieter Ernst Koorts (211195863), hereby declare that the dissertation for MTech Chemistry to be awarded is my own work and that it has not previously been submitted for assessment or completion of any postgraduate qualification to another University or for another qualification.

…………………………………………………………..

Waldo Pieter Ernst Koorts

i. Summary

Hydrogen has gained interest as fuel recently as the harmful effects of fossil fuels on the environment can no longer be ignored. Hydrogen, which produces no pollutants, forms the feed for cleaner fuel cells systems currently in use. Fuel cells, although not as economically viable as fossil fuels, have found a foothold in the energy market in various markets like power backup and use in remote locations.

Production of hydrogen is still largely done via fossil fuel reforming and this technology has received renewed interest for use with fuel cells in the form of micro- reformers or fuel processors.

This study entailed the performance benchmarking of a so called Best-in-Class commercial micro reformer (as available in 2010), the 1 kW *WS FLOX Reformer, and* was undertaken under the auspices of the national HySA programme. The study's focus was primarily on reformate output quality (carbon monoxide concentration), and start up time, thermal efficiency and hydrogen output (15 SCLM).

The reformer consisted of a combustion section encased in an outer reforming section consisting of three reactors in series, steam reforming, water gas shift and selective methanation. As-provided temperature control is simplified though the use of only one temperature setpoint in the combustion chamber and temperature control in the CO clean up stages obtained through means of heat transfer with incoming water being evaporated. Combustion takes place through flame combustion or by means of the supplier's patented FLOX (flameless oxidation) combustion.

The purchased *FLOX Reformer* assembly was integrated into a fully automated unit with all balance of plant components as well as microGC and flue gas analysis for measurement of outlet conditions. The *FLOX Reformer* was tested at multiple combustion temperatures, combustion flowrates, reforming loads and steam-to-carbon ratios to obtain a wide set of benchmark data.

From the testing it was found that the reformer was able to produce the necessary 15 SCLM hydrogen with a carbon monoxide purity of less than 10 ppm as required in fuel cells for all testing if the reaction temperatures were within the recommended limits. Intermediary water gas shift analysis showed methane and carbon monoxide conversion in the reforming and water gas shift stages to be identical to thermodynamic equilibrium conversion – 95% and higher for all temperatures.

Selective methanation conversion obtained was 99%, but not always at equilibrium conversion due to increased selective methanation temperatures, where carbon dioxide methanation was also observed at the higher temperatures.

Temperature control through heat exchange with incoming water in the CO removal stages was found to be less than ideal as the temperature inside these stages fluctuated dramatically due to inaccuracies in the water pump and a lagged response to flowrate changes.

Startup times of less than an hour was observed for multiple combustion flowrates and the reformer boasts a standby function to reduce this to less than half an hour.

The thermal efficiency was independently confirmed and tested and found to be higher than 70 % for flame combustion and on par with other commercially available fuel processors. The suppliers trademark FLOX combustion only reaching 65% due to decreased combustion efficiency.

ii. Acknowledgements

Firstly I would like to thank both *NMMU Innoventon* and *UCT Centre for Catalysis Research* for allowing me to pursue my masters and for providing me with the opportunity to further my studies.

Great thanks goes out to my supervisor Mr. Stephen Roberts for all his help and input in the completion of my studies. Also thanks for the great patience you have shown in this long process.

Thanks also goes out to Dr. Gary Dugmore, my co-supervisor for his assistance and help in all admin related queries as well as Ms. Natasha Luiters for administration assistance.

Thanks goes out to the HySA research group for the funding of this project and of which I am proud to be a part of as well as staff like Niels Luchters, Yi Zhou and Jack Fletcher Jr for their valuable help and input in all technical matters.

A special word of thanks goes out to Jacobus Van der Merwe and Willie Loubser for the construction of my unit including the tubing as well as my heat exchanger assembly and mounting of all components.

More thanks goes out to Kyle Hauslaib, Bill Randall and especially David Lwabona for all their help in terms of electronics and the manufacture of my LabVIEW PLC system which without this project would not have been possible.

Lastly thanks goes out to my family, friends and girlfriend for all their support throughout this time.

iii.   Table of Contents

iv. List of Figures

v. List of Tables

vi.   List of Symbols

Symbol	Description	Units
n, m	Numeric placeholders	-
ΔH_{RXN}	Heat of reaction	kJ/mol
λ	Excess of oxygen in air during combustion	%
$\eta_{Ref,id,LHV}$	Thermal efficiency of reformer with respect to lower heating value	%
LHV	Lower heating value	kJ/mol
HHV	Higher heating value	kJ/mol
Δm	Change in mass	grams
Δt	Change in time	seconds/minutes
m	Mass flowrate	grams/minute
M	Molar mass of component	grams/mol
n	Moles of component	mol
V	Volumetric flowrate	SCCM/SCLM
ρ_i	Density of component	grams/SCCM
F_i	Molar flowrate of component	mol/minute
X_{CH4}	Molar conversion of methane	%
X_{CO}	Molar conversion of carbon monoxide	%

vii. Glossary

BIC	Best in class
BOP	Balance of plant
CCFF	Control card of the FLOX Reformer
CHP	Combined heat and power
DAQ	Data acquisition hardware
DST	Department of Science and Technology
FGA	Flue gas analysis
FLOX®	Flameless oxidation
FPM	Fuel processing module
GC	Gas chromatograph
HTS	High temperature shift
HySA	National Hydrogen and Fuel Cell Technologies Research, Development and Innovation Strategy (Hydrogen South Africa)
JUMO	Safety control switch for the FLOX Reformer
LPG	Liquefied petroleum gas
LTS	Low temperature shift
NI®	National instruments
PCI®	Precision combustion Inc.
PEM	Proton exchange membrane fuel cell or polymer electrolyte membrane fuel cell
PGM	Platinum group metals
PLC	Programmable logic controller
PPM	Parts per million
PROX	Preferential oxidation
PVC	Polyvinyl chloride
S/C	Steam-to-carbon ratio
SCCM	Standard cubic centimetres per minute
SCLM	Standard cubic liters per minute
SMET	Selective methanation
TCD	Thermal conductivity detector
WGS	Water gas shift
WS®	Company supplying the FLOX reformer

1. Introduction

Fossil fuels have, since the onset of industrialisation, been the primary source of energy production across the world [1]. However due to the detrimental effect of its by-products, and limited supply of fossil fuels, future generations might have to find a different cleaner energy source to cope with the world's energy demands.

Hydrogen is such a potential source of energy as it produces totally clean emissions upon combustion and can be used for storage of energy created through renewable energy sources like wind- and solar energy via the process of electrolysis [2]. Hydrogen can be used as fuel to generate heat or power through fuel cells or internal combustion engines, with fuel cells being of special interest for this project.

Steam reforming of hydrocarbons remains the most economical path of hydrogen production – hydrogen production from hydrocarbons typically entails reforming by either steam- or by autothermal reforming processes [3]. This is followed by the water gas shift reaction (shift or WGS) to increase hydrogen production and remove excess carbon monoxide and lastly a final carbon monoxide clean-up stage, either by selective methanation (SMET) or preferential oxidation (PROX). Other methods such as pressure swing adsorption and membranes are also used for producing pure hydrogen.

This method of hydrogen production, although not environmentally ideal due to the associated carbon dioxide production, does pose opportunities for small scale energy production and can be linked up directly to fuel cells [4]. The concept of "fuel processors" is currently used widely and sold commercially by companies like WS®, H_2 Powertech and Precision Combustion Inc. to name a few.

South Africa's Department of Science and Technology (DST) launched its "National Hydrogen and Fuel Cell Technologies Research, Development and Innovation Strategy" (HySA) initiative in 2008, to implement research into fuel cells – primarily low temperature PEM fuel cells – as well as the production, storing and handling of hydrogen as fuel for fuel cells. Within this programme, fuel processing technology of hydrocarbons is seen as a key early market opportunity.

The research conducted in the HySA/Catalysis Centre of Competence, whose mandate it is to develop portable power devices in the 50W to 5 kW range, focuses specifically into all the various reactions involved in fuel processing, including steam reforming, combustion, desulphurisation, water gas shift reaction and CO clean-up in the form of selective

methanation and preferential oxidation, with the aim of producing a commercially viable fuel processor of its own for the current hydrogen market within the next five years.

The aim of this study is the scoping of a so-called *"Best-in-Class"* commercial micro-reformer (fuel processor) to establish standardised benchmark data of the device. Information of key interest includes reformate output, temperature stability, start-up and shut-down time, and CO output levels achievable at varying load levels and for different feedstocks. Issues including sulphur in the feedstock have not formed part of this study.

The reformer selected for this study was the *WS*$^®$ *FLOX Reformer FPM C1* (herein after referred to the *FLOX Reformer*) [5] and was, at the time of project initiation (2010), one of only two commercially available micro-reformers available to the fuel processor market and engineered specifically for connection up to a low temperature PEM fuel cell. The *FLOX Reformer* incorporates a combustion section as well as steam reforming (using methane, propane or LPG feedstock) with water gas shift and selective methanation for final CO clean-up. A desulphurising module is included and the reformer comes complete with control hardware for appropriate system control.

The supplier states that the fuel processor in question has some intriguing features, including the thermal decoupling of feed and fuel streams, combustion using flameless oxidation (or FLOX), short start-up time, high energy efficiency, and CO levels of less than 20 ppm in the reformate stream. It also gives the user the ability of easy control through a simple control strategy as well the ability to measure not only reformate composition, but an intermediate water gas shift [5].

2. Literature review

2.1 Moving away from fossil fuels

For centuries the world's energy demands have been met by means of fossil fuels, with the main fossil fuels being coal, petroleum and natural gas [1]. These fossil fuels cover more than 80% of the world's energy production and consumption needs, as shown in table 2.1.

Table 2-1 Breakdown of world energy consumption in 2015 (adapted from the BP Statistical Review of World Energy) [6].

Consumption (mil. tonnes oil equivalent)	Oil	Natural Gas	Coal	Hydro	Nuclear	Renewable
North America	1025	845	488	213	156	67
South/Central America	317	151	33	5	160	17
Europe/Eurasia	869	954	508	262	202	115
Middle East	382	393	10	1	5	0.2
Africa	172	108	96	3	26	2
Asia Pacific	1412	598	2730	78	311	82
World	4179	3052	3867	563	861	283

The amount of fossil fuel consumed has increased greatly in recent years. The global energy demand has increased as a consequence of the increase in global population and the effect of more of the global population coming out of poverty and thus using greater amounts of energy. The amount of fossil fuel reserves remaining, however, is limited and estimates predict that we may run out of these reserves within this century [6]. It must be noted, conversely, that new resources are regularly discovered. The global trend has therefore recently begin to shift towards cleaner, renewable energy sources. An agreement was established in 1974, where the International Energy Agency agreed to the production and utilization of hydrogen as fuel [7]. The motivation behind this decision came from the world's increased energy demands which could no longer be sustained by fast depleting fossil fuels and the looming threat of increased global CO_2 emissions, as shown in figure 2.1, and its detrimental effect on the global climate as stated by Barbir [2].
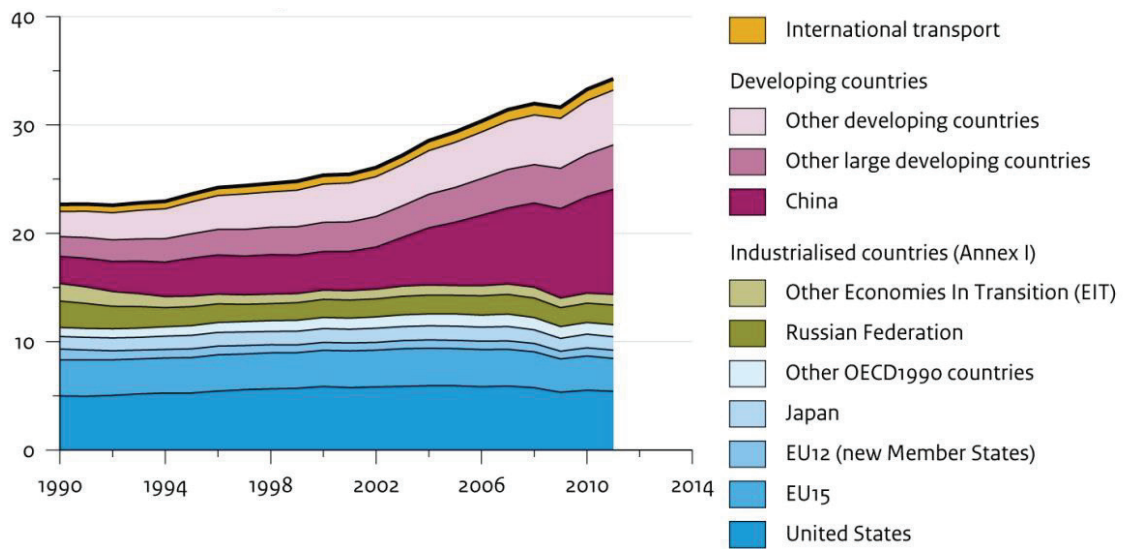
Figure 2-1 Global CO$_2$ emissions in 1000 million tonnes (Netherlands Environmental Assessment Agency 2013) [8].

Due to the establishment of the Kyoto Protocol various countries have enforced legislation to reduce emissions and increase research efforts into alternative or renewable energy sources. Today a great deal of research is performed on all the various renewable energy sources, including solar-, wind- and hydro- and wave energy [2].

2.2 The hydrogen economy

Hydrogen is the lightest element and exists in its normal form as the diatomic molecule H_2. It has many uses in industry including the production of ammonia (Haber- Bosch), production of methanol and hydrochloric acid [3], and also used as a reducing agent in many catalysed chemical reactions in industry or to reduce metal oxides to their metallic form. However its most important use in the future may be as an energy carrier.

2.2.1 Hydrogen production

Hydrogen can be produced by a variety of means in industry. Below are a few of these methods briefly described [3].

2.2.1.1 Steam reforming

Steam reforming is the reaction of steam with natural gas (methane), shown in equation 1 below, or other hydrocarbons including propane, dimethyl ether (DME) or alcohols in the presence of a catalyst at high temperatures. Small amounts of hydrogen is also manufactured by means of steam reforming of naphtha. This method is widely acknowledged as the most common and cost effective method of producing hydrogen in industry.

$CH_4 + H_2O \rightarrow CO + 3H_2$ … (Methane) ……………………...……………….....…… (1)

2.2.1.2 Partial oxidation of hydrocarbons

$C_nH_m + (n + \frac{m}{4})O_2 \rightarrow nCO_2 + \frac{m}{2}H_2$ …………………………………….……....… .. (2)
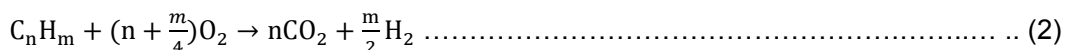
This process entails the partial combustion of hydrocarbons at very high temperatures without a catalyst in a multistage process, as practised in the Texaco process [3], and can be performed utilising most hydrocarbons. It entails the combustion of the hydrocarbon in an oxygen lean environment. The combustion reaction is highly exothermic and consumes virtually all the oxygen. This is followed by the steam reforming reaction where the remaining hydrocarbons react with steam. The reaction temperature can be as high as 1200°C and is highly endothermic, where the preceding combustion stage supplies the energy, thus leading to much less energy requirements than steam reforming alone.

$C_nH_m + nH_2O \rightarrow nCO + \frac{(n+m)}{2}H_2$ ………………………………………….……....…….. (3)
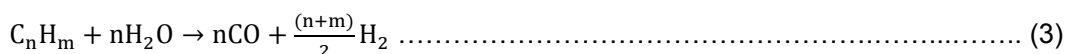
Equation 3 above, the non-hydrocarbon specific form of Equation 1, shows the steam reforming reaction which is typically again followed by a later water gas shift reaction after a heat exchanger. It must be noted that the ratio of CO : H_2 is much higher than obtained through steam reforming alone, as can be seen from the reaction stoichiometry.

2.2.1.3   Autothermal reforming

Autothermal reforming is similar to that of partial oxidation as it again entails a combustion and reforming reaction at high temperatures with combustion providing the heat required for reforming. It is also known as secondary reforming and can be used for a wide range of feedstocks including natural gas and LPG. It has found more application in hydrogen production for ammonia synthesis, however, as air can be fed instead of pure oxygen where nitrogen is utilised as feed during ammonia synthesis [9].

2.2.1.4   Coal gasification

In coal gasification, coal is reacted with oxygen and steam at very high temperatures in a gasifier. The carbon in the coal which is in very high concentrations reacts with the oxygen, forming carbon dioxide and carbon monoxide, which in turn reacts with steam to produce more carbon dioxide and hydrogen in the shift reaction. Carbon also reacts directly with the steam and carbon dioxide in various side reactions.

Methane is also formed through methanation and the hydrogen reacting with carbon. This process does, however, produce significant nitrogen and sulphur based compounds depending on the chemical properties of the coal used.

2.2.1.5   Water electrolysis

Electrolysis is currently the only water splitting technique and produces very pure hydrogen, thus making it very attractive in conjunction with the use of renewable energy sources in the future, although currently it is very expensive technology and only used on a limited scale.

It is achieved by means of passing a current through 2 electrodes in water as shown below:

$2H_2O + 2e^- \rightarrow H_2 + 2OH^{-1}$ ………………………………………………....…… (4)

$2OH^{-1} \rightarrow \frac{1}{2}O_2 + H_2O + 2e^-$ …………………………………....…………….…. (5)
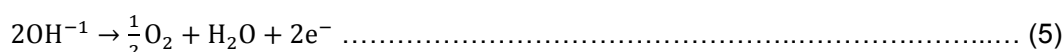
A few different methods of electrolysis exists, either in the form of aqueous alkaline electrolysis using potassium hydroxide as electrolyte or solid polymer electrolyte processes using Nafion^{TM} membranes [3].

2.2.2 Hydrogen purification

In most cases the hydrogen produced by the processes mentioned above are rarely pure enough for use downstream and subsequent removal steps need to be included to achieve the desired hydrogen quality – with electrolysis being the major exception.

In the case of hydrogen use with technologies like fuel cells, carbon monoxide needs to be substantially lowered, if not almost completely removed, since it is a poison for platinum catalysts currently used in fuel cells. Major techniques for minimising the carbon monoxide concentrations include the water gas shift reaction as shown below [10].

$$CO + H_2O \leftrightarrow CO_2 + H_2$$ ……………………………………………………….. (6)

This serves a dual purpose in removing CO whilst also increasing the hydrogen content. After water gas shift further removal of CO might be (and generally is) required, and can be achieved by one of two means listed below.

Selective methanation entails the reaction of carbon monoxide with hydrogen to produce methane and water preferentially to the reaction of carbon dioxide with hydrogen, whilst preferential oxidation is reaction of carbon monoxide with oxygen to produce carbon dioxide above the reaction of hydrogen with oxygen to produce water, both reactions performed over a catalyst.

$$CO + 3H_2 \rightarrow CH_4 + H_2O$$ … (selective methanation)………………………….……….. (7)

$$2CO + O_2 \rightarrow 2CO_2$$ … (preferential oxidation) …………………………………..…….. (8)
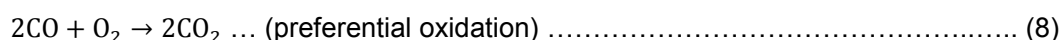
Other compounds that might need to be removed include carbon dioxide, methane, nitrogen and water, but these are highly dependent upon the end use of the hydrogen required. Methods available for removal include cryogenic systems, adsorption onto solids like activated carbon, solvent scrubbing. Hydrogen can also be separated from the rest of the stream by means of pressure swing adsorption. In this process 99.9 % pure hydrogen can be obtained and happens through means of selective adsorption onto certain materials by means of a pressurisation/ depressurisation cycle [3].

2.2.3 Hydrogen storage

In the process of production of renewable energy sources like solar, hydro and wind the energy produced by the renewable is captured in the form of hydrogen by means of electrolysis of water molecules, with the energy obtained for electrolysis from the renewable source.

The hydrogen formed is then stored for later use. The most common methods include:

2.2.3.1 *Gaseous hydrogen*

Hydrogen produced can be compressed and stored in cylinders or tanks of various sizes and pressures and transported for end use. Cylinders currently being sold on the market can be of various purity levels for various different applications. It is currently the most common method although quite dangerous due to the high flammability of hydrogen.

2.2.3.2 *Liquid hydrogen*

Liquid hydrogen is more energy dense than that of gaseous hydrogen and is currently used in NASA's space program. It is, however, harder to maintain as very low temperatures are required to keep it in liquid state.

2.2.3.3 *Hydrides*

Compounds such as LaNi and TiFe are compounds that are able to absorb and desorb hydrogen reversibly depending upon temperature and pressure. This allows for higher density energy storage and is much safer, although is much more expensive.

The use of hydrogen pipelines in the future could also be of great use as well as large geological underground storage facilities [11].

Hydrogen formed can easily be transported off site and used as fuel in various applications e.g. fuel cells, internal combustion engines, etc. [12]. Hydrogen as a fuel has been found to be very efficient as it has a much higher energy per unit mass than more commonly used hydrocarbons [3] and gives off totally clean emissions.

2.2.4 Current hydrogen production and its use for fuel cells

Due to high capital investment and low efficiency, renewable energy sources are not yet the predominant source of hydrogen production. Hydrogen is still predominantly produced by means of steam or autothermal reforming largely due to the huge energy density associated to fossil fuels like natural gas. Although reforming does pose environmental concern due to the large co-production of carbon dioxide which is subsequently released into the atmosphere, it does present an opportunity for a direct link up to a fuel cell which could negate the need for bulky hydrogen storage tanks [4]. Research into hydrogen production via the route of reforming of hydrocarbons has recently found renewed interest especially on small scale in various portable and stationary applications for various combined heat and power (CHP) applications. Other notable applications include jet and rocket engines, steam generation, catalytic combustion and various hydride applications.

Of all current uses of hydrogen as fuel, hydrogen fuel cells have been found to be most efficient and recent government programs have started to develop research in fuel cell technologies, as well as the establishment of limited hydrogen infrastructure, including the production, storing and handling of hydrogen as fuel for fuel cells.

As such, South Africa's Department of Science and Technology (DST) launched its "National Hydrogen and Fuel Cell Technologies Research, Development and Innovation Strategy" (HySA) initiative in 2008, which focuses primarily on low temperature proton exchange membrane (PEM) fuel cells and the use of platinum group metals (PGM) specifically, but not limited to, catalysts. South Africa has approximately 80% of the world's known reserves of PGM's.

Fuel cells are yet to become cost competitive compared to conventional energy production routes, but have found a foothold in the energy market in terms of various small niche markets like leisure, the remote industry and defence, for solar power automobiles and small scale energy production as stated by Muller [4] and Bessarabov [13]. Other notable applications include motor vehicles and transportation, as well as utilities like combined heat and power (CHP) systems.

2.3 Fuel processors

2.3.1 Current commercially available portable fuel processors

There are many other micro-reformers currently commercially available, some manufacturers of these include PCI [14], Innovatek [15], H_2 Powertech [16], WS [17] and Helbio [18], to name but a few. Commercial micro fuel processors are available in a variety load ranges from 50 W – 50 kW depending upon required power. The primary use being portable, transport, auxiliary and back-up power markets [14]. Many vendors of these systems sell devices in conjunction with a fuel cell system, be it PEM or solid oxide fuel cells.

Some prototype fuel processing devices use electrical heating for the reforming stage, however, most commercial systems utilise heat of combustion of the reformer fuel with oxygen (air), either directly in the reforming reactor via autothermal processes, or indirectly via a separate combustion chamber.

Combustion could also be catalytic but this varies from system to system. Most available processors also come available with the option of sulphur removal stages before reforming or combustion depending upon the quality of feed used.

The reforming generally takes place in the presence of a catalyst and is followed by further hydrogen purification stages. These typically include water gas shift followed by either a preferential oxidation (PROX) or selective methanation (SMET) stage to obtain a very pure hydrogen stream and especially remove the carbon monoxide content to very low levels – for low temperature PEM-based fuel cells typically less than 10ppm CO contamination. Lastly a pressure swing adsorption stage could be included to separate hydrogen from the rest of the stream and produce very pure hydrogen.

State-of-the-art catalysts are used to obtain satisfactory outlet compositions, although much research continues to be undertaken to improve performance, notably into novel catalysts, monolith-supported materials and microchannel reactors to obtain the best possible results, whilst ensuring that the total size of the fuel processor stays small and maintains a short start up time for reforming. Microchannel systems, in particular, dramatically increase mass transfer and allow for improved temperature control, thus allowing for a decrease in the amount of catalyst required [18].

Common feeds used could be gaseous in the form of methane, liquefied petroleum gas (LPG), biogas or liquid hydrocarbons, including methanol, ethanol and dimethyl ether.
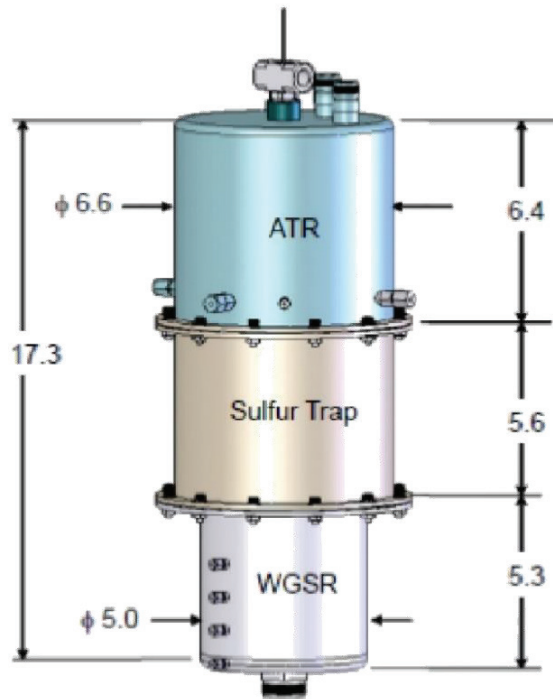
Figure 2-2 Precision Combustion Inc. Reformer schematic with autothermal reformer, sulfur trap and water gas shift stages [14].

Precision Combustion Instruments offers new microlith technology for catalytic reactors in fuel processors and catalytic combustors. This microlith technology entails short metal monoliths coated with state-of-the-art catalysts for reduced contact and startup time. Novel catalysts include high sulfur tolerance and very high thermal efficiencies. A wide range of micro-reformers are available including methane reformers, partial oxidation and autothermal reforming reactors with a wide range of feedstocks.

Innovatek offers the *InnovaGen*® *Fuel Processor* in 1 – 5 kW, 10 – 20 kW and 50 kW fuel cell ranges. It offers multiple different fuels as feedstock and they claim to have great expertise in catalyst, membranes and micro systems technology. The fuel processors sold are adaptable to both PEM and solid oxide fuel cells.

H₂ Powertech is another company offering fuel processing and fuel cell solutions to the current market, especially in the 1 – 5 kW range. This entails reforming using the above three methods including CO clean-up as well as sulphur removal and membrane technology. The standard feed used in this system is a water/methanol mixture.

Helbio offers solutions in the form of combined heat and power units, auxiliary power and standalone hydrogen generators for remote and household use. It includes fuel processor with

reformer and CO clean-up with low temperature PEM fuel cells using natural gas as well as biogas.

WS [5], [19] is an owner operated enterprise which was founded in 1982. Since then, it specialized on highly efficient, low emission burner systems for industrial furnaces. Activities include research, engineering and design, production, sales and service worldwide. They are known industry wide for the patented *"FLOX"* combustion principle and at the time of the inception of this study was an industry leader in small scale fuel processors [19].

2.3.2 Best-in-Class fuel processor evaluation

This study has focussed on the scoping of a commercial micro-reformer considered to be one of the so-called *"Best-in-Class"* (BiC) available for the current (as of 2010) portable or transportable market. Specifically, the study has focussed on the establishment of standardised performance data of this so-called BiC device in terms of quality of reformate output, impurity CO levels (and hence CO removal efficiency) and stability towards load, temperature and pressure changes for various different hydrocarbon feedstock e.g. methane and propane.

There are many critical issues surrounding reforming and its possible use in conjunction with fuel cell technology. Start-up time for reforming usually takes sometime in the order of tens of minutes due to the high temperatures required for reforming, energy efficiency, the effect of sulphur containing compounds in hydrocarbon feedstock, load and steam-to-carbon ratio changes as well the poisoning effect of CO in the reformate stream (<10 ppm CO), on fuel cell catalysts.

All testing and scoping done will give an indication as to the commercial viability of such a micro reformer for hydrogen production in portable fuel cell applications. The commercially available reformer in question encases all the various different stages of reforming and CO removal in one unit; steam reforming, water gas shift, to maximise H_2 production (and simultaneously convert CO) and final CO removal via selective methanation and presents the opportunity of direct connection to a low temperature PEM fuel cell for clean energy production. This project runs concurrent with catalyst screening and testing of all the individual stages by various other postgraduate students and gives HySA a clear indication as to its current position in relation to the current commercial market before any further catalyst development will take place.

2.4 FLOX Reformer

The reformer selected for this study was the *WS® FLOX Reformer FPM C1* (hereafter referred to as the *FLOX Reformer*) made especially for small scale and portable hydrogen production applications and ideally suitable for connection up to a low temperature PEM fuel cell, and was at the time of project initiation (2010), one of only two commercially available micro-reformers, hence its classification as *"Best-in-Class".* The reformer boasts new flameless oxidation technology and is packed with the best commercial catalyst available and claims to not only be energy efficient, but to deliver high quality reformate [19].

The purpose of the study was to develop a comprehensive set of operation benchmark conditions and performance characteristics, against which all future HySA/Catalysis Fuel Processor developments could be compared. The system is specifically designed for use in conjunction with a fuel cell system, similar to those being developed by the HySA Fuel Cell research group, a low temperature PEM fuel cell.

Developed by *WS®* the *FLOX Reformer* is an ultra-compact, ready to install micro-reformer ideally made for reforming of natural gas with deionized water that boasts some very good features, including a short start up time, stand by ability and fast responses to changes in load. The *FLOX Reformer* is a 1 kW reformer capable of producing enough hydrogen for a 1 kW low temperature PEM fuel cell [20].

2.4.1 FLOX Reformer feedstock

General feedstock used with the *FLOX Reformer* includes natural gas (methane) with demineralised or deionised water, however feedstock is not just limited to natural gas and can be used in conjunction with LPG (liquefied petroleum gas) or propane feed. WS, the producer of this reformer also states that with a few modifications it could be used in conjunction with liquid feeds. The use of deionised water is specified as critical due to the low levels of impurities present compared to levels in normal tap water, which can contribute negatively to the overall life span of the reformer by deactivating the catalysts in the various stages.

2.4.2   The *FLOX Reformer* feed and product flowpath

$H_2/\,CO_2$ H_2O/CH_4 CH_4/O_2 CO_2/H_2O

Selective Methanation

Water Gas Shift

Reforming
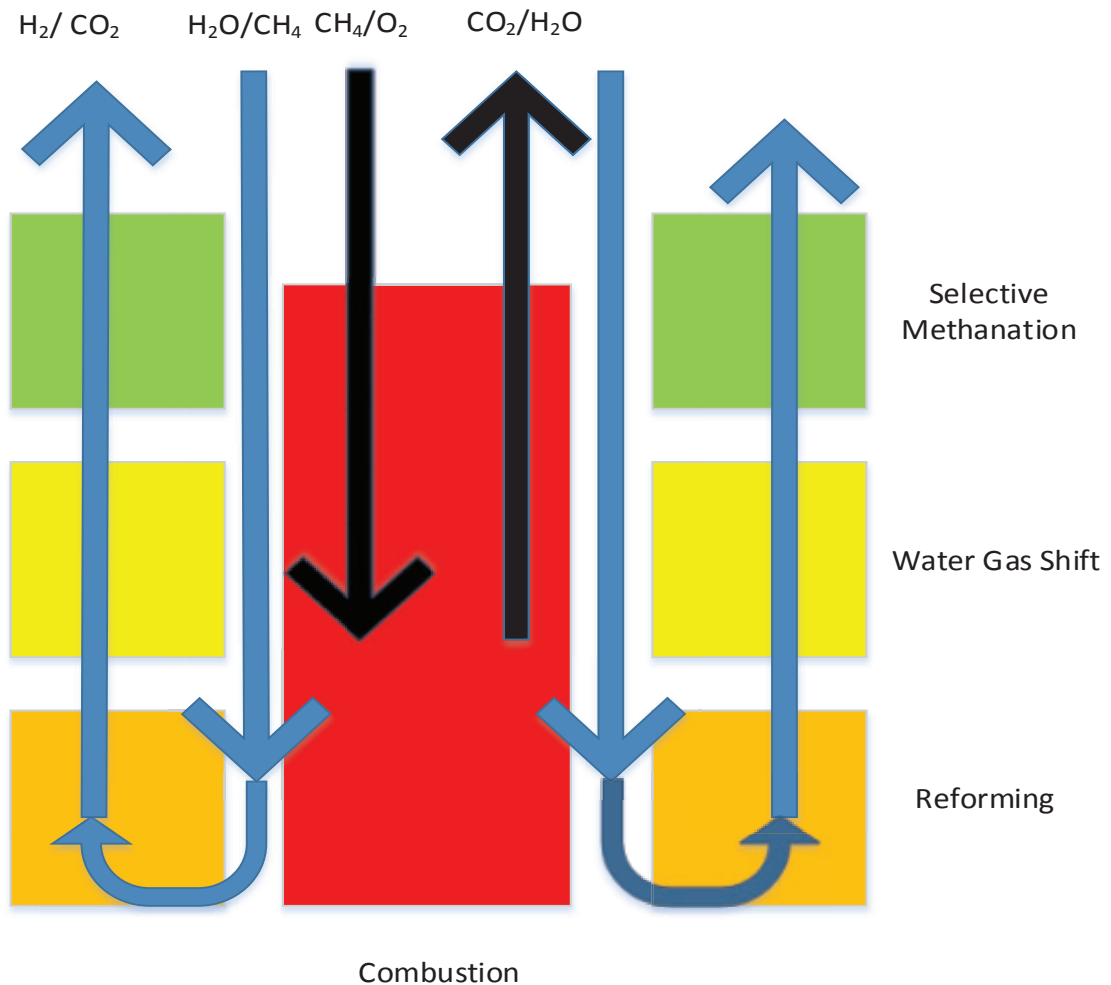
Combustion

Figure 2-3 General flowpaths inside the *FLOX Reformer*.

As shown in figure 2.3, there are two general flow paths existing inside the *FLOX Reformer*. The fuel section where combustion occurs, is housed centrally in the device, and fuel is burnt in the presence of air provided by means of an electric air blower. Gas flowrate is controlled by means of pressure differential. The heat from the combustion chamber passed in the radial direction to the respective fuel processing reaction chambers.

The reforming section, located concentrically around the combustion chamber is where the feed components are reacted to form a hydrogen rich stream. Reformate produced in the first (and bottom-most) 'Reformer' chamber is subsequently directed through two further concentric reaction chambers, a water gas shift reaction stage and a final selective methanation stage in series [20].

These last two stages serve the purpose of further increasing the hydrogen content in the outlet stream whilst also reducing the carbon monoxide to levels suitable for use in a fuel cell system where carbon monoxide levels have to at least below 10 parts per million.

These combustion and reforming/fuel processing sections are completely separated from one other, with no dilution of the hydrogen rich reformate stream with combustion products occurring. All combustion products exit separately out of the combustion chamber with a pure hydrogen rich reformate exiting the reformer for use in the fuel cell.

2.4.3 FLOX combustion

Combustion inside the reformer is able to take place by two different means. Initial combustion takes place by means of a classical flame diffusion combustion where a flame is generated through an ignition electrode creating a spark. This classical combustion takes place at the initial heating stages to get the temperature of the chamber above that of the self-ignition temperature of the fuel.

This method is very effective as it has a very high efficiency, yet with the drawback of localised temperature spikes caused by the flames, especially areas close to the flames. It therefore does not provide a uniform temperature distribution. These temperature spikes in turn can lead to very high NO_x emissions which can be very harmful to the environment as a whole [21]. With flame combustion the issue of flame stability also remains an issue as the correct mixture of fuel and air needs to be perfectly maintained. Any interruption in either feed component flow leads to the flame being extinguished, and the subsequent need for re-ignition. This can also pose a problem with any fuels with highly varying calorific values like hydrogen/methane mixtures [21], [22].

At temperatures above that of the auto-ignition point of the gas, through means of the included control system, the system can switch over to flameless oxidation, or so-called FLOX, combustion. In FLOX combustion mode, there is no further need for a spark to generate a flame, but instead the fuel is merely introduced into the combustion chamber at elevated temperatures. Since the fuel is above its auto-ignition point combustion takes place automatically. The temperature profile across the combustion chamber formed through this process can be shown to be more even throughout the entire volume of the chamber and not have any temperature spikes and thus less NO_x emissions [20].

2.4.4 Heat integration

Figure 2.4 below shows a more detailed flow- and heat exchange pattern occurring inside the *FLOX Reformer*. Once again, it confirms that there is no physical contact between the fuel combustion and feed reforming sections, yet allowing for the required heat transfer taking place throughout the body of the reformer. The reformer is described as "a co-current or counter current reactor which includes a monolithic element with many conduits parallel to one another which are divided into two groups" [23], the two groups being the reforming and the combustion section, respectively.
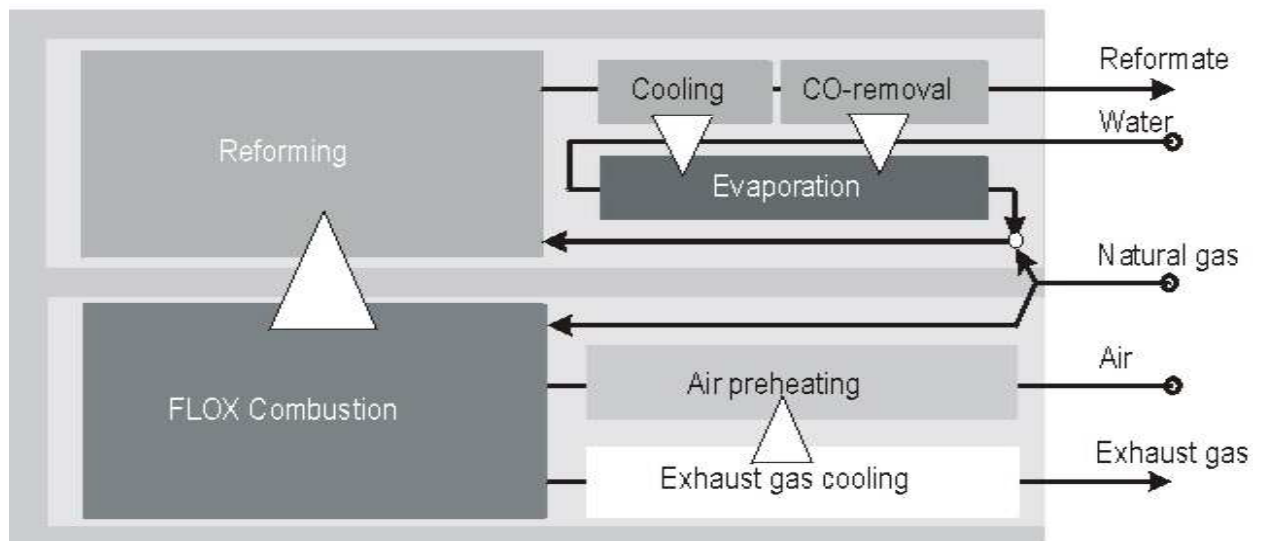
Figure 2-4 Heat integration of the FLOX Reformer (WS Documentation Manual 2010) [20].

Combustion provides the heat required for the entire unit – it not only sustains the heat required in the endothermic reforming stage, but also ensures sufficient light off temperature for the subsequent water gas shift and selective methanation zones. It has a very simple control strategy whereby only one setpoint is controlled, namely the temperature at which combustion takes place inside the combustion chamber.

Air entering the combustion chamber is pre-heated prior to combustion by means of heat transfer with the outgoing combustion product or flue gas, which is in turn cooled down from very high combustion temperatures. Furthermore, water for the reforming (and shift) stage is evaporated by means of heat transfer with the outlet of the steam reforming section and the two CO removal stages through contact in a parallel flow heat exchanger.

2.5 Reactions occurring in the *FLOX Reformer*

2.5.1 Desulphurisation

The *FLOX Reformer* assembly comes complete with a separate removable unit for the purpose of removing all sulphurous compounds before they enter the system. This is for the protection of the catalysts in the downstream reactors – the catalysts are very susceptible to any sulphur containing compounds, whilst sulphur is also detrimental to the operation of any fuel cell system thereafter. Sulphur is also very corrosive in nature and can give off harmful pollutants upon combustion, the most notable being sulphur dioxide, which is very harmful to humans and the environment.

The contents of this desulphurising agent is not known, but has a guaranteed lifetime of 5000 hours as stated by the manufacturers. Common sulphur containing compounds include mercaptanes, H_2S and COS. These can commonly be found in natural gas or LPG and obviously need to be removed prior to any reforming. Common desulphurising agents used in industry and research include MEA (monoethanolamine), potassium carbonate and MDEA (Methyl diethanolamine) [24].

2.5.2 Combustion

2.5.2.1 *Fundamentals*

Combustion is the reaction of a substance with oxygen in the presence of heat or an ignition source. The reaction is highly exothermic, giving off substantial amounts of energy and in the process sustaining the reaction. A few combustion reactions are given below, including the heat of combustion.

$$2H_2 + O_2 \rightarrow 2H_2O \quad \Delta H_{RXN} = \text{-286 kJ/mol ... (Hydrogen)} \dots\dots\dots\dots\dots\dots\dots\dots\dots\dots\text{ (9)}$$

$$CH_4 + 2O_2 \rightarrow CO_2 + 2H_2O \quad \Delta H_{RXN} = \text{-889 kJ/mol…. (Methane)} \dots\dots\dots\dots\dots\dots\dots\text{ (10)}$$
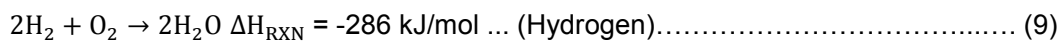
Exhaust products are also given off in the reaction. If the fuel is carbon-hydrogen based the products are carbon dioxide and water vapor, whilst pure elements give off oxides as with hydrogen producing water vapor.

2.5.2.2 *Role of combustion*

Combustion is one of the oldest reactions known to man and has been used primarily for power generation ever since the onset of the industrial revolution. In fossil fuel powered plants,

for example, the heat of combustion is used to evaporate water to steam to drive turbines generating power using the Rankine cycle [1]. Combustion is also the main chemical process used in internal combustion engines of motorized vehicles.

Much research has also been done on the topic of catalytic combustion, especially in the area of environmental engineering where catalytic combustion is employed in catalytic converters in automobiles and flue gas cleaning in industry to eliminate harmful pollutants from the environment, including carbon monoxide and methane [25]. Most catalytic combustion studies have focused on PGM-based catalysts containing platinum and palladium. Gold has also been reported to be useful as combustion catalyst especially for removal of carbon monoxide.

Catalytic combustion has the advantages of lower required temperatures for combustion, thus reducing NO_x and SO_x emissions and allowing its use in very lean fuel/air mixtures.

2.5.2.3   Combustion in the FLOX Reformer

Incoming natural gas and air enters the reformer and is ignited by means of a start burner until the temperature increased beyond the auto-ignition point of the mixture. The flame is monitored by means of ionisation probe which provides a constant and controlled reaction according to Wunning [21]. The incoming fuel and air is also preheated by means of contact with the exhaust or flue gas exiting the reformer, as described earlier. The combustion equations for the incoming gas are shown in equations 11 and 12 below.

$CH_4 + 2O_2 \rightarrow CO_2 + 2H_2O$ ... (for methane) …………………………………………… (11)

$C_3H_8 + 5O_2 \rightarrow 3CO_2 + 4H_2O$ ... (for propane) …………………………...............…. (12)
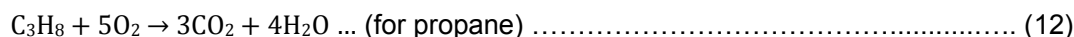
The theoretical amount of air required for combustion can thus be calculated. In practice, however, excess air is used so as to ensure complete hydrocarbon combustion, since under stoichiometric conditions 100% conversion is unattainable for the combustion process, due to thermodynamic equilibrium. Generally a surplus of 10 – 30% of air is fed to the burner. This is known as the lambda (λ) value and can also be controlled by means of measurement of the oxygen content in the flue gas line via lambda sensor or equivalence ratio (air fuel) meter [20]. Lambda is calculated as:

$O_{2_{flue}}$: measured O_2 content in flue gas ($Vol\%_{dry}$)

$$\lambda = \frac{O_{2\_flue}}{O_{2 \text{ in air}} - X\% O_{2\_flue}} + 1 \text{ ……………………………………………..………..... (13)}$$

For methane the auto-ignition point is generally above 580°C, whilst propane is 470°C. These temperatures are well below the recommended running temperature of the FLOX

system which, according to manufacturer, is recommemded to operate in the 750 – 850°C range, and with only temperatures above 800°C to be used in FLOX mode – the control between *'Flame-'* and *'FLOX mode'* being performed by means of the manufacturer supplied control system.

Once a sufficiently high temperature has been obtained (800°C) the start burner ignition is switched off by means of a burner control unit, whilst the fuel and air flowrate is maintained. In this phase the reaction is self-sustaining by means of extensive air recirculation [26] since it is at temperatures above the auto-ignition temperature of the gas mixture. This concept of so-called flameless oxidation or *FLOX* is used in industrial applications including bio gas burners and gas turbines [26]. Flameless oxidation *(FLOX)* mode, so named since no visible flame exists, has the advantage over normal flame ignition in that substantially lower NO_x levels (<25ppm) in the flue gas are present, because of reduced temperature spikes and better heat transfer inside the combustion section which leads to higher overall efficiency. Flame control and monitoring issues as experienced with normal reformers is thus avoided and fuels with highly varying calorific values can be used [26]. There is also the advantage of possible use of fuel cell anode off gas as fuel during this mode.

2.5.3   Steam reforming

Steam reforming has historically been used primarily for the production of hydrogen in industry either as its end use or for further refining to produce methanol and ammonia. Steam reforming could be used for a wide range of feedstock ranging from methane and LPG to even methanol. For the purposes of this study only methane and propane will be covered.

The reaction occurring in the steam reforming chamber are shown in equations 14 and 15, depending on the hydrocarbon feed employed, methane or propane respectively.

$$CH_4 + H_2O \rightarrow CO + 3H_2 \text{ … (methane)} \text{ …………………………………….…………....…} (14)$$
$$C_3H_8 + 3H_2O \rightarrow 3CO + 7H_2 \text{ … (propane)} \text{ ……………………….……………....……} (15)$$

2.5.3.1   *Thermodynamics*

The reaction is highly endothermic (ΔH_{RXN} = 206 kJ/mol for methane), meaning that a substantial energy is consumed during the making of the products. Steam reforming is often combined with partial oxidation to supply this energy demand. In the *FLOX Reformer* the energy for the reaction is supplied by means of the separate combustion reaction occurring,

providing the energy through heat transfer. Due to the endothermic nature of the reaction large temperature drops are possible, leading to lower conversions unless more energy is supplied.

According to Le Chatelier's principle the forward reaction is favoured at low pressures and high temperatures due to its endothermic nature. Steam reforming generally takes place at close to atmospheric pressures to increase the hydrogen output, although it could be used at higher pressures depending upon downstream requirements – especially when used in ammonia production.

Very high temperatures in the range of 600 – 1000°C are typically employed. Although higher temperatures for the reaction are sometimes also desirable, these are often limited by reactor material of construction. In the case of reforming with liquid feeds like methanol lower temperatures in the range of 400°C are typically practiced.

The reaction is also favoured by using an excess amount of the water in the feed so as to shift equilibrium conversion in favour of product formation – industrially steam-to-carbon ratios of 3 – 5:1 is used. Too little water can have a detrimental effect, however, as it can lead to coking of the catalysts through excess carbon deposition.

2.5.3.2 Catalyst development

Through modern catalyst development the reaction can be pushed virtually to equilibrium in the range of 700°C and above using a space velocity of 5000 – 8000 hr^{-1}. Historically nickel catalysts on alumina have been the major catalyst used in steam reforming due to its high activity [3]. Promoters like potassium is often used to inhibit coke formation.

In recent times more research work has been undertaken on PGM-based catalyst and precious metals like rhodium and ruthenium have been found to be adequate substitutes for reforming, at least in terms of activity. Studies performed at the University of Cape Town using microchannel reactors has shown that the space velocity required to achieve near equilibrium conversion can be increased ~100-fold, thus greatly reducing catalyst cost. Equilibrium conversions at gas hourly space velocities in the range of 300 000 hr^{-1} have been achieved through tests done at the University of Cape Town.

2.5.3.3 Outlet composition and side reactions

Apart from steam reforming, the water gas shift reaction (as shown by equation 16) also occurs appreciably, especially at elevated temperatures. An equilibrium outlet composition of less

than 1% methane can be achieved, while 12% carbon monoxide and 10% carbon dioxide is typically expected due to the combined reforming and shift reactions.

2.5.4 Water gas shift reaction – CO clean up

The water gas shift (WGS) reaction is practiced commercially for the purpose of increasing the hydrogen content in synthetic gas. Water gas shift is the reaction of carbon monoxide with water to form carbon dioxide and hydrogen, as shown in equation 16.

$$CO + H_2O \rightleftharpoons CO_2 + H_2... \ (\Delta H_{rxn, 25°C} = -41.1 \text{ kJ/mol})............................ (16)$$

Typically, water gas shift is undertaken in a two stage process, depending upon the quality of hydrogen required. The first is the so-called high temperature shift reaction (or HTS) stage, taking place in the range of 350 to 450°C in the presence of iron oxide catalyst. This iron oxide catalyst is more robust and can withstand high impurity levels whist exploiting the rapid kinetics at this higher temperature. A typical outlet CO concentration for this high temperature shift stage is approximately 2 – 4% [10].

This is followed by the second low temperature shift (LTS) stage, which takes place between 190 and 250°C. The catalyst used for low temperature shift commercially is a copper oxide/zinc oxide based catalyst. Outlet concentrations for the low temperature shift is approximately 0.1 – 0.3% CO. This is obtained by means of the more favourable thermodynamic equilibrium concentrations at lower temperatures [3].

2.5.4.1 Catalyst development

PGM-based catalysts have been extensively studied in literature, notably because of their activity at low temperatures (and thus favourable equilibrium conversion levels), and their resistance to oxidation (and thus non-pyrophoric nature and stability after reduction).

2.5.4.2 Thermodynamics

Due to the exothermic nature of the reaction it should be noted that the formation of products is greatly favoured by low temperatures. For commercial LTS catalysts, reaction kinetics are adequate at typical commercially viable space velocities above 190°C, but with increasing reaction temperature an associated decrease in equilibrium conversion attainable. Thus middle ground between reaction kinetics versus reaction thermodynamics has to be obtained.

It should also be noted that due to the exothermic nature, temperature increases in the reactor can also affect the equilibrium conversion [10].

Water gas shift is an equimolar reaction with equivalent moles of reactants and products, with pressure therefore not affecting the equilibrium (Le Chatelier's principle). Reaction rates are, however, slightly affected by pressure and thus water gas shift is practised at approximately 20 bar industrially.

An excess of water in the reaction also leads to an increase in the equilibrium conversion of CO. Industrially a steam-to-carbon ratio of 2 – 4:1 is typically used [3].

2.5.4.3 Combined reforming and shift

Steam reforming and WGS can be summarised in a combined reformer shift reaction to give the following:

$CH_4 + 2H_2O \rightleftharpoons CO_2 + 4H_2$ … (methane) …………………………………………..……… (17)

$C_3H_8 + 6H_2O \rightleftharpoons 3CO_2 + 10H_2$ … (propane) ……………………………..……....….. (18)

Assuming that there is an excess of water, especially at higher steam-to-carbon ratios of 3.0 – 4.0, the reaction can be changed as follows:

$CH_4 + 4H_2O \rightleftharpoons CO_2 + 4H_2 + 2H_2O$ … (methane) …………….…………….………… (19)

$C_3H_8 + 12H_2O \rightleftharpoons 3CO_2 + 10H_2 + 6H_2O$ … (propane) ………………………….……… (20)
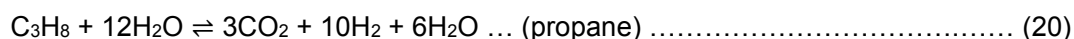
The surplus of water is the key to the high conversion as it shifts the equilibrium more in favour of carbon dioxide and hydrogen formation, as this promotes the forward reaction. Conversely, liquid water condensation on the copper-zinc catalyst in the WGS (typically below 150ºC in pressurised reactors) is known to cause catalyst deactivation [20].

An excess of the feed (methane or propane) is, however, not preferred as it leads to carbon deposition or coking of the catalyst.

2.5.5 Selective methanation

The use of methanation historically has been applied for the removal of carbon oxides from reformate streams, especially in the production of hydrogen or for later use in the production of ammonia where these carbon oxides have a poisoning effect on subsequent catalysts. For ammonia plants bulk carbon dioxide is removed by other means with methanation used to reduce the remaining oxides to very low levels (well below 10ppm). Methanation has also

been used commercially in the production of methane. This reaction takes place in the range of 300 – 400° C industrially normally in the presence of a nickel catalyst [27].

For use as feed to a PEM fuel cell the carbon monoxide levels become critically important as CO acts as poison to the platinum catalyst used in a PEM fuel cell – levels of below 10ppm are required to ensure operation of a fuel cell without degrading of any catalysts. Selective methanation, where CO is preferentially methanated to CH_4 instead of the more abundant CO_2, is a primary focus for the removal of CO from a hydrogen product stream.

The CO methanation reaction is given by equation 21:

$$CO + 3H_2 \rightarrow CH_4 + H_2O$$ …………... (21)

The reaction is the reverse of the steam reforming reaction and thus converts carbon monoxide and hydrogen to methane and water. The reaction of carbon dioxide with hydrogen also occurs in a side reaction and is given by equation 22:

$$CO_2 + 4H_2 \rightarrow CH_4 + 2H_2O$$ …………………………………….………………..………. (22)

Although not utilised in the *FLOX Reformer*, preferential oxidation, where CO is preferentially oxidised to CO_2 as opposed to the very abundant H_2 being oxidised to water, is also a possible method for the lowering of CO to acceptable levels.

2.5.5.1   Thermodynamics

The reaction is highly exothermic with a heat of reaction of -206 kJ/mol. The reaction is thus favoured by low temperatures, as is the side reaction of CO_2 methanation with a heat of reaction of -165 kJ/mol. The temperature range for selectively removing CO is, however, rather narrow – too low a temperature decreases catalyst kinetic performance as well as increases the risk of catalyst deactivation by the condensation of liquid water, whilst too high a temperature compromises the selectivity of the reaction, leading to substantial amounts of hydrogen being consumed for the methanation of CO_2 [28]. Temperature ranges for efficient removal of CO is between 150 and 250°C.

Pressure does have an effect on the reaction as there are more reactant moles than product and should thus be improved by an increase in pressure, although sufficient removal of CO can be obtained at low pressures.

The water gas shift product stream contains an excess of hydrogen (in the range 35 – 65% of the stream composition, depending on the feed and type of reforming initially undertaken).

This excess of hydrogen, one of the reactants in methanation, drives the reaction to virtual completion.

2.5.5.2 Side reaction

At temperatures in excess of 250°C the reverse water gas shift reaction can have a negative impact on CO conversion as shown in equation 23, as CO is produced through the reaction of CO_2 and H_2:

$$CO_2 + H_2 \rightarrow CO + H_2O \ldots\ldots\ldots\ldots\ldots\ldots\ldots\ldots\ldots\ldots\ldots\ldots\ldots\ldots\ldots\ldots\ldots\ldots\ldots\ldots \quad (23)$$

This could be partially negated by means of excess water in the feed [28].

2.5.5.3 Catalyst development

Historically nickel has been used as methanation catalyst whilst work using ruthenium and cobalt have recently garnered more attention. Ruthenium, especially, has shown a high selectivity for CO methanation [28].

2.6 Energy efficiency
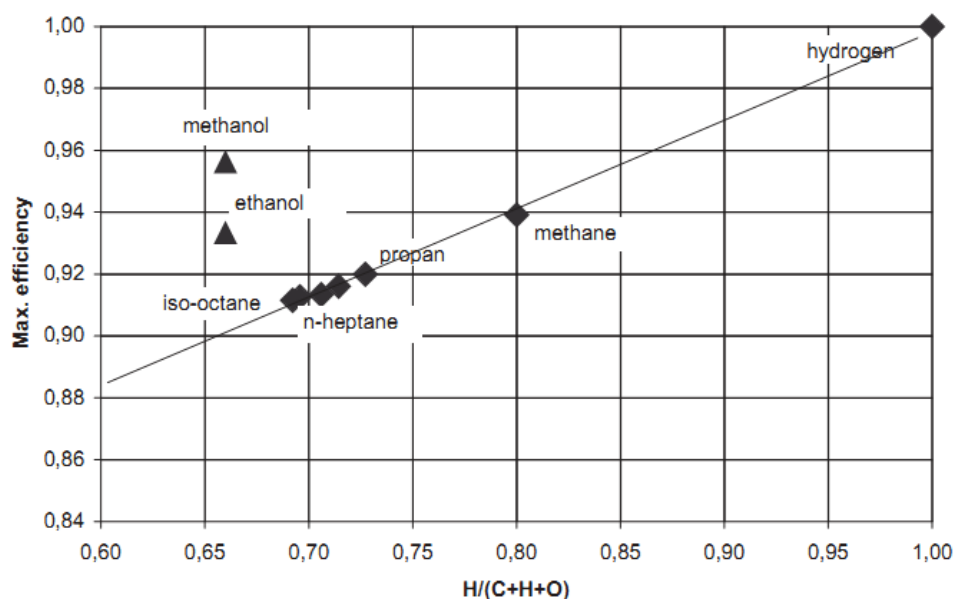
Figure 2-5 Maximum thermal efficiencies of various fuels [29].

$$\eta_{\text{Ref,id,LHV}} = \frac{LHV_{H2}}{HHV_{H2}} \cdot \frac{HHV_{CnHm}}{LHV_{CnHm}} = 0.845 \cdot \frac{HHV_{CnHm}}{LHV_{CnHm}} \quad \dots\dots\dots\dots\dots\dots\dots\dots\dots\dots\dots\dots\dots \quad (24)$$

The maximum possible reformer efficiency can be derived from equation 24 and 25 as stated by Schmid [28] where both the higher and lower heating values of hydrogen and the hydrocarbon is taken into account. It can also be expressed in terms of volume of gas. This is the theoretical efficiency and assumes no heat losses, total hydrocarbon and carbon monoxide conversion at a steam-to-carbon ratio of 2 [28].

$$\frac{V_{H2,max}}{V_{CnHm}} = \frac{HHV_{CnHm}}{HHV_{H2}} \quad \dots\dots\dots\dots\dots\dots\dots\dots\dots\dots\dots\dots\dots\dots\dots\dots \quad (25)$$

For reformers to be viable for use with hydrogen fuel cells there needs to be a very fast adaptation of the water production to load changes and should have a hydrogen yield very similar to large scale reformers. An energy conversion of about 75 – 80% efficiency can be achieved, equating in output terms to approximately 2.6 m^3 of hydrogen generated for every m^3 of natural gas consumed.

Moreover, there is also a need for reformers capable of quick start-up and of the ability to generate steam at fast load changes as a change in evaporation leads to a load change [28], which in turn affects the flow of reformate and power output of the reformer. According to the manufacturer, this is possible in the *WS® FLOX Reformer* as all the reaction vessels are synchronised chronologically. The thermal inertia thus has no inhibiting effect, but creates a heat buffer needed to obtain a 100% load change in seconds.

2.7 Performance analysis

Table 2-2 Predicted responses for changes in key variables.

Parameter		H₂ Output	CH₄ Content	CO Content	Fuel Demand
Pressure	↑	↓	↑	↓	↓
Steam: Carbon	↑	↑	↓	↓	↑
Load	↑	→	→	→	↑
Reforming Temperature	↑	↑	↓	↑	↑

Table 2.2 gives rough predicted responses to possible operating parameter changes. As expected, a higher steam-to-carbon ratio will lead to higher hydrogen and lower methane and

carbon monoxide production as it drives the reforming and shift reactions to virtual completion as a consequence of excess water, but will increase fuel load as more water and fuel is needed for combustion.

Higher pressures affects the steam reforming reaction most notably as the conversion for this reaction is lower at higher pressures (as stated by Le Chatelier's Principle), thus decreasing H_2 and CO content, whilst increasing methane and in turn lowering fuel demand.

A load increase will bring about higher fuel requirements while an increase in the temperature of combustion will cause more H_2 and CO production, since reforming conversion increases with temperature. This increase in temperature adversely affects the shift reaction as higher temperature leads to less conversion of CO to CO_2.

3. Objectives of this study

The aim of this study is the full commissioning, control parameter and operating window scoping and reformate product composition specification of the *WS® FPM C1 FLOX Reformer* unit to obtain standardised benchmark data for a commercially available *"Best-in-Class"* reformer device.

This will be done by means of the following objectives:

- The complete design, integration and automation of the *FLOX Reformer* into a complete system with all necessary balance of plant (BOP) components;
- The complete analysis of the outlet reformate stream to monitor the H_2, CO_2 and CO production at various operating conditions;
- The analysis of the intermediate shift stream composition to establish reforming and shift conversions at various operating conditions;
- The scoping of the unit's performance at various loads (i.e. fuel flowrates), combustion control temperatures, steam-to-carbon ratios and analysis of the change in reformate quality at these conditions;
- The scoping of start-up time from cold start and standby conditions;
- Establishment and independently confirm the thermal efficiency of the reformer.

Key questions include:

- What is the effect of steam-to-carbon ratio on the amount of CO in the reformate output and is it below the threshold of 10ppm CO required?
- What effect do load changes have on the stability of the system?
- How does changes in temperatures effect the reformate composition?
- What is the normal start-up time for the reforming unit?

4. Experimental

4.1 Experimental apparatus

The experimental setup used in this study can be divided into 3 different sections, namely i) the as-purchased FLOX assembly, ii) balance of plant components and iii) operating hardware and software control system.

4.1.1 FLOX assembly
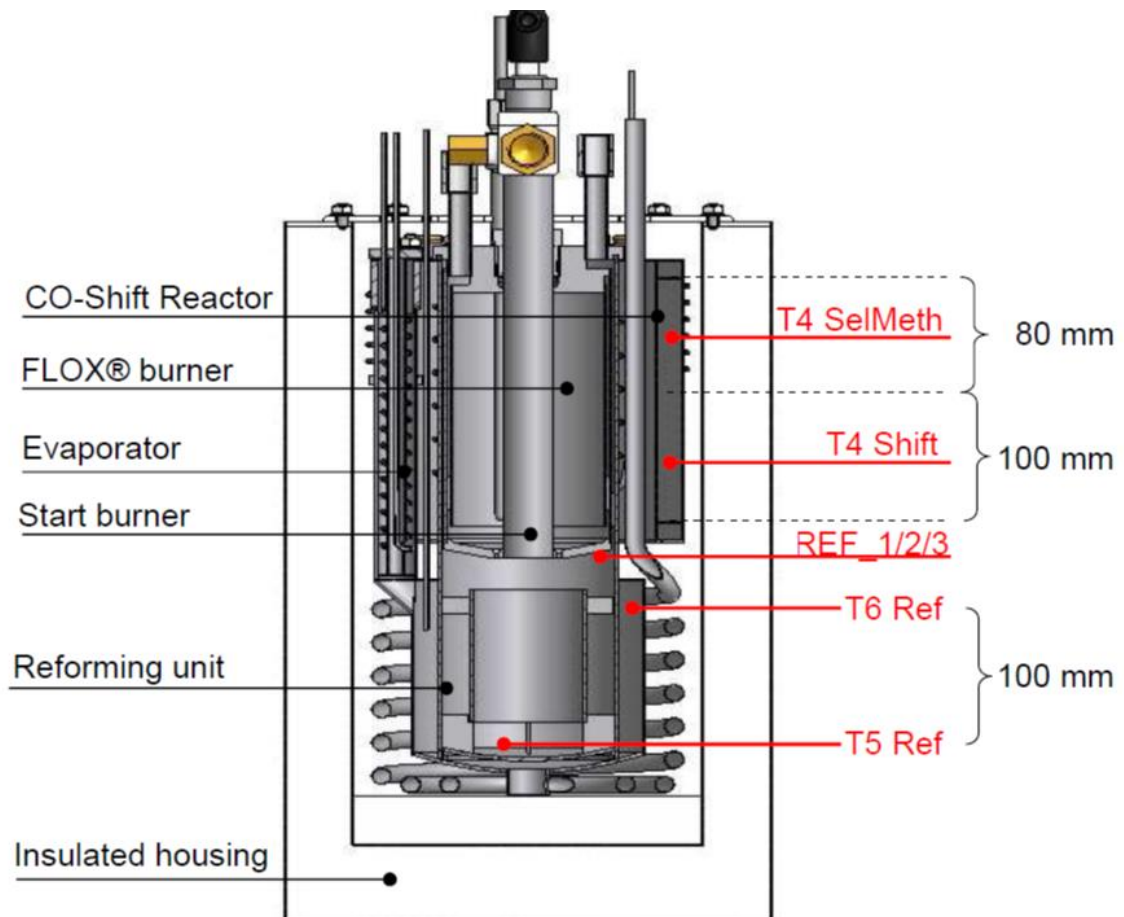
Figure 4-1 Schematic representation of the *FLOX Reformer* assembly [20].

The *WS FLOX® Compact Steam Reformer C1,* the reformer used for this study, is shown in figures 4.1 and 4.2. It consists of the following sections:

4.1.1.1   Combustion chamber

Centrally located in the body of the FLOX assembly is the combustion chamber. It comes complete with a start burner with an ignition electrode to provide a spark for the initial combustion phase. The chamber also has a secondary *FLOX* burner for combustion temperatures above the auto-ignition point of the fuel, consisting of various smaller nozzles injecting the fuel into the chamber. The chamber has a thermal well located close to the level of the flame for effective temperature control, which is accomplished by means of a thermocouple. Start burner has a capacity of a 3.3 kW transformer which is included.
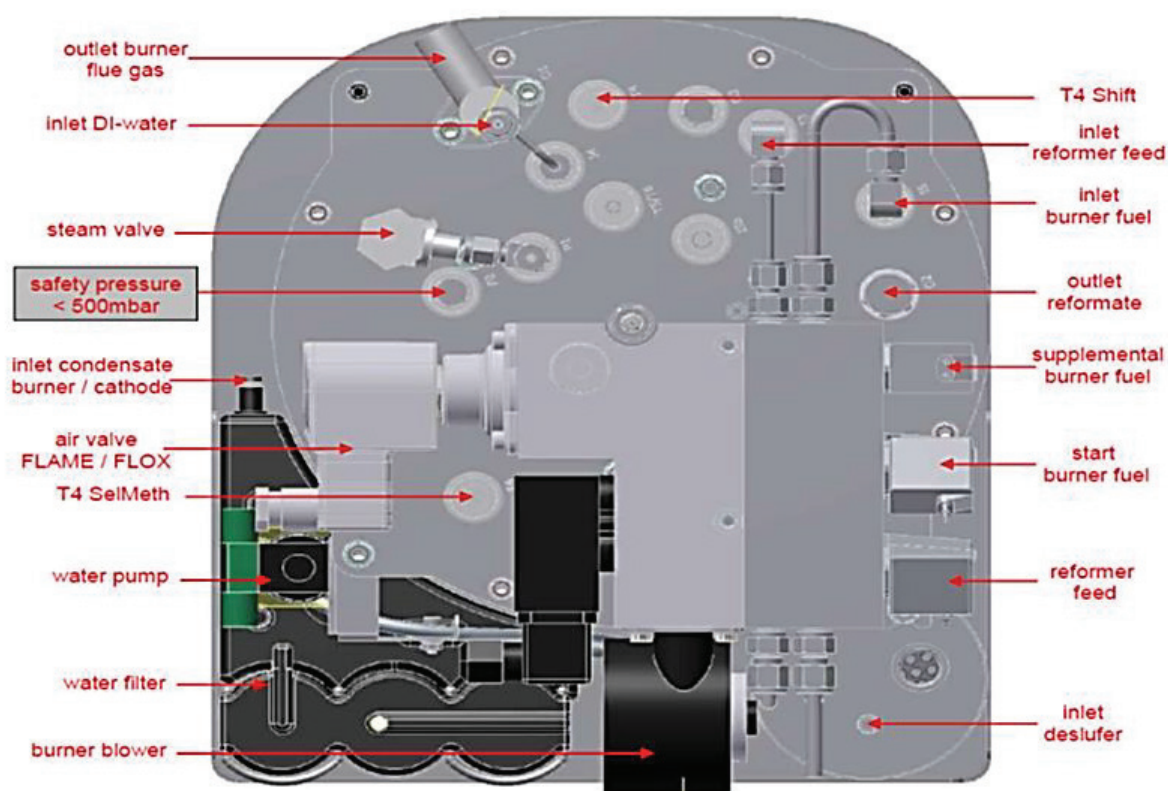
Figure 4-2 Schematic representation of the top view of the *FLOX Reformer* assembly [20].

4.1.1.2   Desulfurization unit

A desulfurizing unit is attached to the reformer for the removal of, specifically, mercaptanes in the feed and fuel sections. It is a separate removable unit consisting of adsorbents – the unit has a single inlet and two outlets to allow for the splitting of desulphurised gas into a feed and fuel section.

4.1.1.3 Burner air supply with control valve

An electronic radial air blower is supplied with the unit for the supply of air into the combustion chamber. The air blower has a 24 V power supply with digital setpoint control to obtain the required air flowrate into the system. This is achieved by means of 0 – 10 V control signal. A two-way solenoid valve is included to shut off the supply if required. The system comes complete with a pressure differential switch as safety precaution, the purpose of which is to measure pressure difference of air flowing into the combustion chamber. If no air flow to the system is detected within a limited time period (approximately 5 seconds), the system is programmed to shut down.

4.1.1.4 Process water pump

Water is supplied into the reformer by means of an electronic water pump, powered by a 24 V power supply and controlled by 0 – 5 V voltage regulation.

4.1.1.5 Gas valves

Three separate solenoid valves are included in the system for on/off control of gas flow into the system. Included are solenoid valves for fuel entering the combustion chamber, feed entering the reformer and a supplemental valve for possible use with anode off gas from a PEM fuel cell.

4.1.1.6 Evaporator and injection pump

The system comes complete with an internal coiled evaporator where incoming deionized water is evaporated by means with heat transfer with the reforming and shift stages. A steam pressure release valve is included to ensure that pressure in the line does not build up to critical levels. Incoming steam and fuel is mixed and pumped into the system by means of an internal injection pump.

4.1.1.7 Steam reforming reactor

The first reaction chamber of the system, reforming contains a packed bed of commercial nickel-based catalyst. No further details about this catalyst (or any other used in the subsequent reaction sections), either in terms of catalyst quantity or supplier, are provided by

the manufacturer. The system includes a thermowell for independent temperature monitoring throughout the axial length of the reactor.

4.1.1.8   Water gas shift and selective methanation reactors

A second reactor chamber containing commercial copper/zinc-based catalyst and subsequent reactor chamber containing semi-commercial ruthenium-based catalyst for the water gas shift (referred to as *Shift or WGS*) and selective methanation (referred to as *SMET*) reactions, respectively, follow in series after the reforming reactor section. Both chambers have accompanying thermowells for monitoring of axial temperature profiles.

4.1.1.9   Housing

The system is encased in a cylindrical stainless steel housing and internally packed with high temperature heat resistant powder insulation material to ensure that external casing does not become hot during operation. All inlet/outlet gas and liquid connections are 316 stainless steel Swagelok™ fittings.

4.1.1.10 Control system

Included with the system is a control module consisting of a so-called *CCFF* card and *JUMO* safety switch.

The *"JUMO"* safety switch is a temperature control device that allows the user to control the temperature at which the switchover between *"Flame mode"* and *"FLOX mode"* occurs – the system control temperature – and has a hardwired shutoff that occurs if a temperature above 910°C is reached.

The *"CCFF"* card is the "brain" of the control system and controls many features including the startup procedure, temperature control, powering the transformer, opening and closing the included solenoid valves and inputs and outputs for a link between the control system and a programmable logic controller (PLC) for external control.

4.1.2 Balance of plant components

An in depth layout of the integrated unit can be seen in figure 4.3 in the form of the system Piping and Instrumentation Diagram consisting of many components as stated below.

4.1.2.1 Test unit frame for unit assembly

A custom built, movable, stainless steel frame assembly, as used for other research projects in the laboratory of the Centre for Catalysis Research at the University of Cape Town, was constructed for the entire integrated FLOX assembly with balance of plant components.

4.1.2.2 Gas distribution

Gas used in this study is supplied by means of the Centre for Catalysis Research's central reticulated gas manifold from high pressure cylinders, all gases used in this study were supplied by Air Products. The gas lines are connected to the frame by means of high pressure Swagelok stainless steel tubing and fittings.

The on-frame gas distribution network consists of 2 separate gas lines for nitrogen and methane, respectively. Nitrogen is used as inert and flushing gas throughout the *"FLOX Reformer"* and methane as reaction gas.

Both incoming gas lines include the following:

- In-line gas filter to ensure that no particulate impurities enter the system via the gas. The filter body contains a 0.5 μm interchangeable filter element;
- Standard *Tescom* low pressure regulator to regulate gas pressure from 50 bar gas network pressure to below 10 bar for system;
- Manual and electronic solenoid 2-way valves for shut off of gas supply. Manual valves are standard , supplied by Swagelok and Burkett, respectively;
- Check (non-return) valves, supplied by Swagelok, to ensure that gas flow only occurs in one direction.

In addition, N_2 gas flowrate into the reformer feed port/line is controlled by means of a *Brooks* electronic mass flow controller (0 – 1000 SCCM).
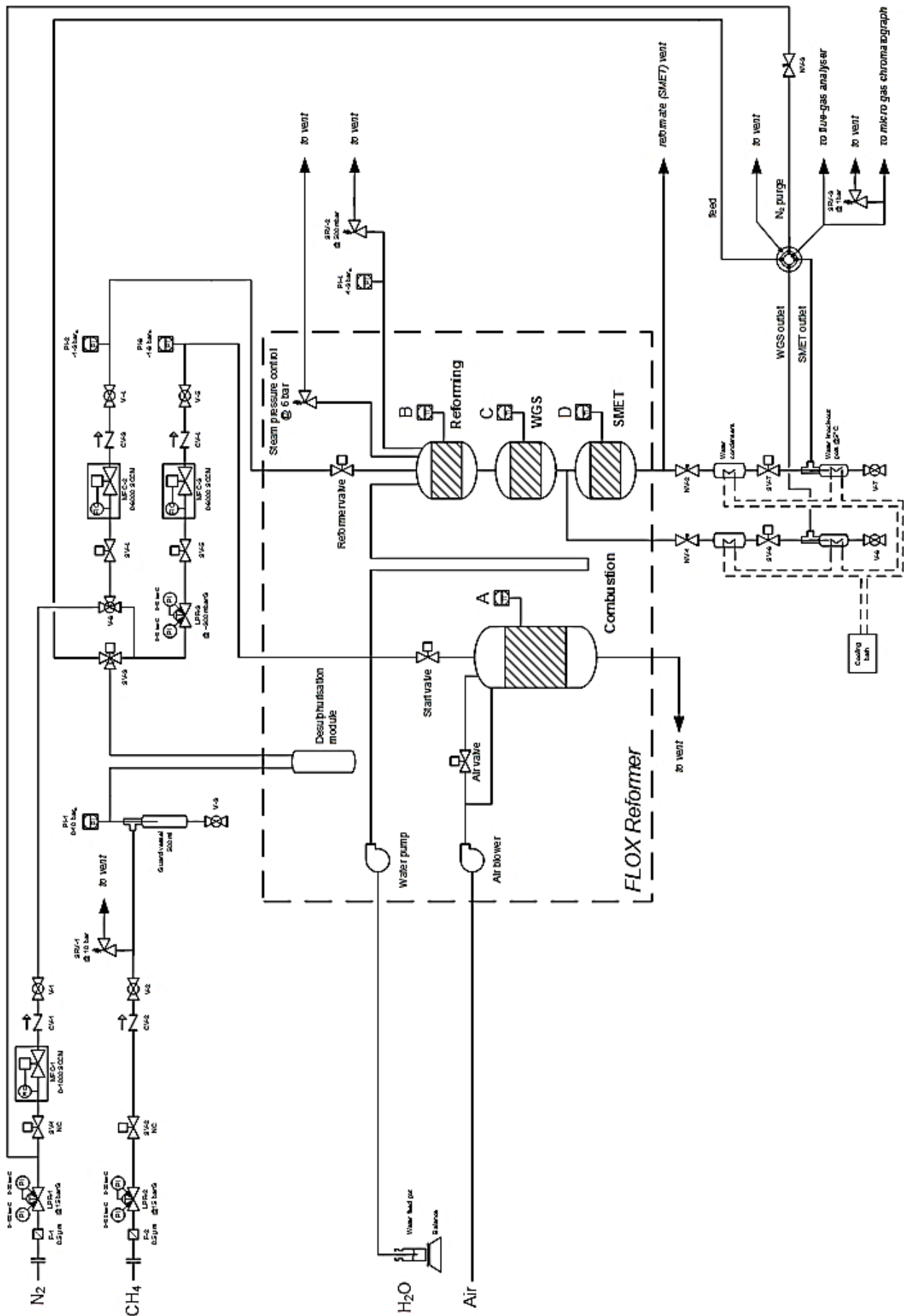
Figure 4-3 Piping and Instrumentation diagram (PID) of the automated reformer assembly.

4.1.2.3   Guard catch pot assembly

After the shut off valves, the methane gas line enters a 500 ml Swagelok vessel with appropriately designed diptube, the purpose of which is to act as guard catchpot to prevent the possibility of water flowing back through the system and thus preventing any damage to the upstream mass flow controllers or contamination of the reticulated gas network. The guard catchpot has a manual drainage valve at the bottom to drain water if required. The pot also serves a dual purpose as mixing and buffer tank, should it be decided to use mixed gas in any future studies.

A safety relief valve (*Swagelok*) is also connected in-line in case of gas pressure buildup. The safety relief valve has a spring assembly, preset to release at 10 bar, with outlet connected to a common vent. The assembly includes an electronic pressure transducer to monitor/log the upstream feed gas pressure.

From the guard catchpot, gas is directed towards to a 3-way electronic solenoid valve, going either to the (manufacturer supplied) desulphurising module and further as fuel or feed to the reaction stages, or to a bypass line for online feed component analysis.

4.1.2.4   Fuel inlet line

Following the desulphurising module, the feed gas is split – one directing fuel to the combustion chamber, and the other directing feed gas to the reforming section. The former line has a second separate low pressure gas regulator to accurately regulate the methane pressure from 10 bar to less than 1 bar so as to control the desired flow required for the combustion reaction.

Furthermore, the line has a *Brooks* mass flow meter (with a full scale flowrate of 0 – 6000 SCCM), i.e. not controlling flow but rather monitoring flowrate set by the low pressure gas regulator, to measure the flowrate of fuel going into the combustion chamber. Additionally, a pressure transducer is connected inline to log gas pressure. A manual shut off valve is located in this line to shut off gas supply, if required, as part of the safety strategy.

4.1.2.5   Feed inlet line

After exiting the desulphurising module, methane is directed to the reformer feed line where gas flowrate is controlled by means of a *Brooks* mass flow controller (with a full scale flowrate of 0 – 6000 SCCM). A manual 2-way shut-off valve as well as electronic solenoid valve are also included. A check valve and pressure transducer are located in this line.

4.1.2.6 Water supply

A 5 litre feed water tank is used for upfront water supply to the system and is placed on top of a 6 kg analytical balance. The purpose of the balance is to accurately measure the change in mass of the water with time to determine the actual water flowrate to the reformer. Teflon tubing is used to connect the tank to the water pump on the *WS*® *FLOX Reformer.*

4.1.2.7 Combustion outlet line

Combustion product exiting the chamber is at elevated temperatures above 100°C even after contact with incoming air. This exhaust product is connected to a high temperature steel reinforced rubber hose and plumbed directly into the takeoff point of the vent extraction system as located in the Centre for Catalysis Research laboratory for safe operation as the outlet may contain trace amounts of CO and NO_x.

4.1.2.8 Temperature control and measurement

Effective temperature control and measurement is required for the scoping of the reformer. A range of multipoint thermocouples supplied by Omega Engineering, were used for the different sections inside the reformer.

- Combustion - A multipoint K-type high temperature thermocouple with 3 readout points on the tip is used, and shown as thermocouple A in figure 4.3. Two points are connected to the *JUMO* safety switch and one is connected to the operating PLC, ensuring effective temperature control even if one point fails. The readout point tip is located in the middle of the combustion chamber close to the flame front.
- Reforming – A multipoint K-type thermocouple with 3 uniformly spaced readout points is used, and shown as thermocouple B in figure 4.3. Each readout point is 50 mm apart to allow for a length of 100 mm between top and bottom to be measured and recorded. The catalyst bed in the reforming section is reported to be 100 mm long, and thus the points read the inlet, middle and outlet of the reforming reactor.
- WGS – A multipoint J-type (more accurate for low temperature applications) thermocouple with 3 uniformly spaced readout points 50 mm apart to measure top, middle and bottom of the water gas shift reaction zone is used, and shown as thermocouple C in figure 4.3.

- SMET – A multipoint J-type thermocouple with 3 uniformly spaced readout points 40 mm apart, because of the shorter 80 mm long selective methanation reaction zone, and shown as thermocouple D in figure 4.3.

4.1.2.9 *Outlet pressure and flow control*

Modification to the internal plumbing of the *FLOX Reformer* was undertaken so as to measure both intermediate and final outlet stream compositions. Two reformate outlet stream paths, at different stages of chemical transformation, are shown in figure 4.3 – one intermediate post-WGS stream and one post-selective methanation stream. The final reformate (i.e. post-SMET stream) is further split, the majority of reformate being sent directly to vent whilst a small amount of it is directed towards analysis. The relative flowrate going to each of these sub-streams is controlled by high temperature bonnet valves. Adjusting the bonnet valves controls the operating pressure of the reactor as well as the flow going into each section.

4.1.2.10 *Water knock-out assembly*

Either reformate that is to be sampled is passed through a custom-made water knock-out assembly. It consists of a two stage assembly with initial condenser where reformate goes through a coiled tube encased in an outer PVC vessel containing circulated cooling water. Water is condensed and flows downwards under gravity into the second knock-out vessel with diptube mechanism for gas/liquid separation. The knockout vessel is encased in a larger heat exchanger vessel containing the same circulating cooling water as in the condenser.

The water knock-out vessel has a manual drainage valve for draining of the collected water. The cooling water is controlled at a constant 5°C to ensure that most of the water in the reformate is removed prior to analysis – the water content of the reformate stream at this temperature being approximately 0.8 %. The circulated cooling is supplied by a Lauda chiller water bath via silicone tubing.

4.1.2.11 *Selection valve*

Dry gas leaving the water knockout vessel for both SMET and shift analysis streams are passed through an electronic stream selection valve. This selection valve (supplied by *VICI-Valco*) is a micro-electric actuator valve with 4 inlet ports and common vent. In this study three ports were used for the SMET sample, shift sample and feed bypass, 1, 4 & 3

respectively, with the fourth port used in conjunction with the flue gas analyser as discussed in the *Analysis* section (see section 4.4).
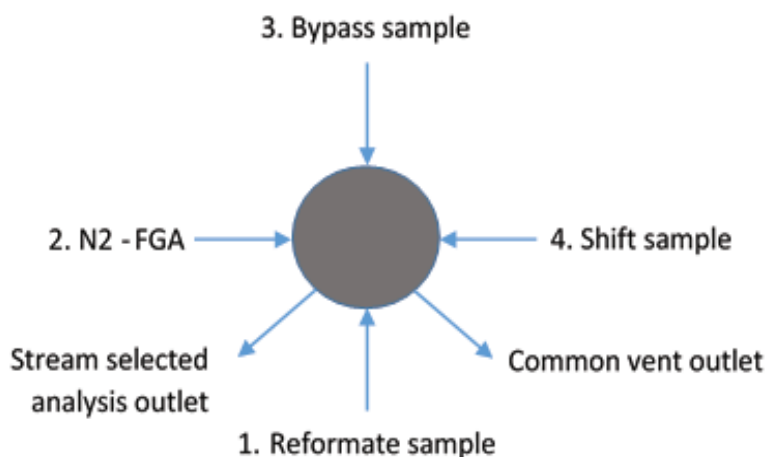
Figure 4-4 Schematic of the sample selection configuration of the stream selection valve.

The selection valve has two outlets with the stream selected going through one, in this case to the stream being sampled. All other non-selected streams pass to a common outlet to the vent section.

4.1.2.12 Flue gas and microGC analysis

From the selection valve the selected stream goes to both micro gas chromatograph and flue gas analyser to determine its composition. The analytical techniques are discussed in detail in the *Analysis* section (see section 4.4).

4.1.2.13 Vent pot and extraction

All reformer outlet streams and safety relief valve outlet lines are connected together in a final mounted 2 litre vent vessel before exiting to the extraction system. A drainage valve is connected at the bottom of the vent vessel to drain water that predominately collects from the bulk reformate stream flow.

4.1.3 Operating software and control

Due to automated nature of the system used for this study a suitable Programmable Logic Controller or PLC was used. The control strategy was programmed using LabVIEW (Laboratory Virtual Instrument Engineering Workbench). It can be described as a system design platform and development environment that uses a visual programming language.

The software, created by developers National Instruments, is ideally suited for use in data acquisition, instrument control and automation of systems and can operate on multiple platforms including Microsoft Windows, LINUX and MAC. In this study a PC running on Microsoft Windows is used.

The software connects to the different instruments through means of a CompactDAQ real time acquisition platform that connects to the software via USB or Ethernet. The DAQ used for this study is an 8 slot chassis with an extra thermocouple input module. The different modules are described below:

- **Thermocouples inputs module:** NI-9213 (16 Channel)

Input module for viewing temperatures of all thermocouples for Reforming, Combustion, and WGS and SMET reactors. Signal generated in millivolts.

- **Analog inputs module:** 2 x NI-9201 (8 Channel)

Input module to view mass flow controller setpoints and actual flowrates for nitrogen (0 – 1000 SCCM), Reforming (0 – 6000 SCCM), Combustion (0 – 6000 SCCM), pressure transducer readings for the guard catchpot (0 to 10 bar_g), reformer feed (-1 to 3 bar_g), combustion feed (-1 to 3 bar_g) and reactor pressure (-1 to 3 bar_g), flue gas concentration readouts for H_2 (0 – 90%), CO_2 (0 – 30%), CH_4 (0 – 20000 ppm) and CO (0 – 400 ppm), air blower and water pump setpoints.

- **Analog outputs module:** 2 x NI-9263 (4 Channel)

Output module to control mass flow controllers, water pump and air blower setpoints.

- **Digital outputs module:** 3 x NI-9472

Output module to control solenoid valves (24V), mass flow controller commands (open, control and close), VICI-Valco selection valve channel selection and "CCFF" Card commands for heating of reformer, temperature setpoint and reset function.

- **Digital inputs module:** 1 x NI-9401 (Dig I/O)

Input/output module to view status of flue gas analyser and CCFF Card.

Inputs are described as signals going to the software from the various platforms and used for measurement purposes primarily whilst outputs are signals sent from the software to the

instrument as commands to control various instruments. A detailed layout of the software interface as well as FLOX Plant LabVIEW system is included in Appendix A. Included in the software is the option for logging all data in a Microsoft Excel format, where the user can choose the interval time for data logging.

4.2 Experimental operating conditions

The main purpose of this study was the scoping of the reformer to check the validity thereof for use in conjunction with a PEM fuel cell.

This is done by means of:

- Measurement of reformate composition;
- Measurement of the shift composition;
- Establishment of startup time;
- Establishment of thermal efficiency;
- Establishment of temperature profiles throughout reformer reaction stages.

The scope of this study only includes work done on one feedstock, namely methane, with the variables tested being:

- Rate of combustion of fuel;
- Combustion temperature;
- Load (flowrate of feed to the reformer), equating to rate of H_2 production;
- Steam-to-carbon ratio.

4.2.1 Combustion rates

For the scoping of the *FLOX Reformer* it was decided to run the unit using two different methane combustion flowrates. The rates selected were:

- 1600 SCCM CH_4;
- 3200 SCCM CH_4.

To achieve a similar air to fuel ratio for the different methane combustion flowrates selected, 2 different air blower power settings, after appropriate calibration, were used.

4.2.2 Combustion temperature

Three different temperatures at which combustion occurs were selected for investigation, namely:

- 750°C (Flame combustion);
- 800°C (Flame combustion);
- 840°C (Above FLOX setpoint – i.e. FLOX combustion).

To reiterate the description of the operation of the *FLOX Reformer*, the entire system has been designed to be operated based on the control solely of the combustion temperature – appropriate heat integration and relative reactor placement and heat shielding by the manufacture reportedly allows for all three reaction chambers, the Reforming, Shift and SMET sections, to operate within their respective correct temperature operating windows.. The highest temperature of 840°C is above the setpoint of the JUMO temperature switchover from so-called Flame-mode to FLOX-mode and is thus done using flameless oxidation. All three temperatures have been tested with the two different combustion rates.

Figure 4.5 below shows the temperature control strategy applied in the *FLOX Reformer.* A temperature setpoint is chosen via the PLC after which the reformer initiates the heating sequence. If the setpoint is below the Flame/FLOX switchover temperature, the system will heat up until the setpoint is attained. The system temperature is controlled by periodically opening and closing the fuel gas valve and starting the flame initiation sequence along with opening the gas valve. The control is thus cyclic as the valve closes above the setpoint and opens again below it. For this system an up-down temperature hysteresis of 5°C was used to ensure that the burner stayed on for at least 20 second intervals, as shown in figure 4.5 between 840°C and 850°C.
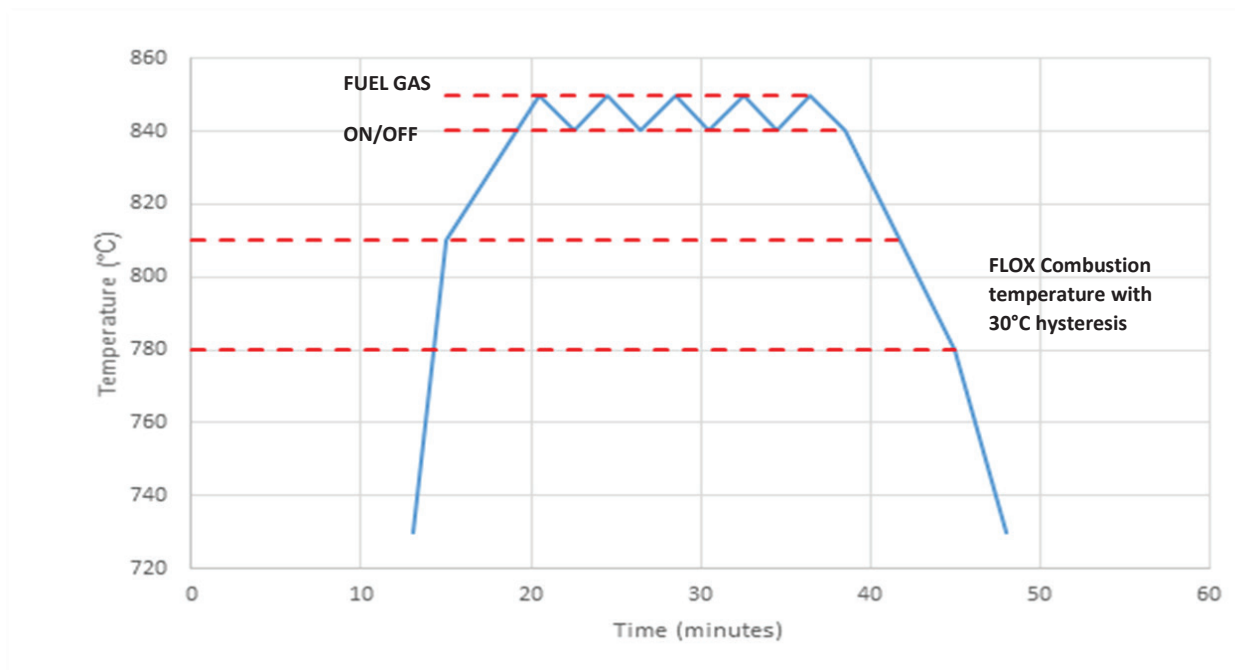
Figure 4-5 Temperature control strategy showing the changeover temperature from Flame- to FLOX-mode, and the cyclic temperature control nature of the fuel gas on/off approach [20].

For temperatures above the FLOX switchover setpoint the same methodology is applied although the control happens only through the periodic opening and closing of the gas valve to the combustion chamber as there is no flame.

The JUMO temperature switch also employs a 30°C hysteresis when switching between Flame- and FLOX-mode as shown above.

Temperatures obtained in all the other reactor areas for each combustion temperature are to be reported in the *Results* section (see section 5).

4.2.3 Pressures

For all tests the pressure was not varied – a reactor pressure of about 300 mbar$_g$ was used throughout. This was obtained by means of bonnet valves to throttle the outlet gas and hence set reactor pressure. The reformer only has a pressure rating of 650 mbar and higher pressures can thus not be used.

4.2.4 Reactor loads

Load or flowrate into the reformer is a key variable in performance testing; the flowrate of methane being consumed for the generation of hydrogen. Although it essentially should be described as relative space velocity, this is not possible as the amount of catalyst used is unknown.

A variety of reformer loads (i.e. methane flowrates for reforming specifically) were tested, namely:

- 600 SCCM;
- 1200 SCCM;
- 2400 SCCM;
- 2700 SCCM;
- 3600 SCCM;
- 4200 SCCM.

Assuming that all reactions proceed according to stoichiometry a total flowrate of hydrogen of nearly 16 SCLM can be achieved, which roughly equates to the hydrogen consumption of a 1 kW PEM fuel cell.

4.2.5 Steam-to-carbon ratio

Along with the different methane loads various steam-to-carbon (S/C molar basis) ratios were tested. As opposed to originally planned, the number of ratios tested has been decreased, as this parameter did not have a significant effect on the *FLOX Reformer* operation.

The steam-to-carbon ratio is essentially determined during the operation of the unit – at high load the S/C ratio is as low as 4, whilst at low load the ratio of over 10 is obtained.

Due to the reformer control strategy of one control temperature in combustion, there seems to be a fine balance between combustion heats supplied, heat of reaction of the other reactions as well as the amount of water sent through the reformer. The range of water flowrates are thus rather limited, as too much or too little causes the reaction temperatures in the other reaction zones to go out of their respective manufacturer specified operating ranges.

The amount of water being evaporated has a great impact on the heat transfer in, especially, the selective methanation and water gas shift stages as it contacts directly with these stages in the evaporator. It would seem that the reformer requires a certain excess of water to operate

optimally. Narrow water flowrate ranges are thus required for normal operation; this is discussed further in the *Results* section (see section 5).

4.2.6 Run summary

All these various operating parameters are to be tested in the form of 6 separate 4 – 8 hour runs. Each run is to be one combustion temperature and combustion rate tested at multiple fuel loads from lowest load to the maximum possible for the system or up until the required 15 SCLM of hydrogen is obtained. For a complete set of run conditions please refer to the Results section (Section 5).

4.3 Experimental operating procedures

4.3.1 System calibration and operability testing

4.3.1.1 *Mass flow controller calibration*

Prior to commencement of the *FLOX Reformer* testing, the ancillary three mass flow controllers were calibrated. This was undertaken by passing the appropriate gas, as specified, through the controllers at various setpoints of its full capacity. The actual gas flowrate, as determined by a calibrated *Brooks* electronic rotameter (0 – 10 SCLM) was recorded and compared to the set-point of the controller.

4.3.1.2 *Calibration of water pump and air blower*

The calibration of the air blower was done by means of varying the air blower control voltage settings (0 – 10V) and measuring the corresponding actual air flowrate exiting the combustion chamber. This air blower calibration was performed without the flow of methane present. Due to the very high flowrates generated by the air blower and the gas exit orifice size of 18 mm, typical flow calibration methods as practiced in the Centre for Catalysis Research could not be performed. An anemometer, rather, was used to estimate the straight line velocity of the air exiting the combustion chamber, and converted to a volumetric flowrate based of geometric cross-sectional area of the pipe.

It was not possible for the water pump attached to the *FLOX Reformer* to be re-calibrated, as the flowrate of water is highly affected by pressure in the chamber and as the pressure of

water and steam in the evaporator is not known, calibrating is impossible to perform. Establishment of water flowrate in the system is rather done by choosing a setpoint and measuring corresponding mass change of the water feed tank whilst performing an experimental run.

4.3.1.3 Setting of relief valves

The three safety relief valves were pre-set prior to installation in the test unit. The 'cracking' pressure was set with a known gas pressure as per manufacturer specifications.

4.3.1.4 Thermocouples

Before operation, thermocouples are inserted into the appropriate thermowells included in the *FLOX Reformer*.

- Combustion thermocouple is inserted to the bottom of its thermowell;
- Reforming thermocouple is inserted to the bottom of its thermowell and thereafter pulled back 10 mm to the bottom of the reformer section. The various pre-defined readout points will now be at the correct height of bottom, middle and top of reformer catalyst zones, respectively;
- Shift thermocouple and SMET thermocouple thermowells are equivalent depth and interchangeable. For Shift the temperature reading thermocouple is inserted to the bottom and lifted 10 mm, for SMET the thermocouple is lifted 110 mm to correspond to the Selmeth catalyst zone.

4.3.1.5 Leak testing

Before commencing with testing, a leak test is performed on the system. This was done by means of introducing pressurized nitrogen into the system, set at 10 bar_g and isolating the system up to the reformer feed and fuel lines. The procedure followed is described in the following *Startup Procedure* section (see section 4.3.2).

An electronic thermoconductivity gas leak detector was used to locate potential gas leak points (a liquid bubble detection method was considered unwise due to the numerous electrical components). Fittings where leaks were found to occur were tightened and the process repeated until no discernible leaks were observed and the system pressure remained constant whilst isolated.

Gas was introduced in the feed lines and the pressure set at 500 mbar in the reactor section using the post-reactor bonnet valves. A leak test thereafter also performed on all visible fittings in this section until the system showed no pressure decrease over time whilst being isolated.

4.3.1.6   Safety chain

The safety of the system is ensured by a variety of methods, including:

- 910°C temperature override shutdown – system shuts down via *JUMO* Safety switch if the reactor temperature of 910°C is exceeded. A triple combustion thermocouple is connected to the system;
- Pressure relief valves – the feed line, reactor and analysis sections have safety relief valves connected to maintain system pressure below critical values. Steam pressure in the reactor is controlled by an extra steam relief valve as supplied by WS;
- Catalysis research lab facilities include a gas extraction system in the case of leaks and has multiple hydrogen and carbon monoxide detectors throughout the facility.

4.3.1.7   Feedstocks

Feedstocks used in this study includes atmospheric air, with all impurities and water vapor included, and introduced into the system by means of air blower. Nitrogen used for purging purposes is high purity nitrogen 5.0 as obtained from Air Products. (The designation 5.0 signifies 99.999% purity).

Methane for combustion and reforming is high purity with 3.5 purity rating (99.95%), with nitrogen being the main impurity. Water used was obtained from the in-house deionising unit delivering water at 12 MΩ purity.

4.3.2   Start-up procedure

Start-up is done by means of the following sequences:

4.3.2.1   Initial nitrogen flushing:

1. Gas supplies are opened and pressure regulator set to approximately 10 bar_g outlet. Initially solenoid valves are kept in the closed position.
2. Nitrogen solenoid valves and mass flow controllers are opened using the software for the system.

3. Nitrogen is passed into the reformer feed line by switching the 3-way valve on the reformer feed line and reformer feed line solenoid valve is opened.

4. Mass flow controller is set to approximately 500 SCCM and all valves are opened on the feed line. Outlet bonnet valves are opened to allow gas flow through reactor. The purpose of this is to flush the reactor with nitrogen and ensuring that no air enters the system.

4.3.2.2 Initiating combustion (cold start)

1. Air blower is set to control voltage required (46% or 4.6V) for specified combustion setting. (Both the air blower and fuel gas regulator have been tested previously to obtain the correct setpoints for successful ignition of the system.)

2. Regulator on the fuel line is set to the correct level for a combustion flowrate of 1600 SCCM.

3. Solenoid valve and manual valves on fuel lines are opened. Mass flow controller is fully opened to use as a meter.

4. Temperature setpoint of 750°C is set on the in-house software.

5. CCFF Card heating order given by manual switch or through software. Card goes through following start up sequence:

- A1 – Air valve open
- A2 – Gas valve open / Transformer on (provides spark)
- A3 – Flame on (wait 5 seconds for stability)
- A4 – Flame stable (heating up)

6. System is now heating up through flame combustion. Wait until combustion temperature reaches setpoint. Cooling bath is turned on and adjusted to a setpoint of 5°C.

7. If the setpoint is above the FLOX temperature the CCFF Card displays A5.

4.3.2.3 Starting reforming

1. The system is now left to heat up until the combustion setpoint is obtained. Once this occurs the fuel gas valve starts to control the temperature through cycling the fuel gas valve. A few minutes later reforming reaches roughly the same temperature as Combustion whilst Shift and SMET temperature continues to increase.

2. Once Shift has reached 200°C and SMET has reached 160°C water can be introduced into the Reformer chamber.

3. Water pump is set to a control voltage of 20% or 1V, initially.

- If system has not been used for some time the pump may require priming as air bubbles are formed in the line. This is accomplished by increasing the flowrate to maximum and by opening a fitting after the pump whilst the water is pumping to allow for the removal of air bubbles. System is sealed up again thereafter.

4. In so doing, water is now being passed through the reformer and brings about a corresponding change to the temperatures in the Shift and SMET chambers as water being evaporated is contacted with these sections.

5. The system is allowed to stabilize at the set water flowrate and if temperatures of both Shift and SMET are between 190 and 230°C reforming can be initiated. If the temperature is not in the above mentioned range water flowrate must be adjusted. An increase in water flowrate brings about a decrease in these temperatures.

6. Water flowrate is measured by means of change of mass of the water supply tank on the balance.

7. Bonnet valves after the reactor are adjusted to keep system pressure at 0.3 bar$_g$.

8. Once the system is stable methane is introduced into the system by switching the 3-way valve on the feed line to the methane section. All accompanied valves on the methane line are opened to ensure this is possible.

9. Flowrate into feed is adjusted to 600 SCCM methane setpoint for the 1st experimental load setting.

10. Bonnet valves for SMET- and shift analysis are opened and adjusted to approximately 500 SCCM each for flow into microGC and flue gas analyser.

11. Selection valve is changed to appropriate channel for either SMET or shift analysis.

In the case of a load change to 1200 SCCM methane load, the following method is prescribed:

1. Control voltage for water is increased incrementally initially. The reason for this is to avoid any CO spikes from decreased steam-to-carbon ratio.

2. Pressure of system is adjusted with bonnet valves to stay at 0.3 bar$_g$ and maintain 500 SCCM to the analysis section. Water flowrate is measured and adjusted if temperature is out of range.

3. Methane setpoint is doubled to 1200 SCCM via the control software.

4. Bonnet valves are again adjusted to maintain a constant pressure.

4.3.2.4 Start-up from standby

For startup from standby the system is started in an identical fashion with the same procedure for nitrogen flushing and initiation of combustion as previously described, but rather using a temperature setpoint of 350°C. The system is left to run on standby for approximately two hours to allow Shift and SMET to reach 200°C and 160°C, respectively. The startup procedure can now be initiated by changing the setpoint of combustion to the required setpoint for the reaction to occur. Startup from this condition takes about 10 minutes before the reforming procedure can be initiated, as only reforming and combustion temperatures need to be increased.

4.3.2.5 Shut-down procedure

Once all required operating conditions have been tested the system can be shut down, using the sequence described below:

1. The reforming mass flow controller is adjusted to 500 SCCM as at the start of testing and switched to introduce nitrogen into the system via the 3-way valve as shown in figure 3 and as done previously during initial purging.
2. Combustion is stopped via the software or by switching off the CCFF Card and all methane valves closed.
3. Water flowrate is decreased to 20% of control voltage as at the start of the test. Water supply MUST remain on to ensure that system temperature in Shift and SMET does not increase too extensively (the temperature is maintained by continuing to allow for the evaporation of water).
4. The combustion and reforming temperature is allowed to cool down to below 600°C whilst system is flushed with nitrogen.
5. Water supply is discontinued once the temperatures have dropped below 600°C and system allowed to cool under nitrogen environment. The system is left to cool further overnight.
6. Nitrogen supply cut off and air blower turned off.
7. Water catch pots and vent vessels are drained of all collected water.

4.4 Feed and Product Gas Analysis

4.4.1 Gas chromatography

4.4.1.1 Chromatograph operational specifications

The gas composition is determined using a Varian 4900 microGC. It is equipped with thermal conductivity detectors (TCD) and consists of 4 modules (with independent injector, column and detector) and operating with two different carrier gases, depending on the module in question. The system is operated by means of Galaxie chromatographic software. A summary of the column specifications and operating conditions in each module is given in Table 4.1.

Table 4-1 Varian 4900 microGC parameters and setpoints.

Module	1	2	3	4
Column	Mol sieve 5A	Mol sieve 5A	CP-SIL 5CB	CP-PoraPLOT Q
Length	10 meter	20 meter	15 meter	10 meter
Carrier Gas	argon	hydrogen	hydrogen	hydrogen
Injector Temp.	50°C	50°C	40°C	50°C
Column Temp.	50°C	50°C	40°C	50°C
Column Pressure	150 kPa	150 kPa	70 kPa	80 kPa
Gases Detected	Hydrogen nitrogen methane carbon monoxide	nitrogen methane carbon monoxide	carbon dioxide water vapor	carbon dioxide water vapor

4.4.1.2 Sampling procedure

For sampling the appropriate stream to be sampled is selected by means of the VICI-Valco electronic stream selection valve. The water-free gas is then directed towards analysis, before passing to the vent system. The sample is teed off to microGC. An injection vacuum pump draws in a defined amount of sample, for a pre-determined time period, and injected into the 4 separate modules inside the microGC.

Galaxie software allows for the setting of methods with different variables as well as the creation of a sequence of samples in succession.

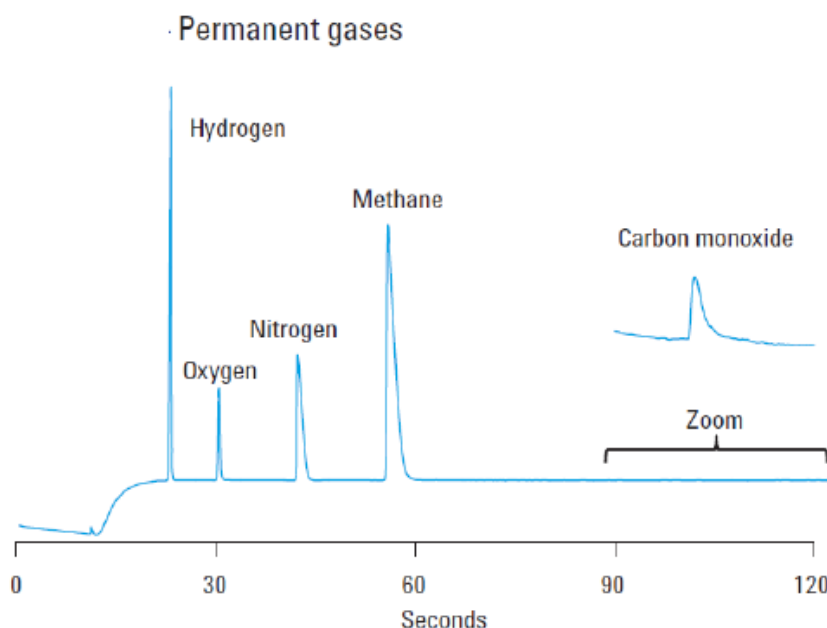### 4.4.1.3   Chromatographic analysis

Figure 4-6 Typical Gas chromatogram for permanent gases in a Mol Sieve column [29].

Figure 4.6 shows a typical chromatogram as obtained from microGC analysis. Mol sieve columns are used for the separation of various permanent gases, specifically hydrogen, methane and carbon monoxide in this study. Each gas species has a specific retention time (shown illustratively by the x-axis in figure 4.6) causing each gas specie to elute separately. This process is gas and column specific. The size of the peak in the signal is relative to the concentration of a specific component in the analysis stream. Gas species have different relative response in signal intensity, related to their thermal conductivities.

For detection of carbon dioxide a *PoraPLOT Q* or *CP-Sil 5CB* module is used. The retention times are generally consistent for species in a specific column, except for the mol sieve columns where frequent sampling leads causes a shift of the peaks to shorter retention times, and thus less separation. This is remedied by "baking out" the column – exposing the column to high temperatures with flushing gas for an extended period, typically overnight.

4.4.1.4   Calibration

Calibration of the microGC for all the specific component species needing to be identified and quantified was undertaken by a multi-point calibration technique. Calibrated mass flow

controllers were used to mix individual gases in specified relative ratios to simulate a known gas mixture. This gas mixture was then analysed.

This absolute signal response of the individual gas species is ratioed to the composition of the known gas to yield its calibration factor.

4.4.2 Flue gas analysis

Analysis of the shift and SMET streams is also undertaken by means of ABB flue gas analyser. The main purpose of this supplementary technique is to achieve real time analysis of some key outlet stream components as compared to microGC where samples are taken periodically (typically only once every 6 minutes).

4.4.2.1 Analyser conditions

The flue gas analyser consists of two different units for measuring four different components, namely the Uras26 and Caldos25.

Infrared Analyser Module Uras26

The Uras26 is an infrared detector using non-dispersive infrared absorption in the λ = 2.5 – 8 µm wavelength range. The setup for this project has 3 different measuring cells as shown in table 4.2 using one beam path. It can typically be used to detect carbon-, nitrogen- and sulphur oxides as well as hydrocarbons (C1 – C6).

Table 4-2 Detection ranges for Uras26.

Component	Carbon monoxide	Carbon dioxide	Methane
Range	0 – 400 ppm	0 – 30 %	0 – 20000 ppm

The carbon monoxide range allows for detection of very small quantities of carbon monoxide in the 4 – 20 ppm range as typically observed after selective methanation, at which CO levels are virtually undetectable with the microGC. Carbon dioxide and methane ranges were chosen to suit typical reformer outlet concentrations.

Thermal Conductivity Analyser Module Caldos25

The Caldos25 is a thermal conductivity analyser with highly corrosion resistant sample cells embedded in glass. It is typically used for detection of hydrogen or sulphur dioxide in other gases. The range is 0 – 90% hydrogen which is more than sufficient for reformate analysis.

Table 4-3 Flue gas analyser technical specifications.

Cell	Uras26	Caldos25
Deviation	1% of span	2% of span
Zero drift	1% of span	1% of span
Detection limit	0.4% of span	1% of span
Flow range	20 – 100 litres per hour	10 – 90 litres per hour
Warm up time	30 minutes	1 hour
Temperature	50°C	60°C
Pressure	Atmospheric	Atmospheric
Response time	3 seconds	10-20 seconds

4.4.2.2   Sampling procedure

The combined analyser consists of two units which have been mounted on the customized frame assembly. The sample line passes through both these units in series and cell concentrations are viewed on the attached display or by means of the PLC connected to the analyser though 4 – 20 mA input signals.

Reformate passing through the analyser is sent to vent thereafter and is kept in the region of 500 SCCM for both shift and methanation outlets using the high temperature bonnet valves. This flowrate is well within the range of the analyser as specified in table 4.3.

A nitrogen flushing line is connected to both units due to the highly flammable mixture being sampled. A flowrate of diluent nitrogen is purged through the cell at all times at a flowrate of 20 litres per hour to prevent buildup of these gases.

4.4.2.3 Calibration

The analyser is calibrated in a variety of ways to ensure that measurements are accurate:

- Zero point calibration – Pure nitrogen or the zero gas (gas not detected by any of the cells) is passed through the cells using the selection valve connected to a nitrogen supply. Signal for 0 % is thus calibrated to minimize zero drift;
- End point calibration of span gas calibration – A gas of known composition can be passed through the analyser. The percentage of known gas in sample is inputted and system auto-calibrates accordingly;
- Calibration cells – The Uras26 has built in calibration cells of known composition for CO, CO_2 and CH_4.

All calibrations are performed by means of the attached display on the analyser units.

4.5 Data work up and calculations

4.5.1 Logging data

All temperatures, pressures, mass flow controller flowrates and water pump and air blower setpoints are directly logged vs. time by means of the PLC and require no further work up.

4.5.2 Calculation of water flowrate and steam-to-carbon ratio

Water flowrate is determined by means of monitoring the loss of water feedpot mass (via balance) relative to time and the corresponding molar flowrates calculated.

$$\text{Mass flowrate} = \frac{\Delta m}{\Delta t} \quad \text{..} \quad (26)$$

$$\text{molar flow rate} = \frac{m}{M} \quad \text{...} \quad (27)$$

Methane molar flowrates is obtained by using the actual mass flow controller volumetric setpoint after calibration and dividing it by the density of methane at STP to obtain firstly the mass flowrate, after which equation 27 is used to calculate the corresponding molar flowrate.

$$mass\ flowrate = \rho * V \quad \text{...} \quad (28)$$

The corresponding S/C ratio can now be calculated.

4.5.3 MicroGC and flue gas analysis

From the PLC all flue gas analyser concentrations in the SMET and shift outlets are directly logged versus time. MicroGC concentrations are calculated by means of the following equation for peak areas using pre-determined calibration factors.

$$\text{Molar fraction } \% = \frac{\text{millivolt signal (peak area)}}{\text{calibration factor}} \dots\dots\dots\dots\dots\dots\dots\dots\dots\dots\dots\dots\dots\dots\dots\dots\dots\dots\dots\dots \text{(29)}$$

4.5.4 Conversions

Once shift outlet composition is known, and assuming that no methane conversion or production occurs in the water gas shift stage (an assumption which is well supported by performance data of commercial Cu/ZnO LTS WGS catalysts), the conversion of methane in the reforming stage can be determined by measurement of the methane composition at the shift outlet.

Molar flowrate into the reformer is determined by mass flow controller methane feed flowrate, assuming ideal gas behavior. Molar flowrate of methane out of the water gas shift stage (and hence out of the reforming stage) is determined by assuming a 100% carbon balance and obtaining the fraction of methane in the carbon exiting the shift stage.

$$X_{CH4} = \frac{F_{CH4,FEED} - F_{CH4,REFORMER\ OUT}}{F_{CH4,FEED}} \dots\dots\dots\dots\dots\dots\dots\dots\dots\dots\dots\dots\dots\dots\dots\dots\dots \text{(30)}$$

The conversion of CO in the shift reaction cannot be obtained as the exact reformer outlet composition is not known. CO conversion in selective methanation however can be calculated:

$$X_{CO} = \frac{F_{CO,FEED} - F_{CO,PRODUCT}}{F_{CO,FEED}} \dots\dots\dots\dots\dots\dots\dots\dots\dots\dots\dots\dots\dots\dots\dots\dots\dots\dots\dots \text{(31)}$$

This is done through measurement of CO concentrations in the shift and selective methanation outlets and assuming a 100% carbon balance in the selective methanation stage.

4.5.5 Thermal efficiency

Once the volumetric flowrates of hydrogen leaving the reformer is known the thermal efficiency of the reformer can be quantified. Equation 17 can be rewritten as the following.

$$\eta_{reformer} = \frac{F_{H2} * LHV_{H2}}{(F_{fuel} * LHV_{fuel}) + (F_{feed} * LHV_{feed})} \dots\dots\dots\dots\dots\dots\dots\dots\dots\dots\dots\dots\dots\dots\dots\dots \text{(32)}$$

The molar flowrate of hydrogen can be calculated by its ratio to the carbon fraction in the SMET outlet and can be converted to volumetric flowrate by equations 27 and 28.

5. Results

5.1 Start-up time

Initial testing done for this study was the establishment of the times required before reforming could be initiated. This can be shown in the form of temperature versus time graphs for all the different reactions zones in the reformer assembly as shown in figures 5.1 to 5.4 below. Startup times were tested using the two combustion flow rates as described in the *Experimental Operating Procedures* section (Section 4.2). Startup for both combustion flowrates were tested using a cold start and startup from standby condition (350°C).

5.1.1 Cold start

Figures 5.1 to 5.2 shows the predicted time taken to obtain the necessary reaction temperatures in the various zones using the two combustion rates from a system at room temperature.
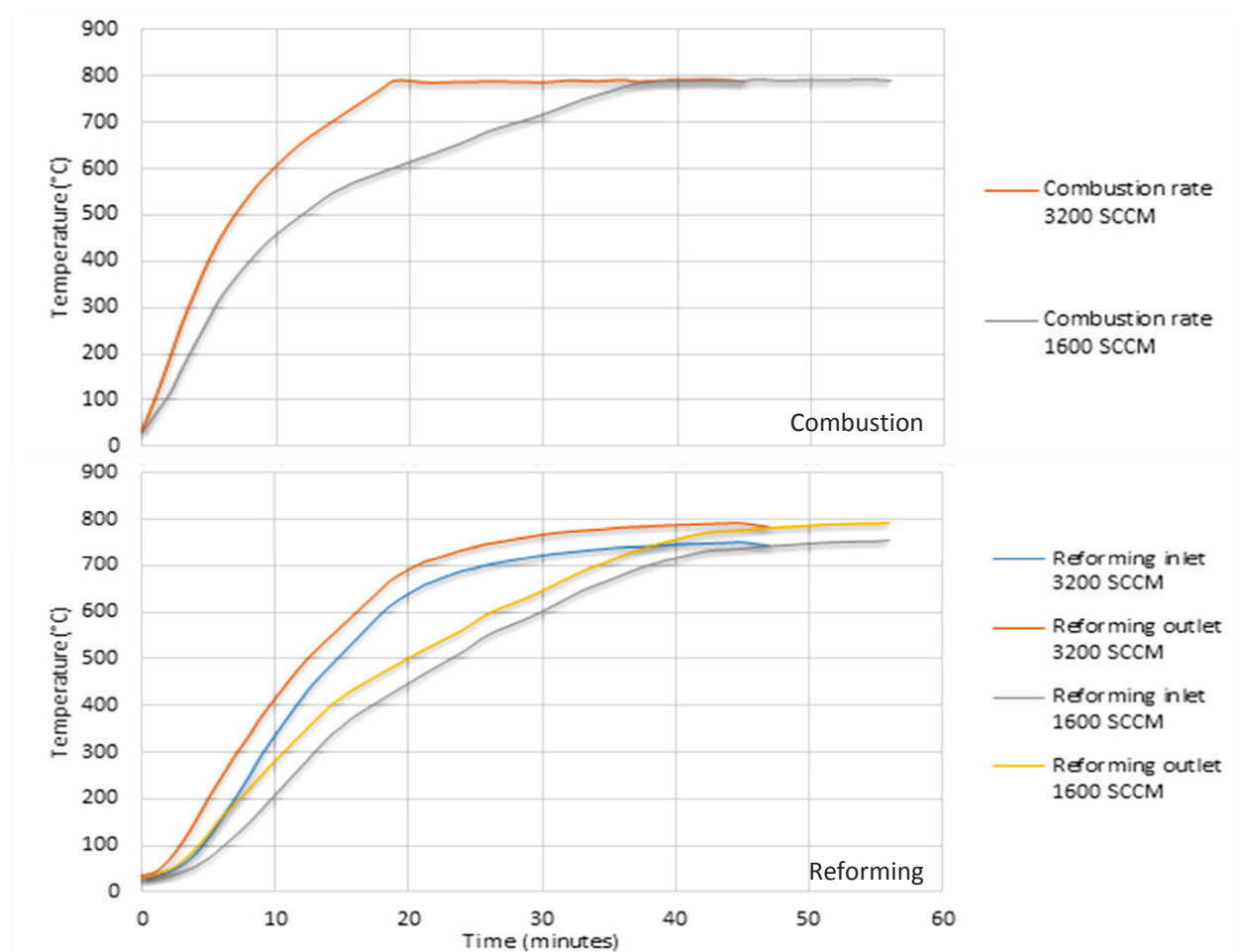
Figure 5-1 Startup times required for combustion and reforming to reach setpoint temperature of 800°C at the two designated combustion flow rates.
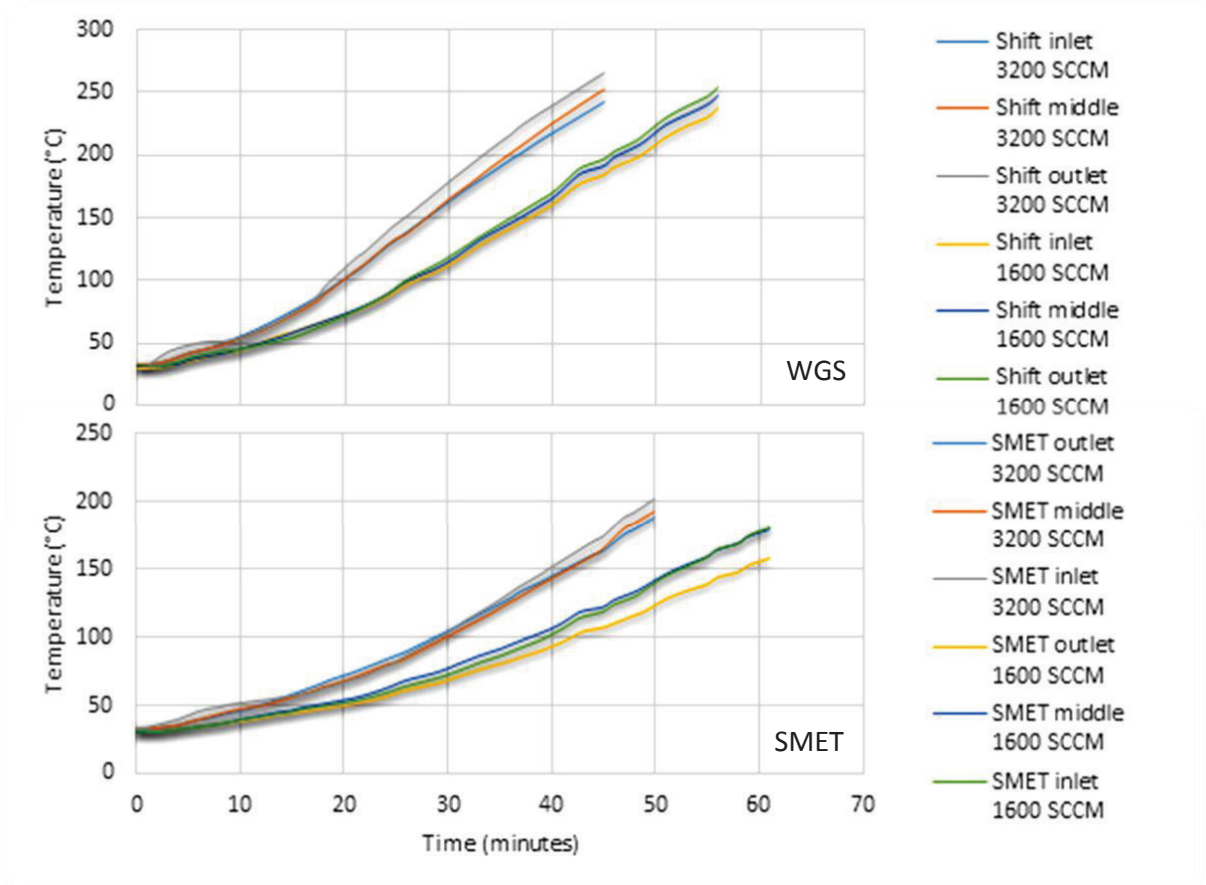
Figure 5-2 Startup times required for WGS and SMET to reach reaction temperatures at the two designated combustion flow rates.

It must be noted that for this start up test a combustion temperature of 800°C was chosen as it is one of the chosen reaction temperatures. A constant air/fuel ratio was used for both combustion flowrates by means of digital control of the air blower setpoint via the operating PLC. Initial startup tests was performed without the logging function inside the PLC as this was still under development.

5.1.2 From standby

Startup from standby is described in section 4.3.2 using a combustion temperature setpoint of 350°C as prescribed by the supplier. The corresponding temperature profiles attained during this stage is given by figure 5.3 which shows the system temperatures for all reactor stages using two combustion flowrates.
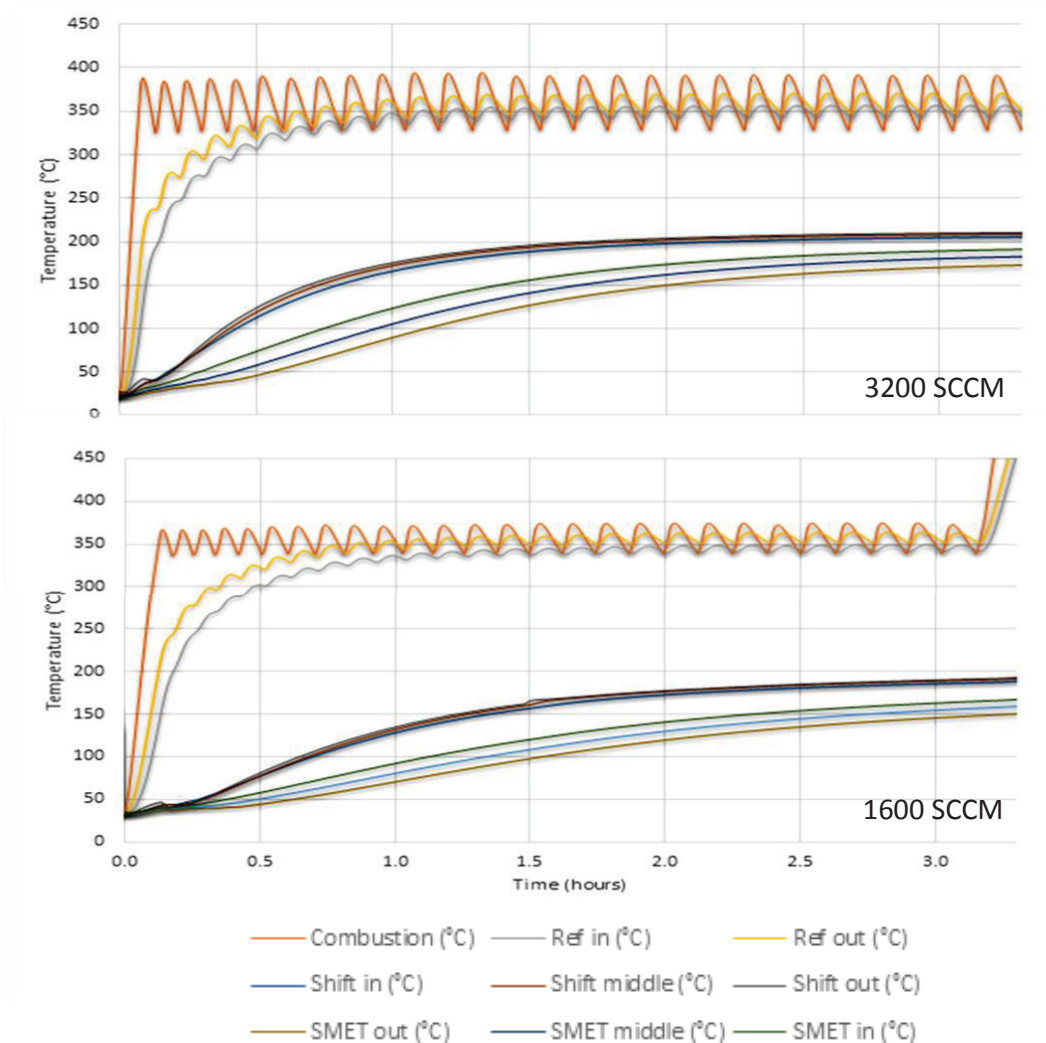
Figure 5-3 Standby temperature profile at i) 3200 ii) 1600 SCCM.

From figure 5.3 it can be seen that during standby the temperatures in both the WGS and SMET stages slowly increase until the reaction temperatures of 190 and 160°C are reached during this standby phase. Combustion and reforming quickly reaches the setpoint and thereafter oscillates around this setpoint.

These standby startup tests have been undertaken with the logging function of the PLC allowing for logging of data every 5 seconds. This demonstrates the cyclic nature of the control system occurring in the combustion chamber. The temperature can be seen to increase and decrease periodically around the chosen setpoint as the system opens and closes the fuel solenoid valve. Furthermore, this has a cascading effect on the temperature inside the reforming stage due to its physical proximity to the combustion chamber.

It must be noted, however, that there is a minimum time period required for standby as it takes roughly one and a half hours to obtain the necessary WGS and SMET temperatures using a combustion rate of 3200 SCCM as shown in figure 5.3. That time period is doubled to about

three hours for the lower combustion rate. During this phase the amount of fuel being consumed is a lot lower than during normal operation at reaction temperatures, as much less energy is required to heat up the system at 350°C than at 800°C.
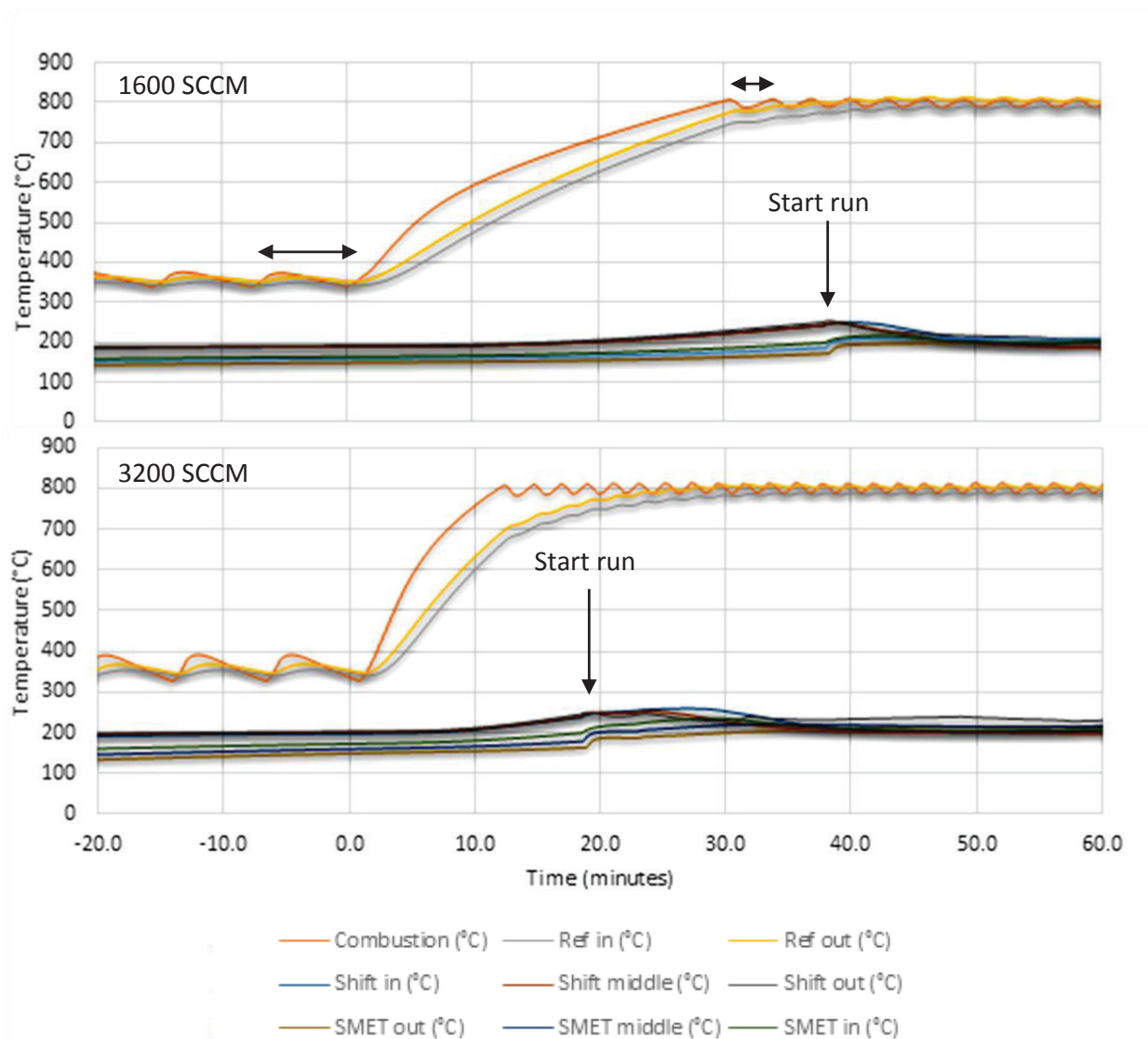
Figure 5-4 Startup temperature profile from standby using a combustion rate of i) 1600 SCCM and ii) 3200 SCCM.

From figure 5.4 it can be seen that the time needed for startup has decreased from 61 minutes to about 30 minutes at a combustion flowrate 1600 SCCM and decreased from 44 minutes to roughly 12 minutes at a combustion flowrate of 3200 SCCM. This standby function thus allows the user to cut down drastically on overall start time required.

The change in length of the cyclic control can also be seen in figure 5.4. At lower temperatures the average time between fuel valve pulses is longer because the temperature gradient driving force is greater at the higher temperature.

The start point of the run is also shown on figure 5.4. This is the point at which water is introduced into the system and will also be used as time zero for all performance testing.

5.2 Performance testing

Performance testing of the *FLOX Reformer* was undertaken by 6 separate runs. Each run was performed using one combustion temperature and one combustion flowrate. Furthermore, each run consisted of testing at various loads from a lowest load of 600 SCCM methane to the maximum load possible for roughly 1 – 2 hours at each condition. These experiments were performed after the initial startup procedure, i.e. the heating of the combustion chamber, had been concluded and the system allowed to stabilise – the time at which water is pumped into the reformer being designated as the start of the performance test.

The stabilisation phase of roughly an hour in duration allowed the WGS and SMET temperatures to stabilise at the preselected water flowrate, after which time methane is introduced. Methane is initially introduced at a low flowrate of 300 SCCM and the system allowed to restabilise. This initial time period also allows for all nitrogen in the system to be flushed out.

A summary of methane flowrates utilised, and the water flow rates and thus steam-to-carbon (S/C) ratios achieved for the six runs is given in table 5.1 below.

Methane flowrates presented below are the actual flowrates after appropriate calibration, and the water flowrates are the average achieved over a designated time period (determined by weight loss from the water feed pot) at each condition or methane flowrate. The corresponding molar flowrates to calculate the S/C ratio were calculated according to the equations given in the *Data Workup* section (see section 4.5).

From table 5.1 it can be seen that the S/C ratios achieved are very high, especially at lower load settings, whilst at the higher load settings it is in the range of 3.6 – 5.0. These values although high are closer to common S/C ratios used in industry.

For the above mentioned conditions a range of temperatures were obtained for the fuel processor stages as detailed in table 5.2. In the reformer stage temperatures were found to be relatively stable with a steady state stable inlet and outlet temperature being reached shortly after a load change is induced.

Table 5-1 Summary of combustion settings and combustion/reformer flowrates for all experiments.

	Combustion Temperature (°C)	Combustion flowrate (SCCM)	Methane feed flowrate (SCCM)		Water feed flowrate (g/min)	S/C molar basis
RUN 1	750	1600	Load 1 -	624	4.71	9.37
			Load 2 -	1248	7.07	7.04
			Load 3 -	2497	8.84	4.40
			Load 4 -	3932	11.58	3.66
RUN 2	800	1600	Load 1 -	624	6.73	13.39
			Load 2 -	1248	9.70	9.65
			Load 3 -	2497	11.50	5.72
			Load 4 -	3870	14.31	4.59
RUN 3	840	1600	Load 1 -	624	4.90	9.74
			Load 2 -	1248	4.90	4.88
			Load 3 -	1872	7.07	4.69
			Load 4 -	2497	7.88	3.92
RUN 4	750	3200	Load 1 -	624	9.46	18.81
			Load 2 -	1248	10.52	10.47
			Load 3 -	2497	11.38	5.66
			Load 4 -	3745	14.86	4.93
			Load 5 -	4367	13.70	3.89
RUN 5	800	3200	Load 1 -	624	11.65	23.18
			Load 2 -	2497	11.67	11.61
			Load 3 -	2809	16.19	7.16
			Load 4 -	4369	17.57	5.00
RUN 6	840	3200	Load 1 -	624	5.11	10.16
			Load 2 -	1248	6.96	6.93
			Load 3 -	2809	9.05	4.00
			Load 4 -	4369	16.30	4.63

The temperature stability of the combustion and reforming stages are dissimilar to those in the water gas shift and selective methanation stages where relatively large changes in temperatures during methane load and water flow rate changes are observed. These stages also exhibit a delay in the response to these changes – they are not directly contacted but rather are effected by heat generated and consumed in the combustion and reforming stages,

respectively, and by the amount of water fed (and therefore evaporated) to the reforming stage. The approximate temperature ranges for these stages are given in table 5.2.

Table 5. 2 is a brief summary of these temperatures obtained and detailed temperature versus time graphs are included in sections 5.2.1 to 5.2.6.

Table 5-2 Summary of reactor stage temperature ranges for all experiments.

RUN	Combustion flowrate (SCCM)	Load	Reforming Temperature (°C)		WGS Temperature (°C)		SMET Temperature (°C)	
			In	Out	In	Out	In	Out
1	1600	1	725	745	220-235	205-217	210-235	190-230
		2	730	735	210-240	220-227	220-240	240-245
		3	700	665	195-198	240-250	207-210	230-235
		4	665	625	193-200	260-270	210-215	225-235
2	1600	1	785	805	190-210	205-210	195-210	195-210
		2	780	790	210-235	210-235	220-245	215-250
		3	760	730	195	255-260	208-210	235
		4	725-690	680-640	200-205	265-285	218	230-240
3	1600	1	835	870	197-223	190-210	192-225	192-225
		2	831	860	188-212	210	197-215	227-230
		3	830	855	200-210	215-245	208-220	240-245
		4	810	825	185-190	240-250	199	230-240
4	3200	1	735	750	195-235	218-230	203-223	205-219
		2	730	730	203-214	233-236	208-215	224
		3	708	675	208-218	250-255	207-213	220-225
		4	665	620	208-210	255-275	214-216	228-230
		5	645	608	207-208	255-260	213-215	224-226
5	3200	1	785	803	200-205	231-237	206	218
		2	780	788	203	244	205-210	217-223
		3	750	717	200-206	270-275	210-215	217-223
		4	700	653	206	271	212	222
6	3200	1	822	858	193-217	190-213	184-223	184-223
		2	820	840	188-218	208-230	200-220	217-227
		3	780	770	207-212	240-260	205-218	220-237
		4	760	720	205-215	261-297	212-230	238-264
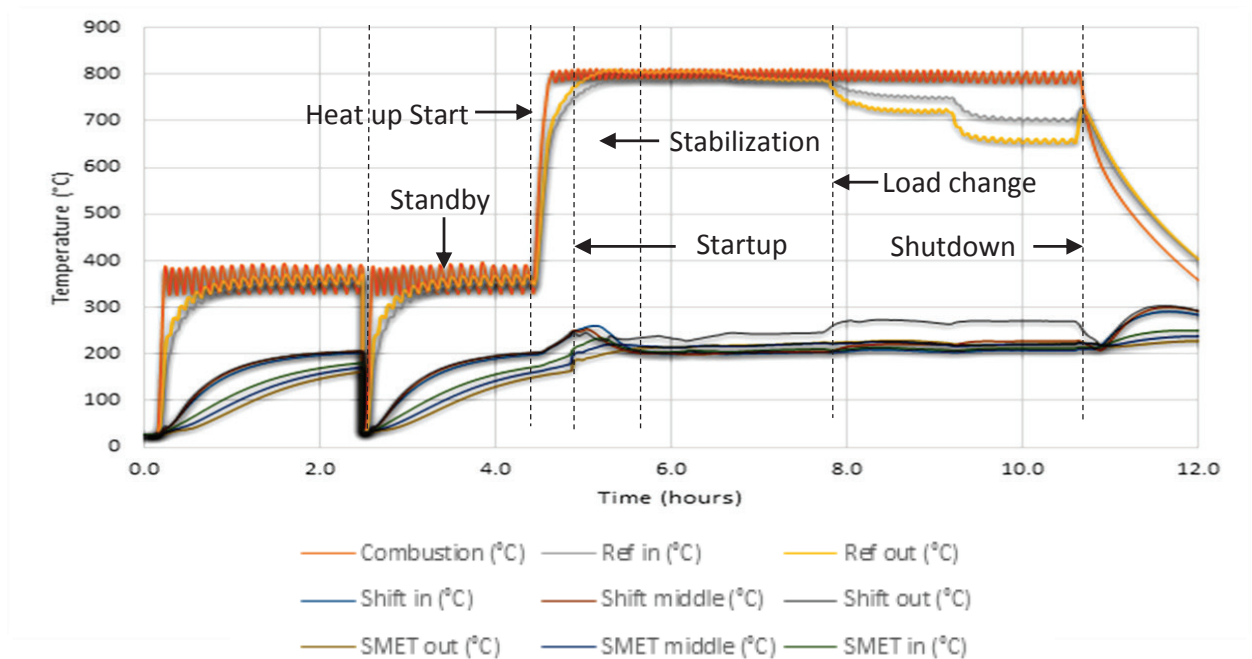
Figure 5-5 Temperature versus time raw data example.

Figure 5.5 shows a typical temperature versus time plot as recorded via the PLC logging system. Time zero is taken as the time at which logging is initiated. The response presented in figure 5.5 shows the various temperatures achieved when the *FLOX Reformer* is taken to standby (at 350°C), followed by a system stop, after which the system is restarted and heated to standby for approximately 2 hours until steady state is re-achieved, and then the system is started by increasing the temperature to 800°C (as an example of appropriate combustion temperature for reforming).

This is followed by performance testing at various load conditions and which shows temperatures changes in the different stages. Once all loads have been tested the system is shut down, signified by a drop in the reforming and combustion temperature, whilst the WGS and SMET temperatures increase for a short period once the water supply is cut off.

Figure 5.6 shows the raw data for the same run as presented in figure 5.5 but as obtained on the flue gas analysis versus time. The concentrations of hydrogen and carbon dioxide is seen to rise during the stabilisation period as methane is introduced into the system. After approximately one hour the concentrations are seen to stabilise as steady state is achieved. During this period the load is cycled and both WGS and SMET analysis is performed during shorter intervals until the system is shut down and the concentrations are seen to decrease.

Both WGS and SMET outlet concentrations are given on the same graph and is manually separated during data workup.
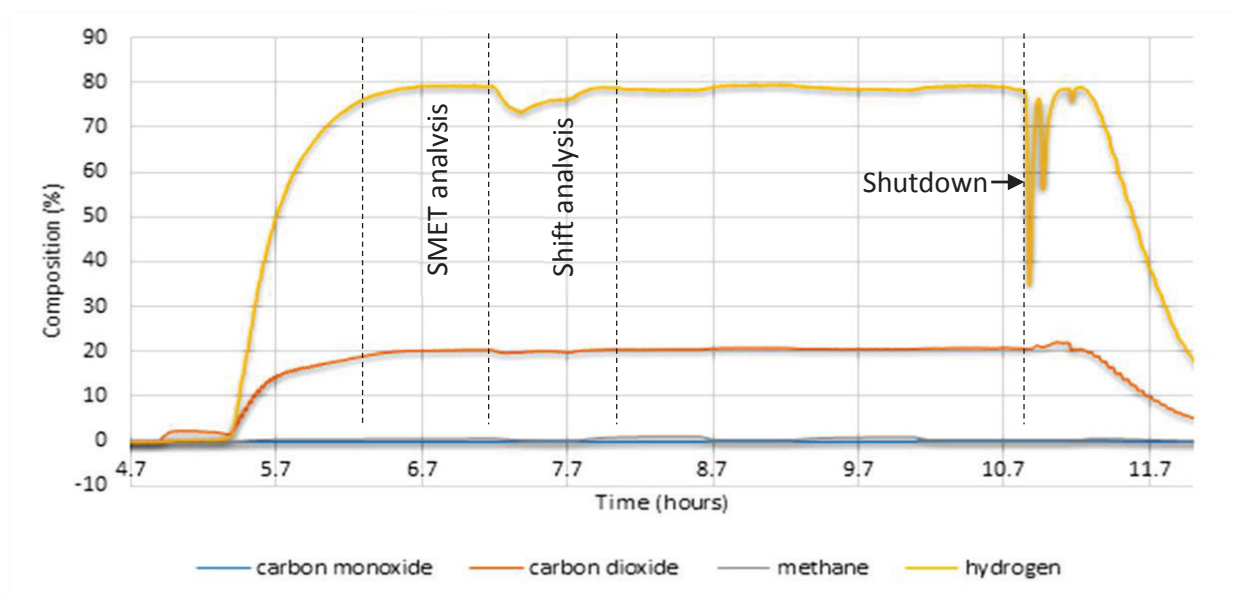
Figure 5-6 Flue gas readouts versus time raw data example.

Appendix D contains all raw fluegas and temperature graphs as recorded via the PLC.

All microGC results are given in Appendix C.

5.2.1 Run 1
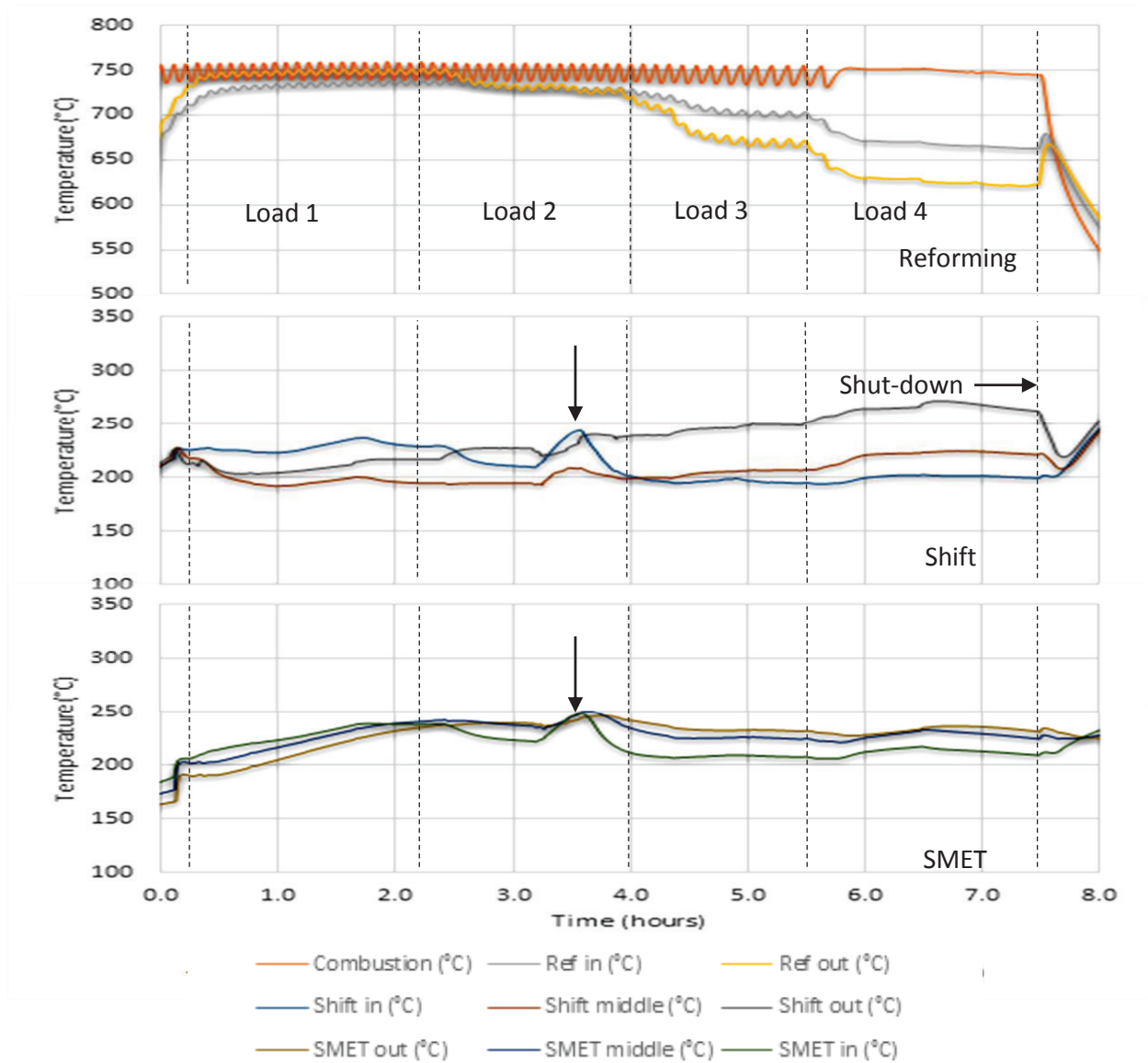
Figure 5-7 Temperature in the various *FLOX Reformer* stages under various load conditions for run 1.

Temperature in the various *FLOX Reformer* stages over time under various load conditions is given in figure 5.7 for run 1. Run 1 utilises a combustion flowrate of 1600 SCCM and temperature of 750°C as shown in table 5.1.

The cyclic nature of the combustion temperature is shown throughout but the time between temperature cycles is seen to slightly increase from load 1 to load 3. At the highest load the combustion temperature is seen to even out completely since at this this heating requirement

the valve stays continuously open allowing the maximum methane combustion flowrate possible.

Changes in the reforming inlet and outlet temperatures are also seen. The reforming outlet is initially higher than the inlet at load 1 and is seen to be approximately 750°C. At higher loads the outlet is seen to decrease dramatically compared to the inlet due to the higher extent of heat of reaction occurring which for reforming is highly endothermic. These temperatures are seen to even out at well below 700°C.

The temperatures inside the WGS and SMET stages are seen to vary quite substantially throughout the run as they are quite sensitive to load and water flowrate changes in the system. The overall trend shows the inlet temperature to be higher at low loads but the outlet temperatures increase dramatically as the load is increased, once again due to the exothermic nature of the reaction. This is especially noticeable at load 4 where an inlet–outlet change of 70°C is noticeable in the shift stage.

A temperature spike is seen in both the WGS and SMET stages after approximately 3.5 hours due to a drop in the water flowrate which may have been caused, although never confirmed, by the water pump not supplying water at a constant flowrate.

Figure 5.8 shows the WGS outlet composition achieved for run 1 as measured by flue gas and microGC analysis. Both analytical techniques show consistent results with hydrogen (in the dry product stream) in the range of 75 - 80% and carbon dioxide at approximately 20%. These compositions point to the fact that both the reforming and shift stages have proceeded virtually to thermodynamic equilibrium for all loads.

Methane composition (in the dry product stream) is seen to increase from 0.2% for load 1, to 0.8% for load 4, whilst carbon monoxide concentrations have also increased slightly from 0.1% to 0.3%. Carbon monoxide analysis was only performed via microGC analysis as the relatively high CO levels were outside the measurement range of the flue gas analyser. Both these increases could be linked to the decrease in S/C ratio as shown on figure 5.8.

Figure 5.9 shows the analysis obtained from the outlet of the SMET stage. Both hydrogen and carbon dioxide outlet composition percentages exhibit very slight decreases which are attributed to methanation taking place within the system, with the methane composition increasing to approximately 2% accordingly.

Of most importance is the carbon monoxide outlet concentration which for all loads was found to be 10 ppm (0.001%) or less as required for fuel cell use.
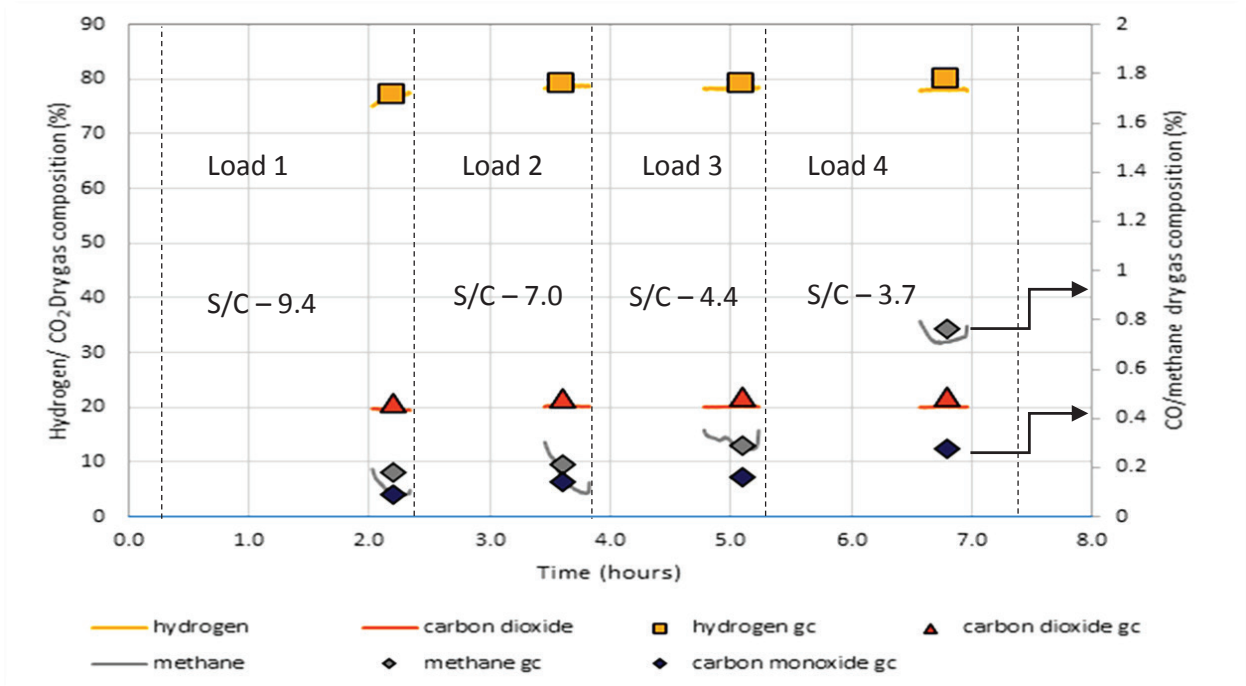
Figure 5-8 WGS outlet dry gas composition at various load conditions for run 1.
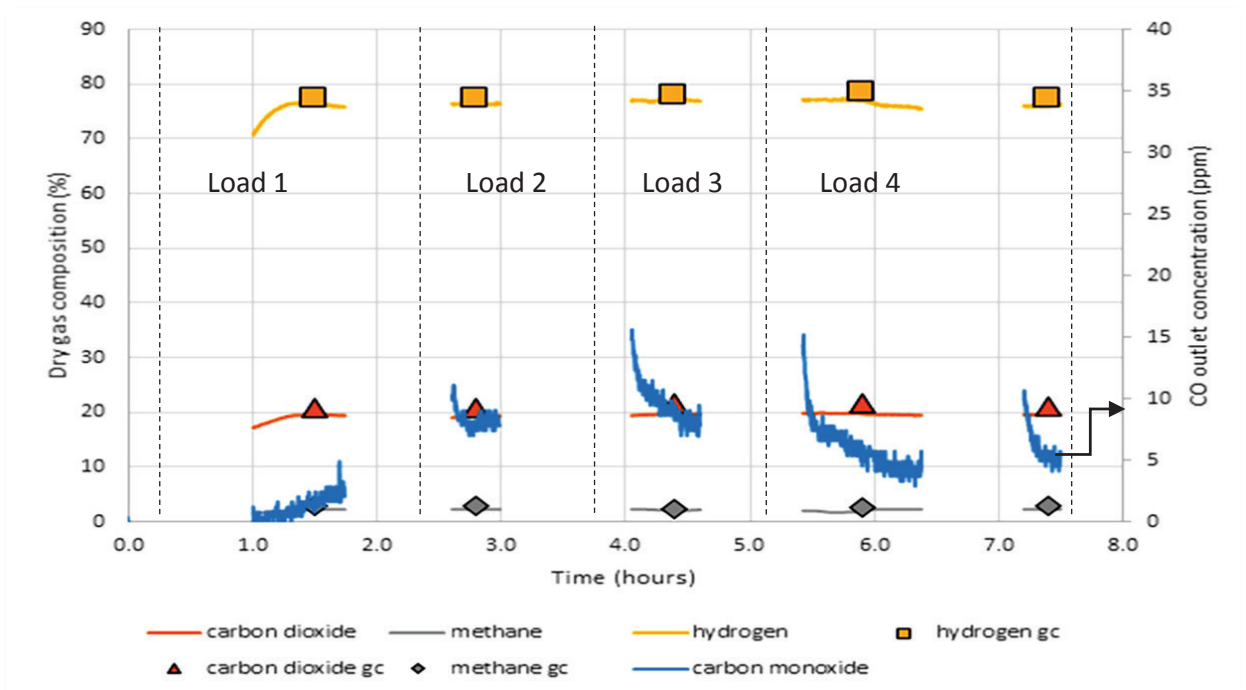
Figure 5-9 SMET outlet dry gas composition at various load conditions for run 1.

5.2.2   Run 2

Figure 5.10 shows the temperature in the various *FLOX Reformer* stages over time under various load conditions for run 2, which was performed with a combustion flowrate of 1600 SCCM and 800°C combustion temperature.

The combustion temperature exhibits the same behaviour as run 1 with an increase in cycle time as the load is increased until load 4 where the energy demand is too high to control the temperature at the set combustion flowrate. In this case the run was stopped when the temperature fell below 800°C.
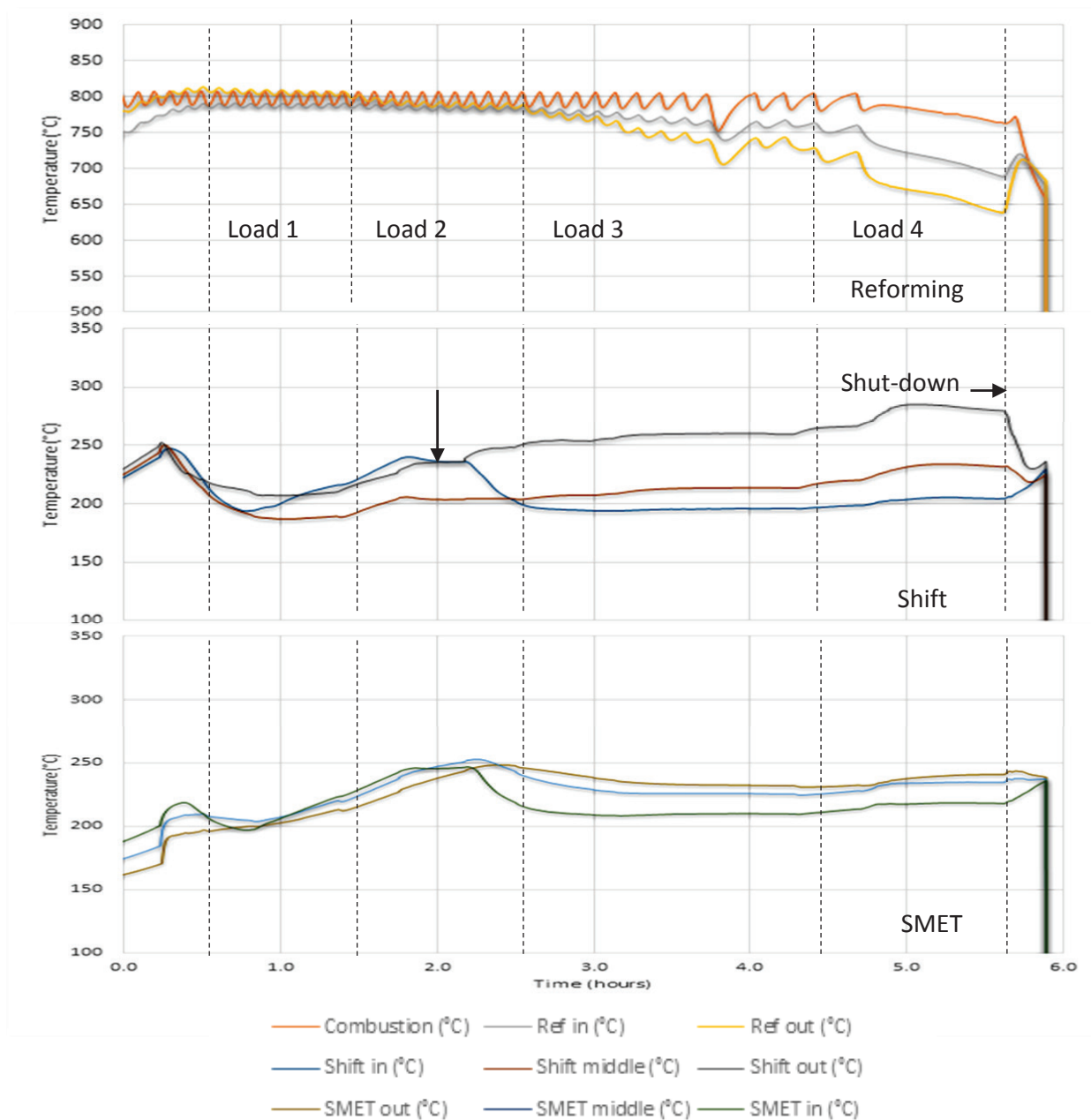
Figure 5-10 Temperature in the various *FLOX Reformer* stages under various load conditions for run 2.

The behaviour in the reforming stage mimics the temperature of combustion but at a slightly lower temperature with the outlet temperature decreasing more compared to the inlet temperature with increasing load.

The WGS and SMET stages are similar to run 1 where, due to the increase in load, a significant temperature increase is found from inlet to outlet, especially in the WGS stage. This change is less pronounced in the SMET stage. For shift, inlet and middle thermocouple readouts are all found to be in the 190 – 210°C range required for optimal shift performance. SMET readout are found to be between 200 – 230°C as in run 1.
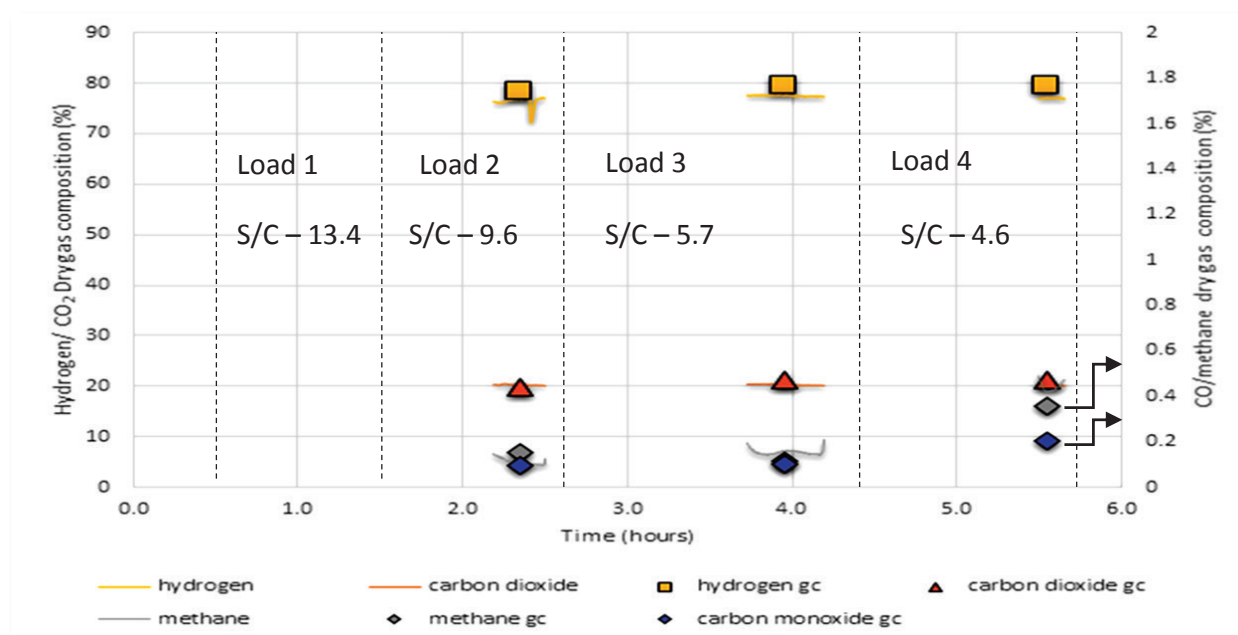
Figure 5-11 WGS outlet dry gas composition at various load conditions for run 2.

Figure 5.11 shows a composition versus time graph of all components in the WGS outlet stream as in run 1 (see figure 5.8), with similar composition observed. Both CO and methane levels is found to be within the range of 0.1 – 0.4% throughout reaching its highest concentrations at the highest load where the steam-to-carbon ratio is also lowest. Methane does not increase as much as for the same load in run 1. This could be attributed to the fact that the corresponding reforming temperatures are much higher than before.

It should be noted that WGS analysis was only performed for loads 2, 3 and 4 for this run.

Figure 5.12 shows the corresponding SMET analysis obtained for run 2. Carbon monoxide concentrations are found, once again, to be less than 10 ppm throughout. All other compound compositions formed through the different stages are given in the figure and closely resembles

results obtained for run 1. The initial increase, after startup, in hydrogen concentration as measured with the flue gas analyser is clearly evident during load 1, and shown in figure 5.12 with an *.
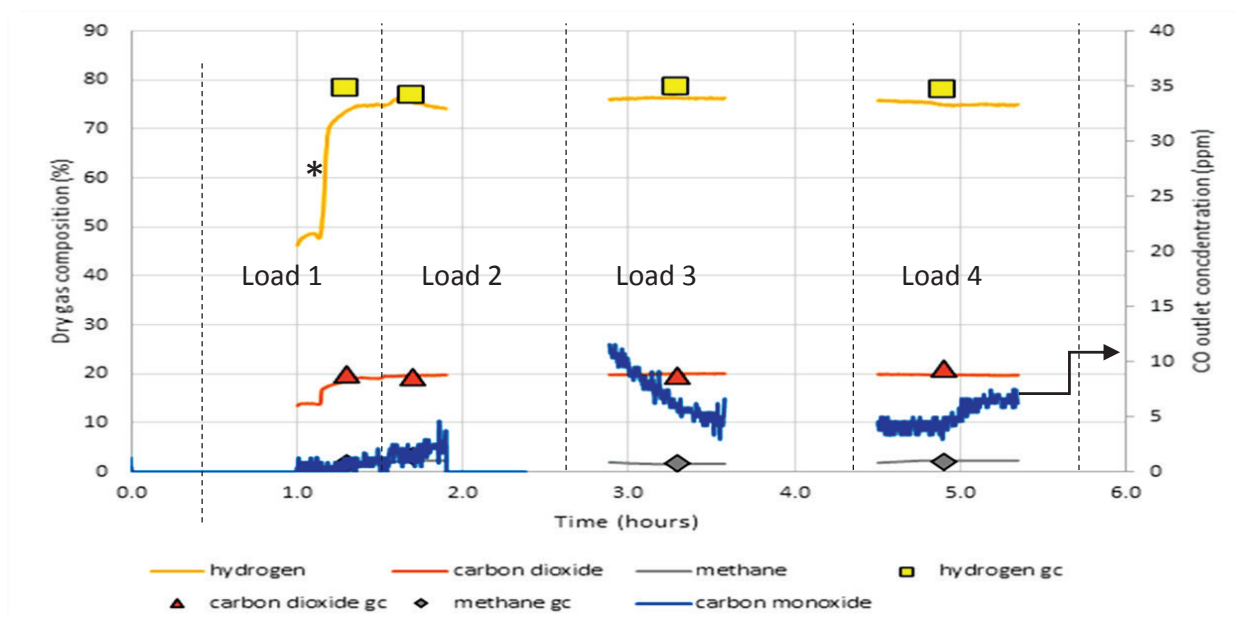
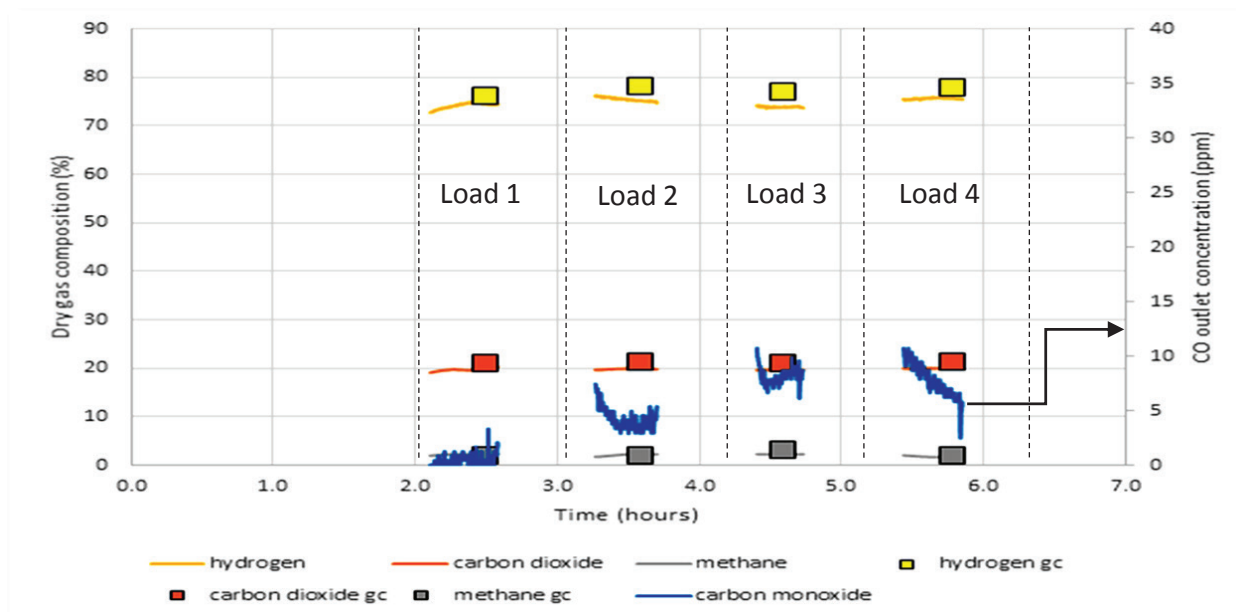**Figure 5-12** SMET outlet dry gas composition at various load conditions for run 2.

5.2.3   Run 3

Run 3 was performed utilising a combustion temperature of 840°C and a combustion flowrate of 1600 SCCM. At this temperature the *FLOX Reformer* operated in FLOX-mode (refer to the Experimental section for clarification. The cyclic control length can be seen to increase with increasing load and at load 3 the control valve switching period is drastically reduced as the combustion rate struggles to handle the increased heat demand. At load 4 the same can be seen with a drop in temperature as the combustion rate is no longer sufficient to cope with the load.

At this FLOX combustion condition it is however interesting to note that there is no significant drop in temperature of the respective reforming stages compared to combustion, as it closely follows the combustion setpoint as shown in figure 5.13.

Even though the total run length was over 6 hours in duration, methane was only introduced as reforming feed after approximately 2 hours, due to the temperature in the shift stage initially being outside of the required temperature range, shown by a # in figure 5.13. Once shift temperatures reached the necessary temperature range the run was started at load 1. The same trend of increase in WGS and SMET outlet temperatures is again observed.

It should be noted that the highest load tested using this combustion temperature was only approximately 2400 SCCM compared to 3600 SCCM for non FLOX combustion.
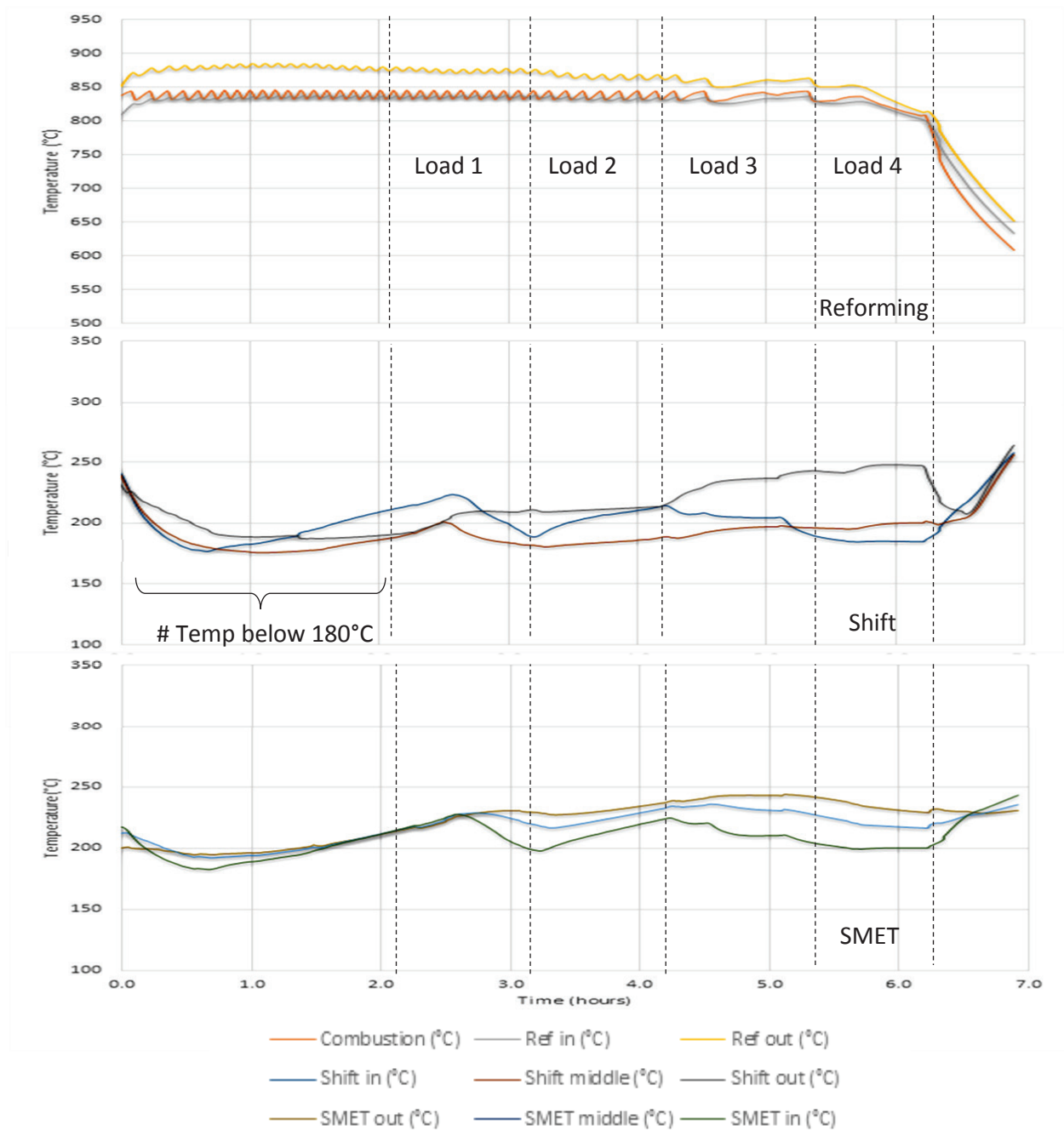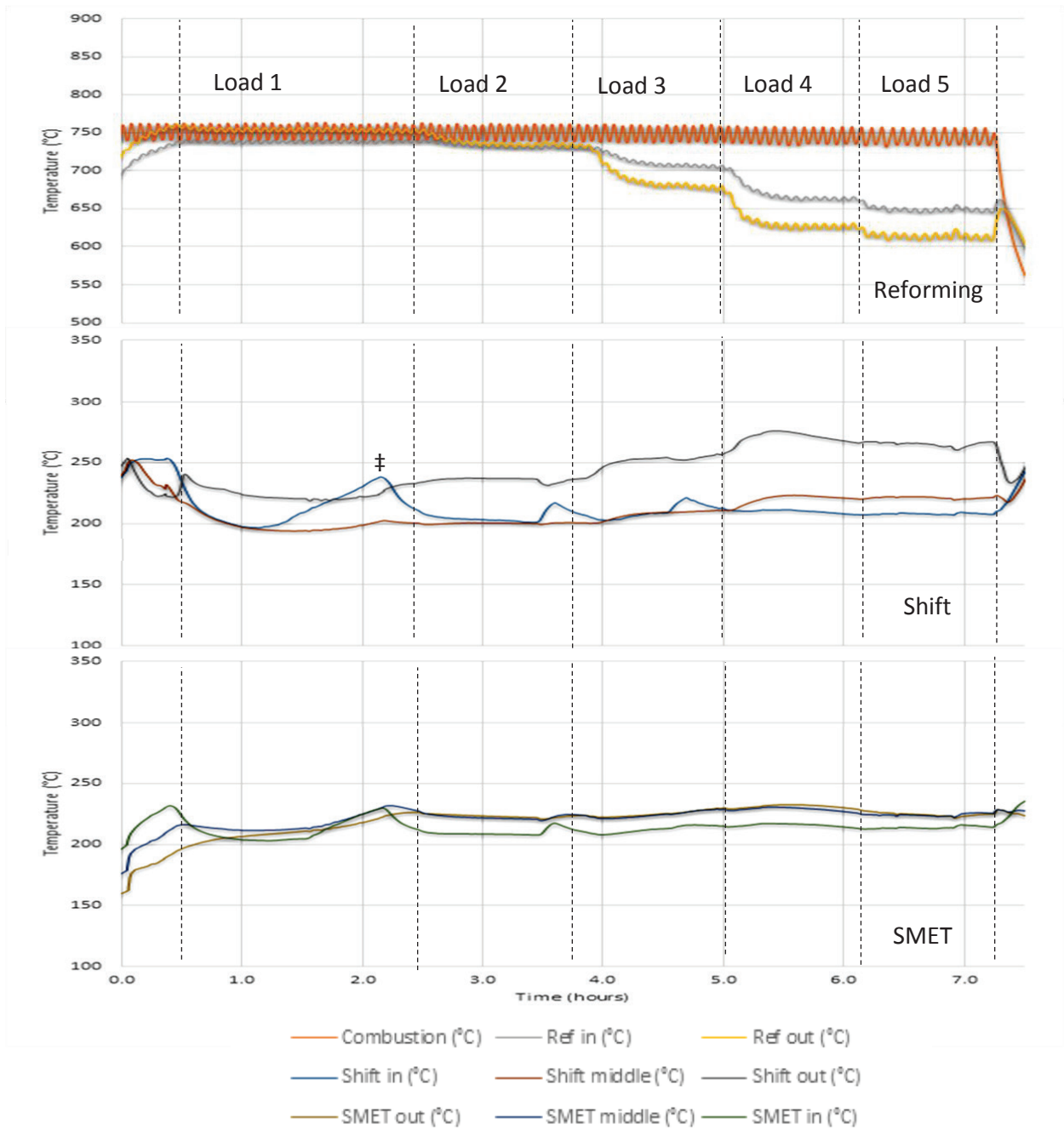

Figure 5-13 Temperature in the various *FLOX Reformer* stages under various load conditions for run 3.
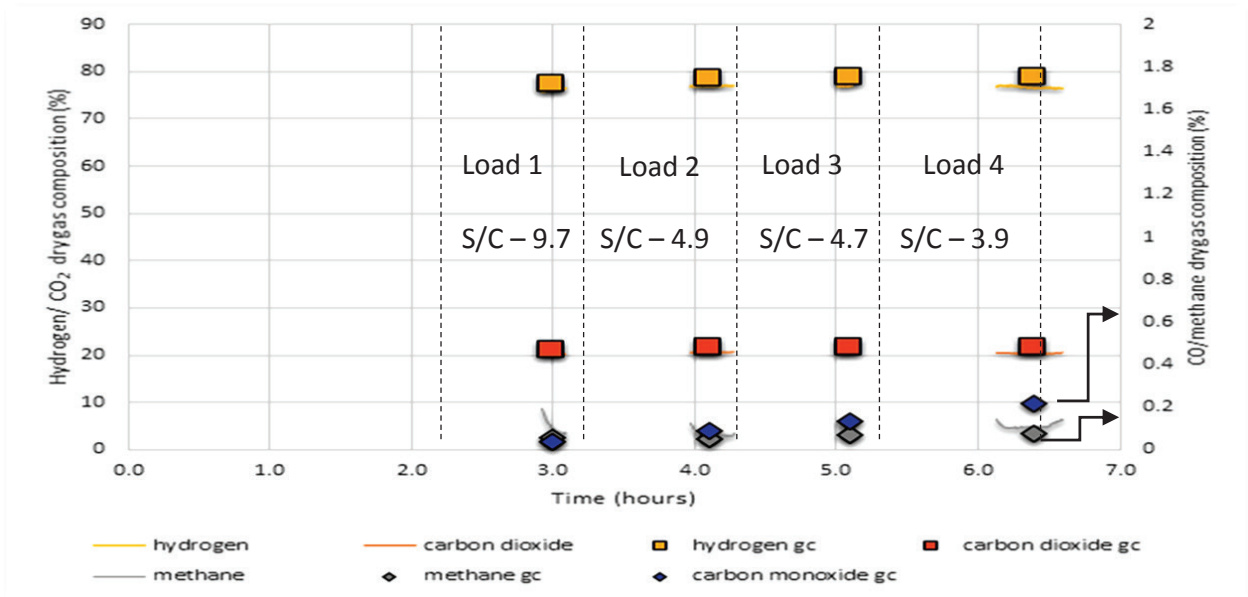
Figure 5-14 WGS outlet dry gas composition at various load conditions for run 3.

Figure 5.14 shows the outlet composition obtained for WGS for all four loads tested as per table 5.1. Hydrogen and carbon dioxide levels remain rather stable with methane and carbon monoxide levels remaining at approximately 0.2% and below in the outlet stream for all the various steam-to-carbon ratios. Carbon monoxide increases marginally with increasing load and decreasing steam-to-carbon ratio, whilst methane remain below 0.1% due to the fact that reforming temperatures are above 800°C.

The SMET product analysis shows a relatively constant outlet composition for all components, with carbon monoxide levels peaking at around 10 ppm.
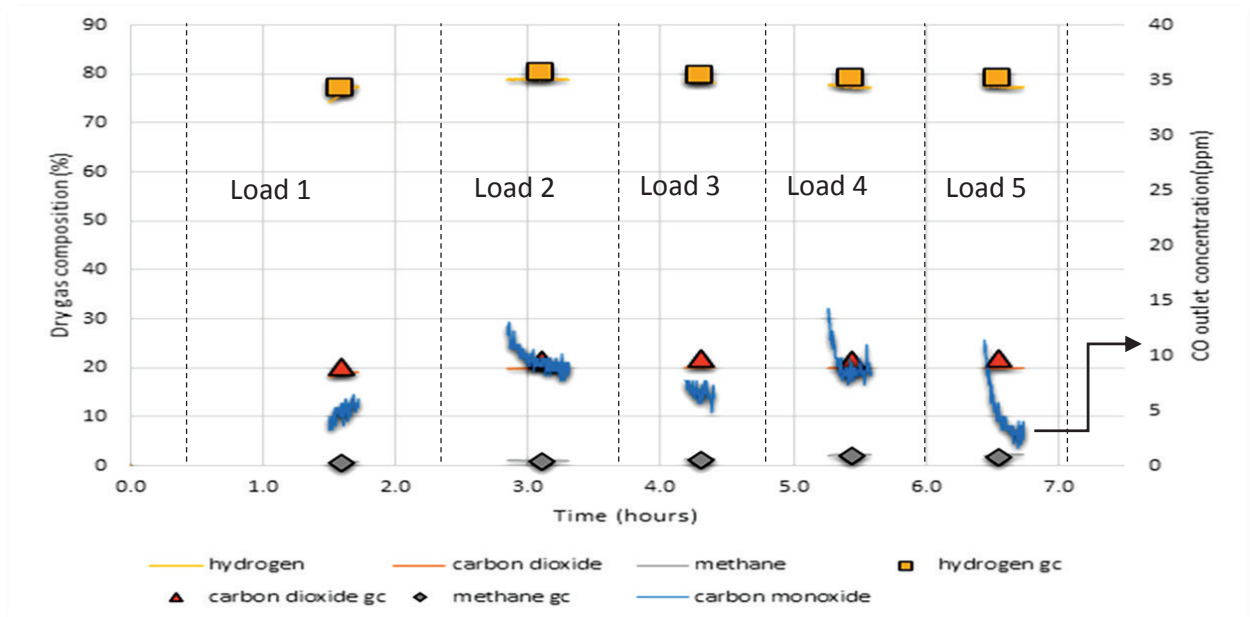
Figure 5-15 SMET outlet dry gas composition at various load conditions for run 3.

5.2.4 Run 4

Run 4 was performed with a combustion flowrate of 3200 SCCM as opposed to the first three runs which were performed at 1600 SCCM. Results for a combustion temperature of 750°C is shown in figure 5.16. Five different loads were tested at this combustion temperature and combustion flowrate condition, as opposed to four for all other runs.

It is clearly evident that the temperature control cycle of the combustion temperature is more rapid at the increased combustion flowrate. The reforming temperature mimics run 1 which was also performed at this temperature and shows a more pronounced temperature drop in the reforming outlet temperature as opposed to the inlet temperature previously observed.

Similar trends as previously noted are observed in the WGS and SMET stages, but overall was remarkably stable apart from a temperature spike at 2 hours caused by a drop in the water flowrate, shown as ‡ in figure 5.16.
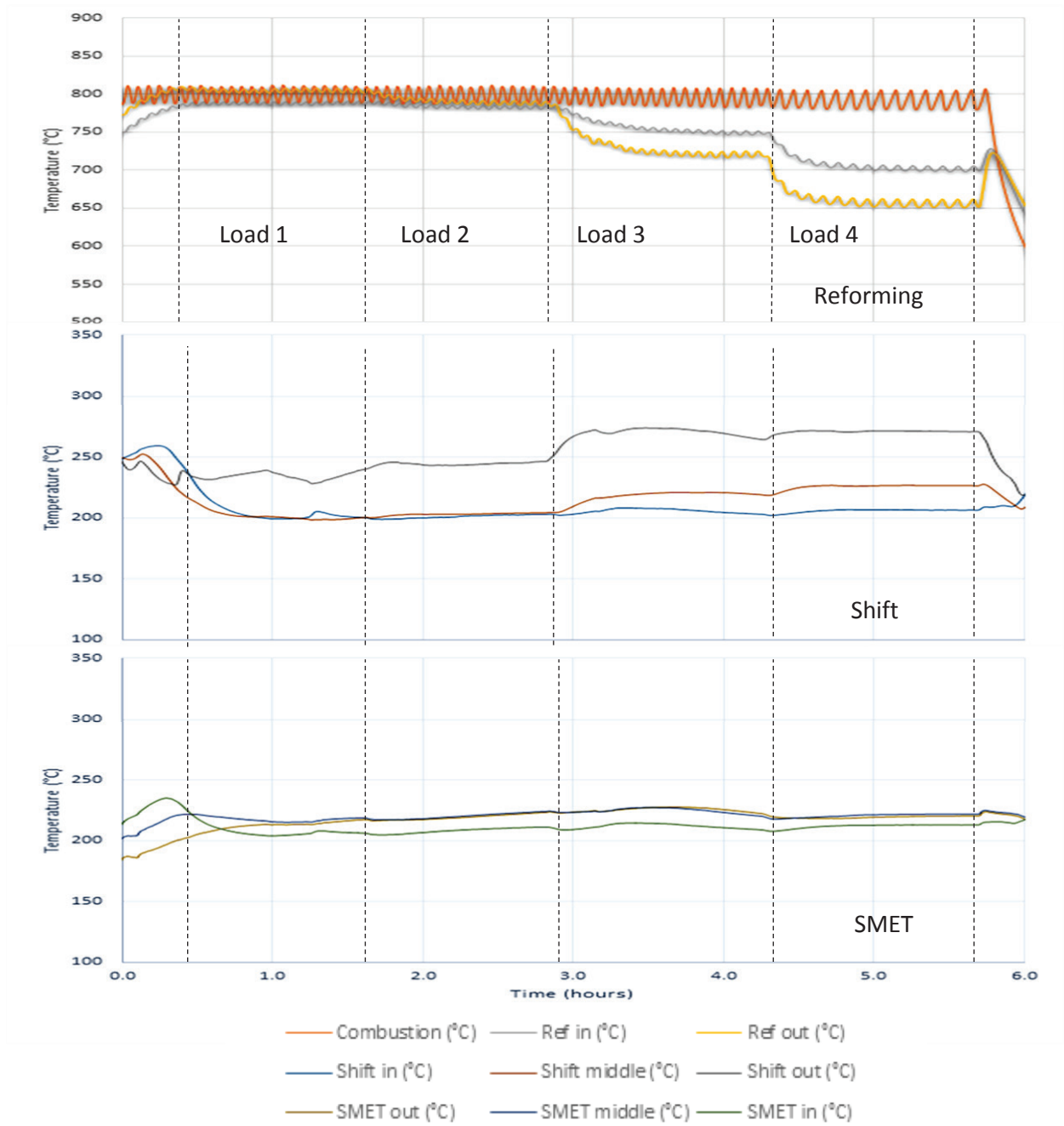
Figure 5-16 Temperature in the various *FLOX Reformer* stages under various load conditions for run 4.
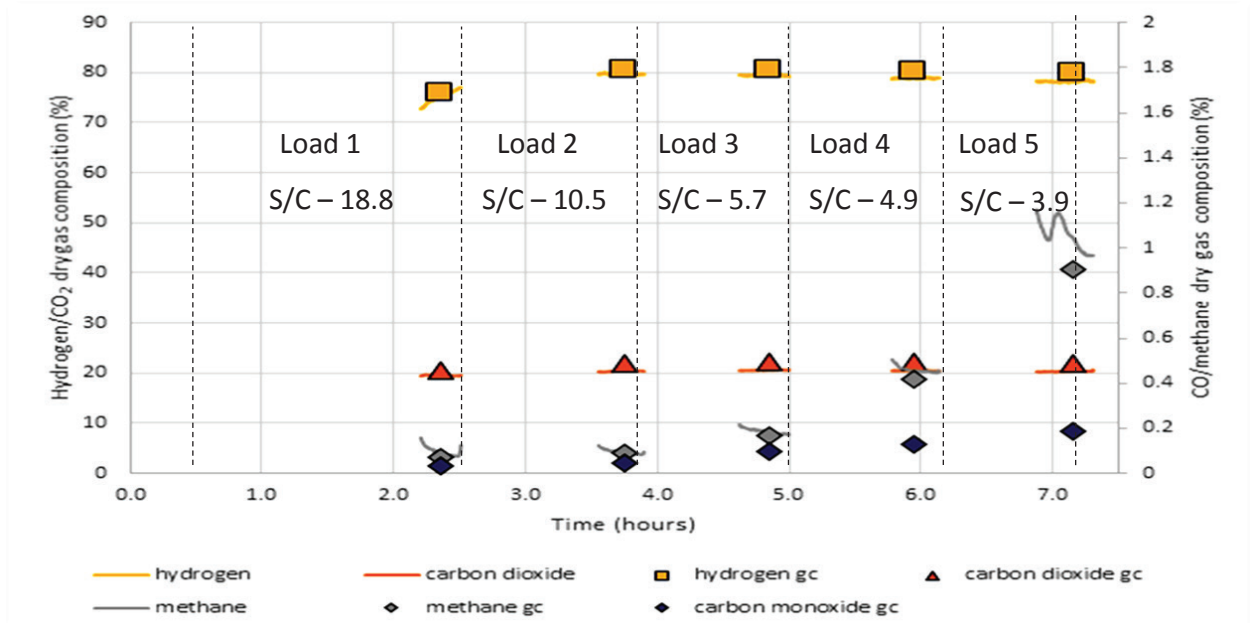
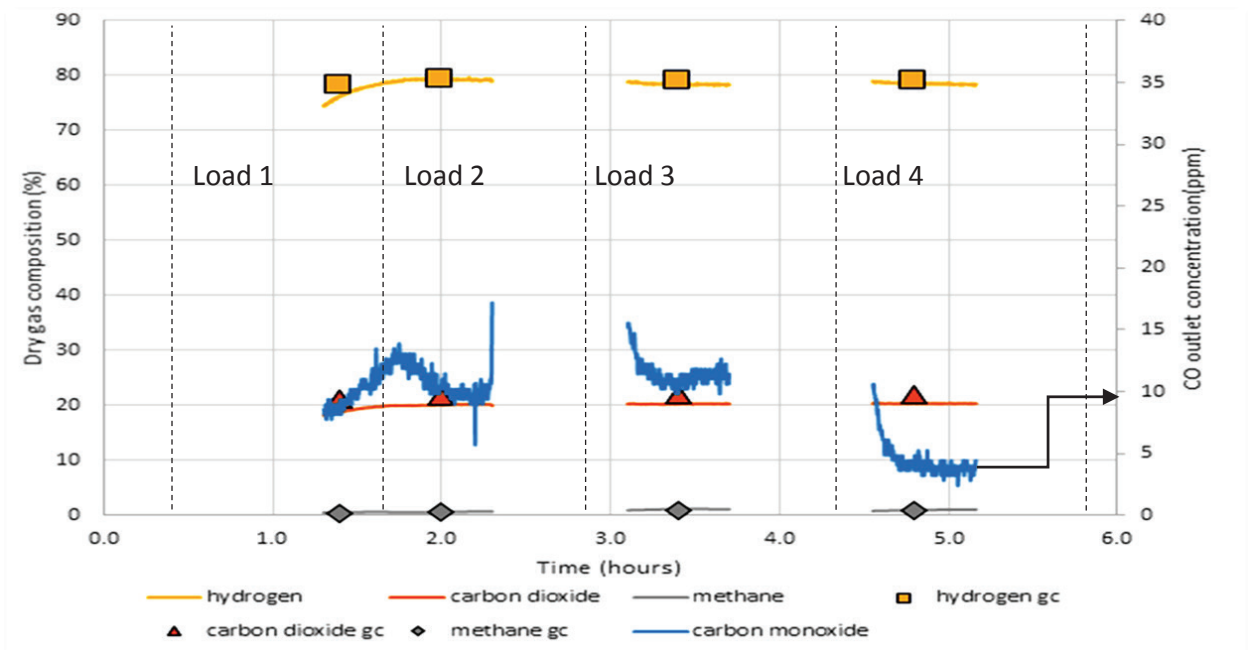**Figure 5-17** WGS outlet dry gas composition at various load conditions for run 4.

From the WGS analysis it can be seen that the methane and carbon monoxide levels increase with increasing load and decrease in steam-to-carbon ratio as previously noted. The methane level spikes to approximately 1% for the highest load as the temperature in the reforming stage is well below 700°C. Carbon monoxide levels, although slightly increasing with increasing load, remains within the 0.1 – 0.3% WGS outlet range.

Carbon dioxide and hydrogen levels remain very similar although a dip can be noted in load 1, compared to the rest as seen in figure 5.17. From figure 5.18 the corresponding SMET analysis for run 4 can be seen showing carbon monoxide levels at a maximum of 10 ppm, but at times even lower than 5 ppm.

Figure 5-18 SMET outlet dry gas composition at various load conditions for run 4.

5.2.5 Run 5

Run 5 was performed with a 3200 SCCM combustion flowrate and at 800°C combustion temperature. All temperature versus time graphs are given in figure 5.19, showing the reforming, WGS and SMET sections. Similar trends as those noted before are once again observed with very stable temperatures for reforming, WGS and SMET after an initial temperature stabilisation phase.

It should be noted that at this combustion flowrate the heat input through combustion is high enough to keep the temperature control cycle going even at a load of 4200 SCCM methane as shown in figure 5.19. WGS and SMET thermocouple readouts indicate that these stages are within the range of 190 – 250°C as required for optimal catalytic performance.

From figure 5.20 the WGS analysis shows a constant outlet composition for all loads as the reaction is pushed virtually to thermodynamic equilibrium throughout, with methane and carbon monoxide increasing slightly with load and decreasing steam-to-carbon ratio. For this run only three loads had WGS analyses performed.
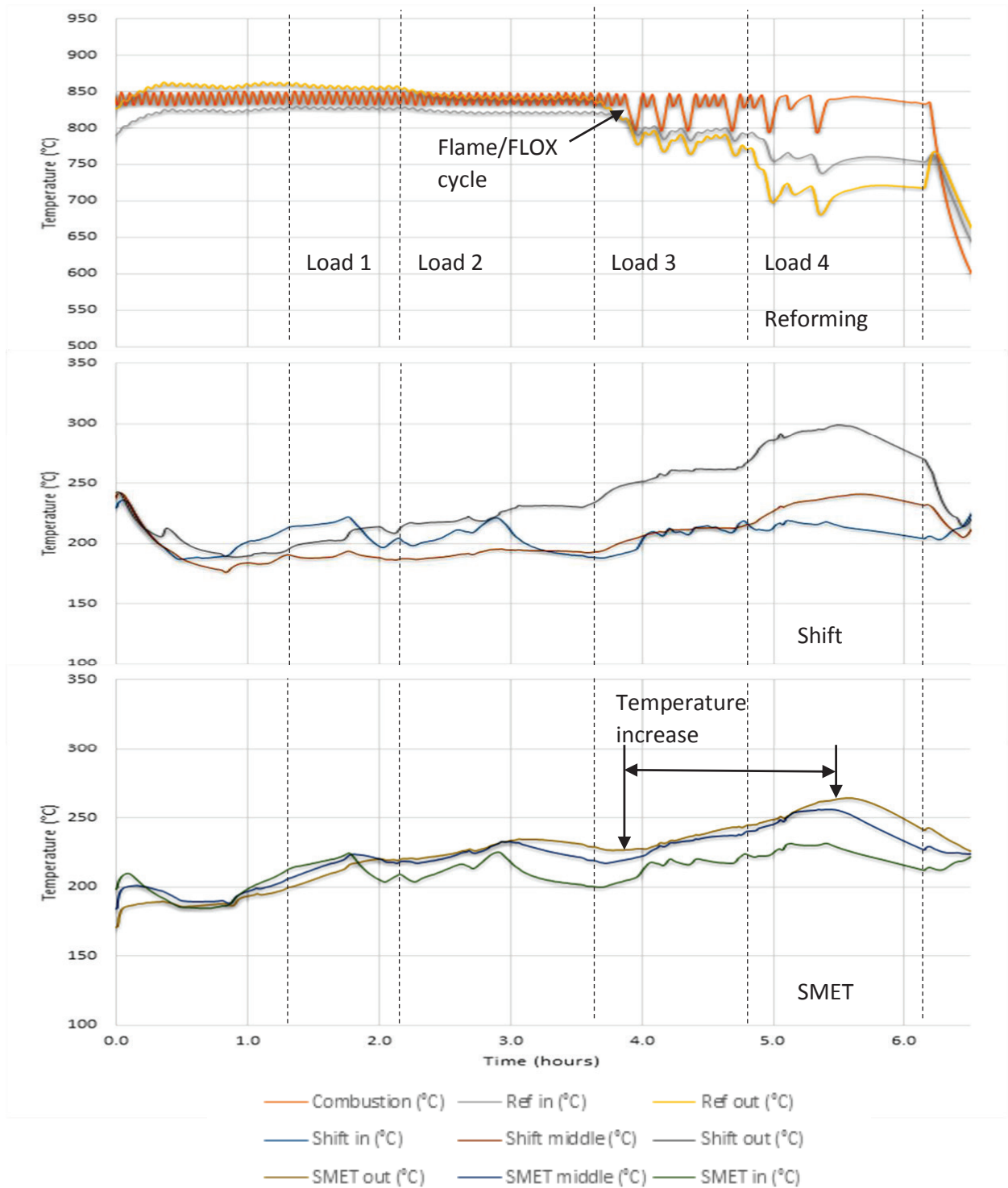
Figure 5-19 Temperature in the various *FLOX Reformer* stages under various load conditions for run 5.
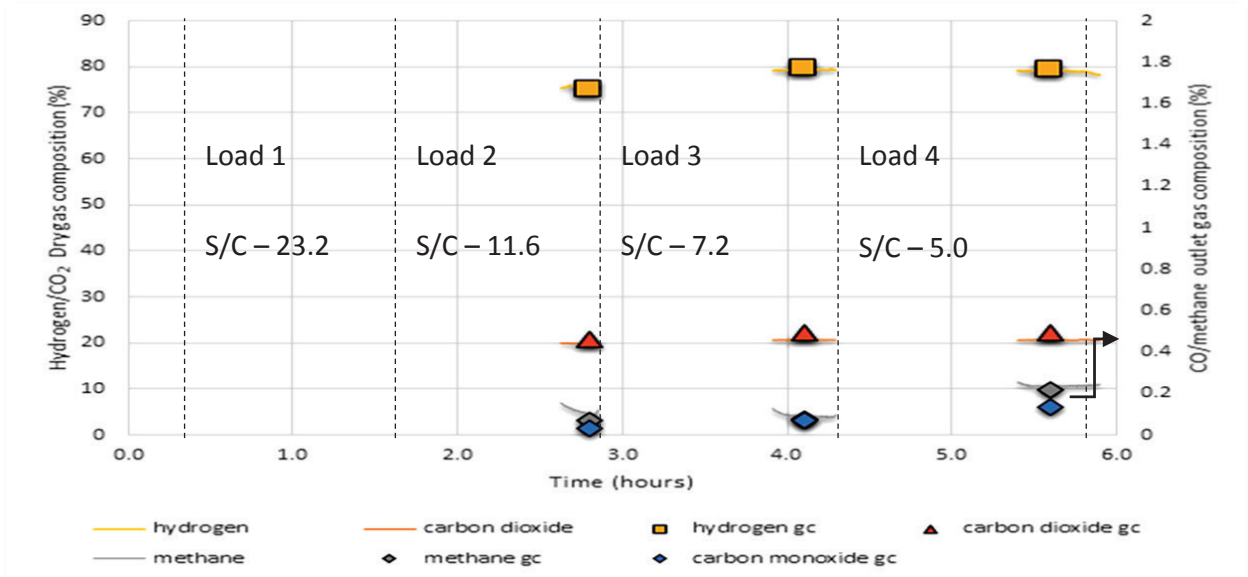
Figure 5-20 WGS outlet dry gas composition at various load conditions for run 5.

Figure 5-21 SMET outlet dry gas composition at various load conditions for run 5.

Figure 5.21 shows the corresponding analysis after the selective methanation stage. As expected methane has increased to approximately 2% whilst the carbon monoxide content has decreased to approximately 10 ppm at lower loads, but as low as 5 ppm for the highest load setting.

A constant SMET analysis was performed throughout a load change from load 1 to load 2. Vary little change is seen in the concentrations of the major components except for a slight CO spike leading to about 15 ppm in this changeover period.

5.2.6 Run 6

Run 6 was performed with the same higher combustion flowrate and utilising a combustion temperature setpoint of 840°C. This was again achieved via FLOX combustion. At load 3 and 4 it can be seen that the combustion temperature fluctuates substantially as it struggles to cope with the heat demand of the system. When the combustion temperature drops below the 810°C threshold the system automatically switches to flame combustion mode from FLOX combustion mode, and vice versa. This is repeated until eventually the system evens out at a constant flowrate and temperature using FLOX combustion.

At lower loads the reforming temperature can be seen to mimic the combustion temperature, however as the system varies between flame- and FLOX-mode the reforming temperature drops and exhibits a similar behaviour as flame-mode observed for previous runs.

Temperatures in the WGS and SMET stages remain relatively stable until this occurrence of flame/FLOX cycling during which the temperature increases noticeably for SMET and exceeds the upper limit of 250°C suggested by the manufacturer. Once the cycling stops the system is able to achieve a stable reforming operating temperature, as shown in figure 5.22, and the SMET temperature decreases again to within acceptable limits. The same behaviour is noticeable in the WGS stage, although not as pronounced.

Figure 5-22 Temperature in the various *FLOX Reformer* stages under various load conditions for run 6.
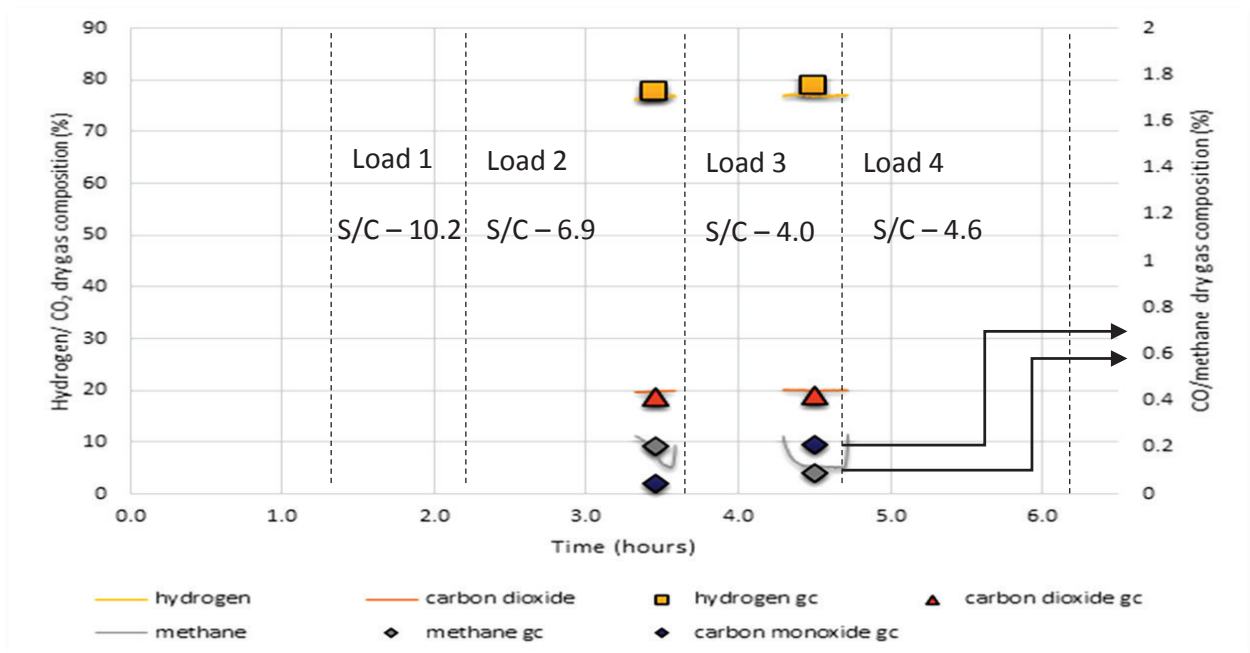
Figure 5-23 WGS outlet dry gas composition at various load conditions for run 6.

From figure 5.23 it can be seen that WGS analysis was only performed for two loads. At these loads the methane content is below 0.2% as the temperature for reforming is above 700°C. From load 2 to load 3 the carbon monoxide content increases due to the decrease in steam-to-carbon ratio from 6.9 to 4.0.

From the corresponding SMET analysis carbon monoxide content exceeds 20 ppm during the combustion cycling period.
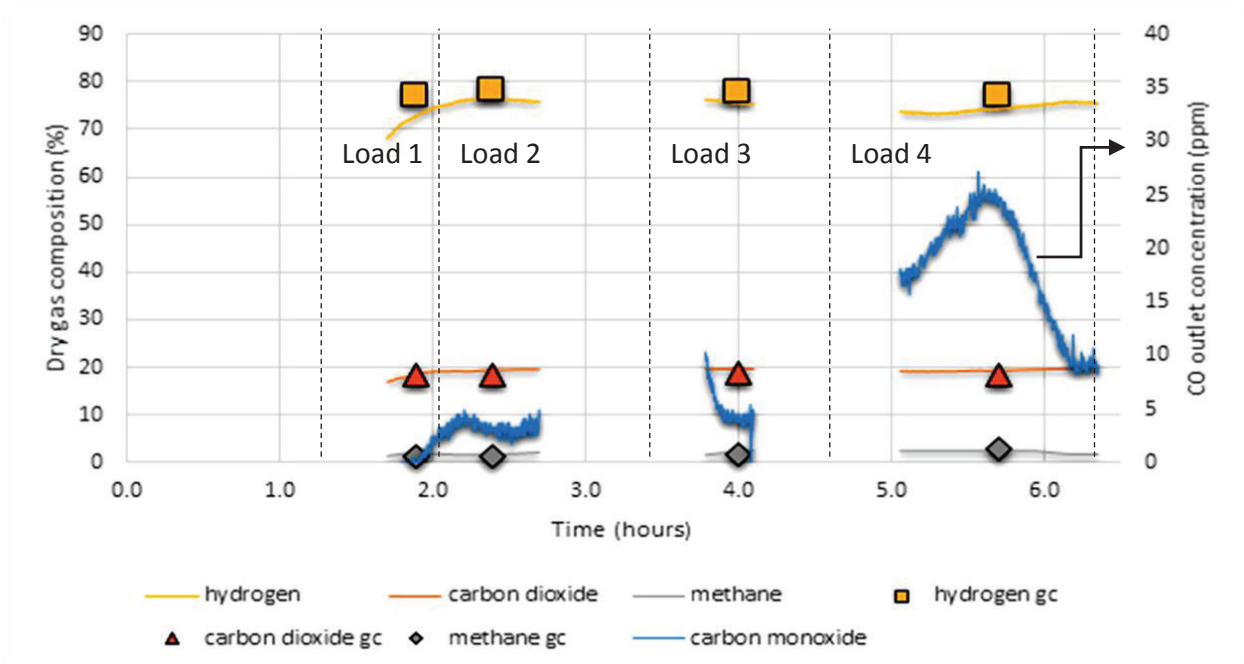
Figure 5-24 SMET outlet dry gas composition at various load conditions for run 6.

5.3 Thermal efficiency of the FLOX Reformer

The thermal efficiency for the *FLOX Reformer* is summarised in table 5.3 below. The efficiency is calculated at the maximum load for all six runs completed. It can be noted that at runs using flame combustion the efficiencies are over 70% and approaches the maximum theoretical efficiency of 80%. Runs performed utilising FLOX combustion are only in the 60 - 65% thermal efficiency range. Methane fuel load for run 4 and 5 is denoted by an asterisk as at these conditions the combustion temperature setpoint was still controlled through opening and closing of the fuel valve.

Table 5-3 the maximum thermal efficiencies of the *FLOX Reformer* operating at various load conditions and combustion temperatures.

Run	Efficiency (%)	Hydrogen flowrate (SCLM)	Methane feed flowrate (SCLM)	Methane fuel flowrate (SCLM)
1	75 – 77%	13.7 – 14.1	3.78	1.6
2	73 – 74%	13.1 – 13.4	3.72	1.6
3	64 – 65%	8.5 – 8.8	2.4	1.6
4	71 – 72%	15.1 – 15.4	4.2	2.13 *
5	73 – 75%	15.9 – 16.2	4.2	2.24 *
6	59 – 62%	14.8 – 15.5	4.2	3.2

6. Discussion

6.1 Startup time

Table 6.1 summarises the times required for startup for both combustion flowrates from cold start and standby conditions. At the set combustion flowrate of 1600 and 3200 SCCM the heat of combustion supplied into the system is on average approximately 1kW and 2kW, respectively.

Table 6-1 Summary of startup tests performed and times achieved.

		1600 SCCM	3200 SCCM
Average combustion flowrate		1600 SCCM	3200 SCCM
Average heat of combustion based on LHV		1 kW	2 kW
From cold start	Time required for combustion	36 minutes	18 minutes
	Time required for reforming	45 minutes	35 minutes
	Time required for WGS (to 190°C)	45 minutes	35 minutes
	Time required for SMET (tom 160°C)	60 minutes	45 minutes
From standby	Time required for combustion	28 minutes	12 minutes
	Time required for reforming	32 minutes	22 minutes
	Time required for WGS	0 minutes	0 minutes
	Time required for SMET	0 minutes	0 minutes
Minimum time to achieve standby conditions		1.8 hours	3.5 hours

At this energy input it takes roughly 60 minutes and 45 minutes respectively to heat up the system from a cold start. This is the time taken for the SMET stage to reach 160°C (the limiting factor) due to its location from the combustion chamber. All other sections heat up according to their position relative to the combustion section heating source and thus quickest to reach their respective reaction temperatures.

The time for combustion is almost exactly halved when the combustion flowrate is doubled. This is as expected as the combustion section is the source of the heat and a doubling of the flowrate should decrease the time required.

The time for reforming, WGS and SMET is also decreased from lowest to highest combustion flowrate, yet not with as much as combustion. These sections heat up through means of heat transfer from the combustion section to the various parts. A doubling of the combustion flowrate does thus not necessarily yield a halving in time for the respective reaction stages, as there are heat losses that can be assumed to take place through the system. These heat losses cause the outside of the *FLOX Reformer* to heat up a bit and it could be argued that an increase in energy input could cause more relative heat losses to occur.

Startup from a standby condition for either flowrate decreases the amount of time for startup significantly, as can be seen in table 6.1. This is due to the fact that the rate temperature of the limiting stages, namely WGS and SMET, have already reached their startup setpoint at standby conditions – the only required time being that for combustion and reforming to reach their required setpoints. The minimum time required to start from standby was also investigated and given in table 6.1 and is the estimated time taken for the SMET stage to reach required temperatures.

During this standby condition the average combustion fuel rate is approximately 500 SCCM and 1000 SCCM, respectively, for the two rates investigated. This is determined by measuring the time of temperature increase relative to the time for temperature decrease of the combustion setpoint to estimate the amount of time the fuel solenoid valve is open.

The startup times achieved could be considered to be on par with other 1 kW reformers available on the market currently, if not better. A similar LPG reformer as made by *Helbio* in 2008 shows an average time required for all reaction stages to reach the desired temperatures at around 80 minutes [30].

Startup times are highly dependent upon the size of the body of the reformer, which for the *FLOX Reformer* is 270 mm diameter and 420 mm height. The thermal mass of the unit therefore negatively affects the startup times achievable. The *FLOX Reformer* does not make use of microchannel or monolith technology in its design as are now more common in recently developed fuel processors – the use of these technologies is reported to decrease startup time well below the capability of the *FLOX Reformer*.

6.2 Reduction of catalysts

This project was started in 2010, but due to unforeseen circumstances was postponed for a number of years and re-initiated again in 2013. The reformer was thus left unused for that time and upon initial project re-instatement performance tests showed less system activity than that

had been previously achieved. It is assumed that allowing the system to be exposed to atmospheric conditions, in particular air/oxygen ingress, allowed re-oxidation of the metallic catalysts to occur, with the associated loss in activity. Water gas shift catalysts, for example, are known to oxidise readily when exposed to air, causing the oxidation from the reduced metallic Cu state to the oxidised CuO state.

Before the re-commencement of the performance testing phase of the project the system was re-reduce under nitrogen. Thereafter, the system was found to exhibit similar activity as was previously observed, and similar to the activity prescribed by *WS*.

6.3 Temperature profiles and control

6.3.1 Combustion

Temperature control of the system is maintained by the setting of a combustion temperature setpoint at which point the temperature control, as described previously, takes place through the cycling of the fuel solenoid valve. Throughout all six runs this cycling is clearly visible and affected by a number of factors. An increase in the combustion flowrate affects the temperature control by decreasing the time the fuel valve is required to be open as more energy is emitted per unit time with the subsequent quicker temperature increase. Furthermore, an increase in the combustion temperature setpoint also affects this control as more time is required to increase the temperature to the point at which the valve closes again. This is due to the fact that more energy is required to heat up a system at elevated temperatures than at lower or room temperatures. This is particularly evident during startup by the shape of the combustion temperature curve which increases rapidly initially, but slows down as the temperature increases.

A major factor affecting temperature control is the reforming load or combined methane and water flowrate into the system. Energy is required to keep methane and water at elevated temperature and an increase in flowrates of these feed components require an increased combustion energy output. Furthermore, the reforming reaction is endothermic and requires heat input to retain the elevated temperatures of the reaction system, again with an increase in the flowrate leading to higher energy demand. This is noted throughout the runs and the cycling can be seen to slow down or even stop completely at high loads as the combustion energy input is equalled, or even surpassed, by the energy requirements of the system.

FLOX combustion also affects this control; this can be observed by the fact that less load brings about a change in the cycling control compared to flame combustion. At a load of approximately 2400 SCCM the system shows the same behaviour as flame combustion at

3600 SCCM, where the energy input and requirements are balanced with no cycling of the fuel valve and a steady combustion temperature.

It can thus be postulated that with FLOX combustion not all the methane is auto-ignited, whereas all or most of the methane is burnt during flame combustion at a specific methane and air flowrate. The conversion of methane during combustion is speculated to be lower using FLOX combustion although this is not verified as no analysis was performed on the combustion chamber outlet.

For run 4 and run 5 at maximum load the system still exhibited the temperature control strategy designed by WS. Although these limits could have been extended to even higher loads than investigated in this study, the hydrogen production was already more than that required for an equivalent 1 kW fuel cell, and therefore no further tests were performed.

During run 6 the combustion temperature exhibited cycling between flame and FLOX combustion as can be seen in figure 5.22. During this period the energy from combustion was seen to struggle to control the necessary temperature setpoint and was repeatedly pushed down to flame combustion, at which the temperature increased again. This happen numerous times and can be attributed to the conversion of the combustion reaction during FLOX mode as the flowrate as measured by mass flow meter remained constant.

6.3.2 Steam reforming

Temperatures in the steam reforming stage is monitored by multipoint thermocouples at both the inlet and outlet positions. These readout positions are stipulated by the supplier, but any error in thermowell by the supplier or by inserting the thermocouple to the incorrect position might lead to the erroneous measurement, since the thermocouple positioning inside the *FLOX Reformer* was never independently verified.

For runs performed in flame combustion mode the same trend was noted throughout with the outlet position being at a higher temperature than the inlet at the start of the performance testing. However as the load is increased the temperature in both readout points is decreased due to increased amount of methane and steam entering the stage.

The outlet temperature is generally found to be lower than the inlet temperature because of the endothermic nature of the reaction. This trend is more pronounced with increasing load and these temperatures are observed to be well below the setpoint of combustion.

Conversely, the trend of decreasing temperature from inlet to outlet at high load in FLOX combustion mode is not as pronounced or, in most cases, non-existent as can be seen in run

3. This could be linked to the fact that during FLOX combustion a more even temperature distribution is achieved and could thus be at a steady temperature throughout. Flame combustion can exhibit large temperature spikes close to the flame but also large temperature drops away from it leading to the drop in temperature as seen in the steam reforming temperature in flame combustion runs. Temperatures obtained throughout FLOX combustion were at similar combustion temperatures above 800°C but can be seen in run 6 to drop during the flame/FLOX cycling.

6.3.3 Water gas shift and selective methanation

Temperatures in the water gas shift and selective methanation stages are both obtained through multipoint thermocouples reading the inlet, middle and outlet temperatures. Again these readout points may not be considered 100% accurate as their position is subject to error.

Before commencing performance testing these temperatures are seen to increase and go above the range of 190 – 250°C. Once water is introduced these stage temperatures are seen to decrease as the incoming water is evaporated through heat exchange with the WGS and SMET stage. If the correct amount of water is fed to the reformer the system stabilises these two stages in the 190 – 230°C range and reforming can be started.

The inlet and middle temperature readout points are seen to consistently stay within the 190 – 230°C range. The outlet thermocouple readout point for WGS can be seen to increase significantly as the load is increased; this also occurs in the SMET stage although not as pronounced. The reactions taking place are both exothermic in nature, leading to an increase in temperature across the catalyst bed during reaction as is noticeable with this outlet readout point – see table 5.2.

From the obtained graphs the vast temperature fluctuations can be noticed for both stages. These are brought about by any change in the flowrate of water entering the system, with an increase in water causing a decrease in temperature in both these stages, and vice versa. This makes the control of water flowrate and the pump as supplied by the supplier crucial.

In a few cases (see figures 5.7, 5.10 and 5.16) especially run 1, 2 and 4, the flowrate can be seen to drop automatically without any adjustment to the flowrate. This is noticed with a sharp sudden increase in the temperatures. The pump, which is a small electric water pump and found to be relatively inaccurate, might not be ideal for this application where a constant water flowrate is required. Better water control, achieved by means of a more controllable and quantifiable pump, is suggested.

The water flowrate is increased before the actual load change or increase in methane flowrate occurs. This can be seen in many cases with a drop in the temperature in these stages. This is to ensure that no spike in CO levels occur during this period as there is no sudden drop in S/C ratio of the system.

It would seem that the system requires a set amount of excess steam in the system so as to ensure that the WGS and SMET stages all remain in their respective appropriate temperature ranges. This excess amount is proportional to the combustion flowrate or energy input into the system and can be seen from the obtained steam-to-carbon ratios to be much higher at a combustion flowrate of 3200 SCCM methane. In FLOX mode (i.e. at combustion temperatures above 810°C), however, the excess water required is significantly lower which could be attributed to the conversion efficiency of FLOX combustion.

The excess is also increased for an increase in combustion temperature with flame combustion, as seen in table 6.2.

Table 6-2 Water excess (g/min) required to keep WGS and SMET in the operating range.

	run 1	run 2	run 3	run 4	run 5	run 6
Load 1	3.7	5.7	3.9	8.4	10.6	4.1
Load 2	5.1	7.7	2.9	8.5	9.7	4.9
Load 3	4.8	7.5	4.1	7.3	11.7	4.5
Load 4	5.2	8.1	3.9	8.8	10.5	9.3
Load 5	N/A	N/A	N/A	6.7	N/A	N/A
Average	4.7	7.2	3.7	8.0	10.6	5.7
Combustion temperature (°C)	750	800	840	750	800	840
Combustion flowrate (SCCM)	1600	1600	1600	3200	3200	3200
Flame/FLOX	flame	flame	FLOX	flame	flame	FLOX

6.4 Performance testing

6.4.1 Steam reforming

Figures 6.1 – 6.6 show the methane conversions obtained for all 6 runs along with the thermodynamic equilibrium conversions applicable to each load condition. Equilibrium conversions were calculated by means of Aspen simulation software using a Gibbs equilibrium reactor. Actual temperatures from the multipoint thermocouple (both inlet and outlet) and methane and water flowrates as experimentally determined for each run and load condition were used in determining an approximation for the thermodynamic equilibrium conversion applicable to each different condition as shown in table 5.1 and 5.2. Equilibrium conversions were calculated for both inlet and outlet temperatures so as to obtain an equilibrium conversion range, shown on the figures as error bars.
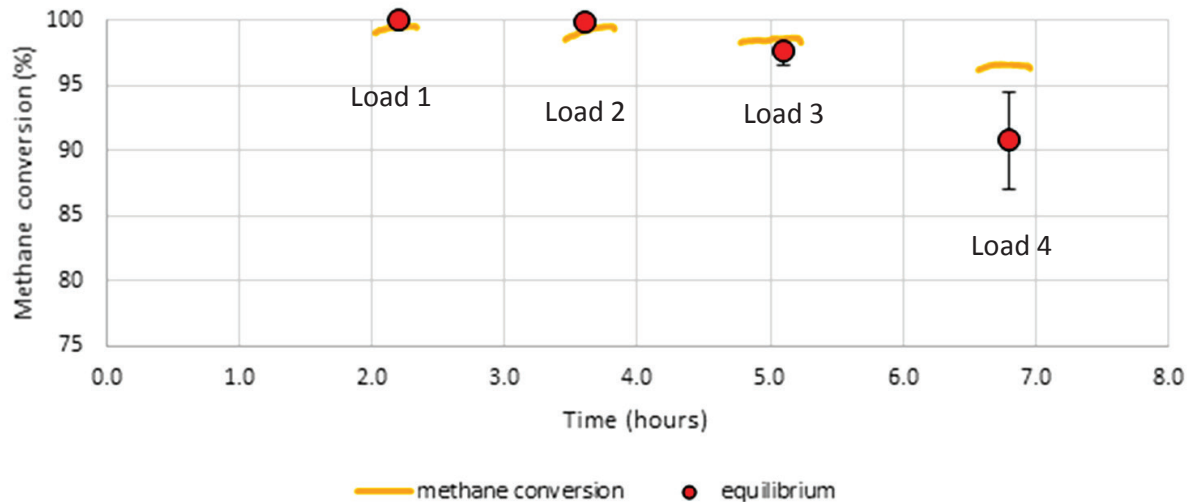
Figure 6-1 Methane conversion achieved in the reforming stage relative to thermodynamic equilibrium conversion for run 1.
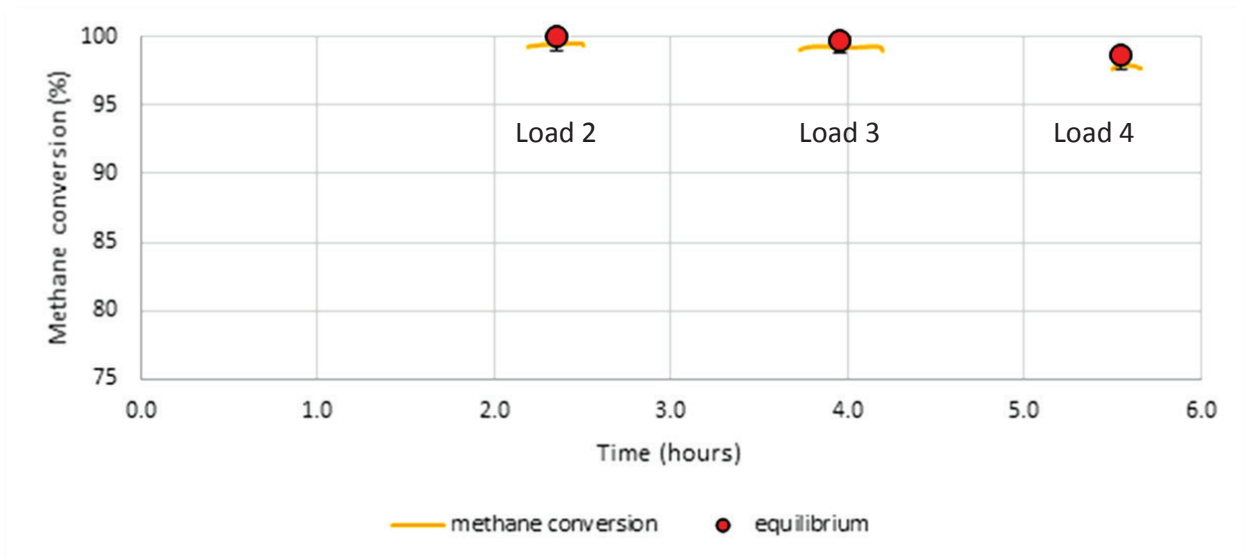
Figure 6-2 Methane conversion achieved in the reforming stage relative to thermodynamic equilibrium conversion for run 2.
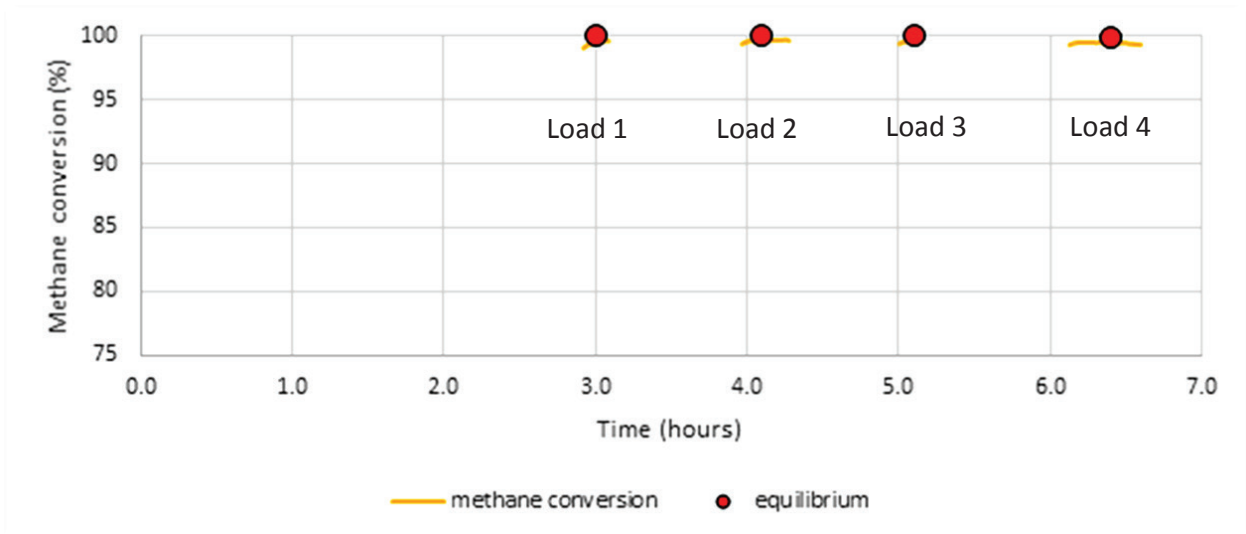
Figure 6-3 Methane conversion achieved in the reforming stage relative to thermodynamic equilibrium conversion for run 3.
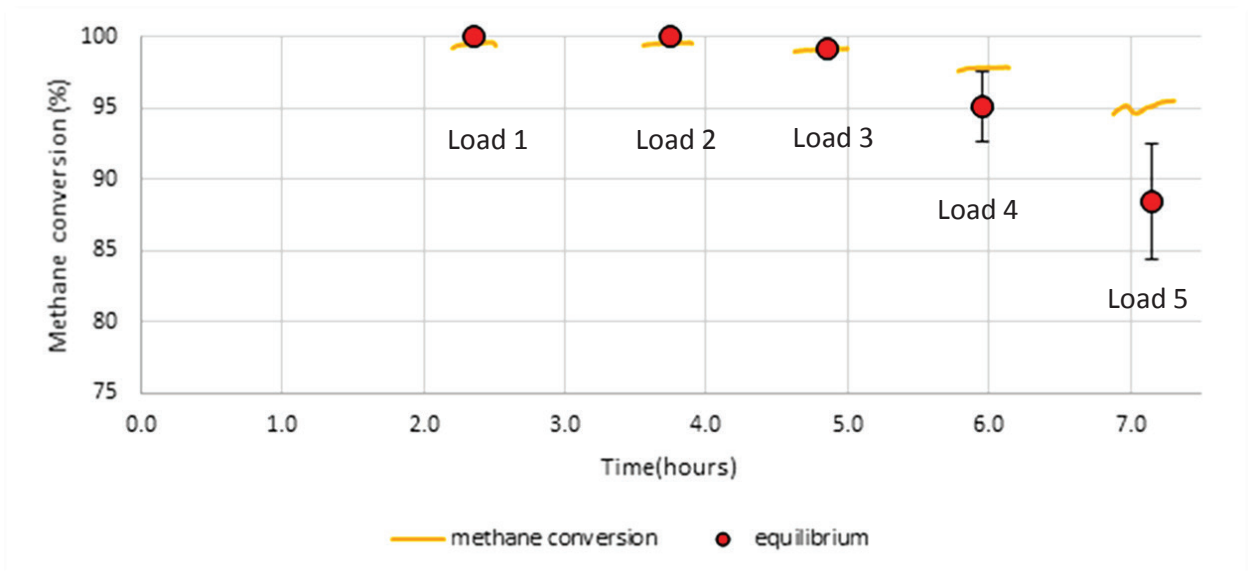
Figure 6-4 Methane conversion achieved in the reforming stage relative to thermodynamic equilibrium conversion for run 4.
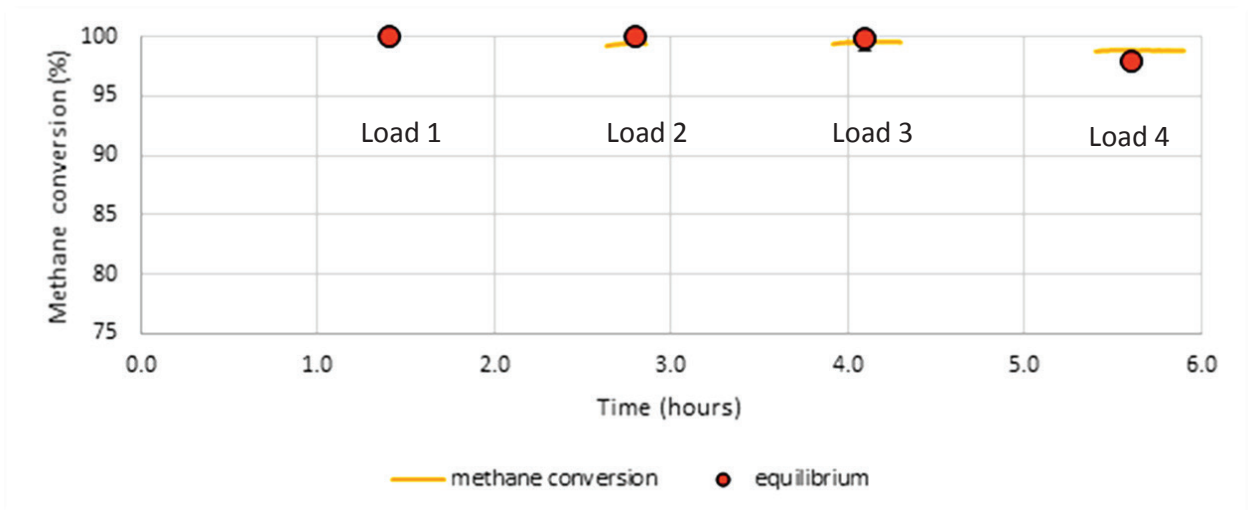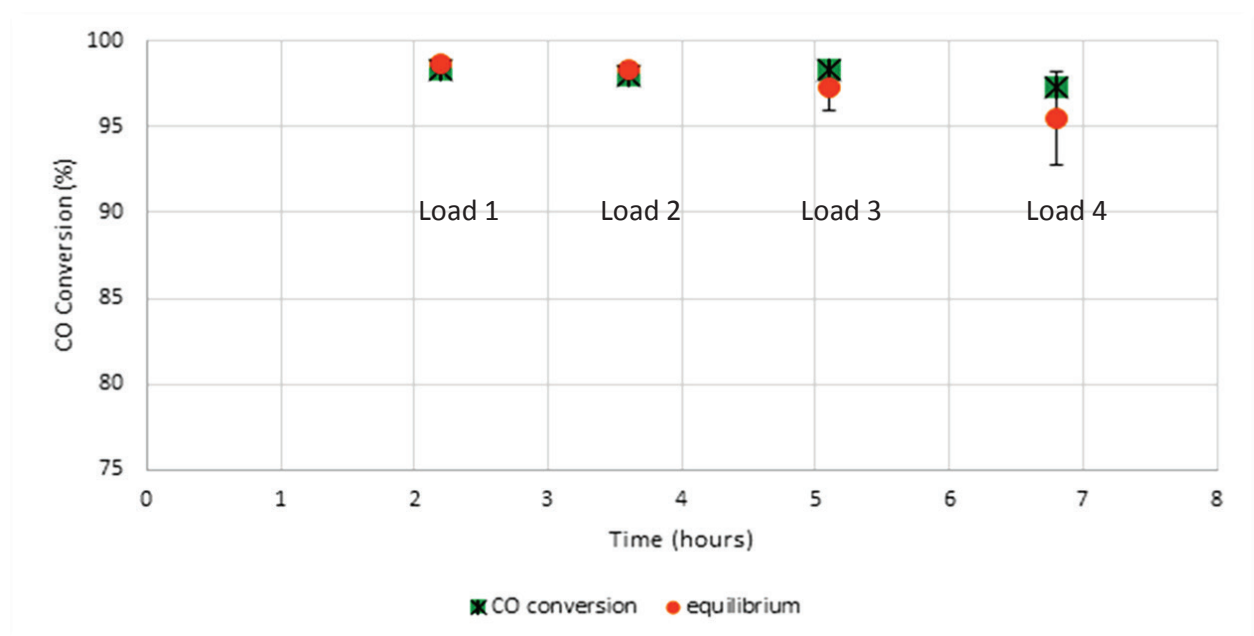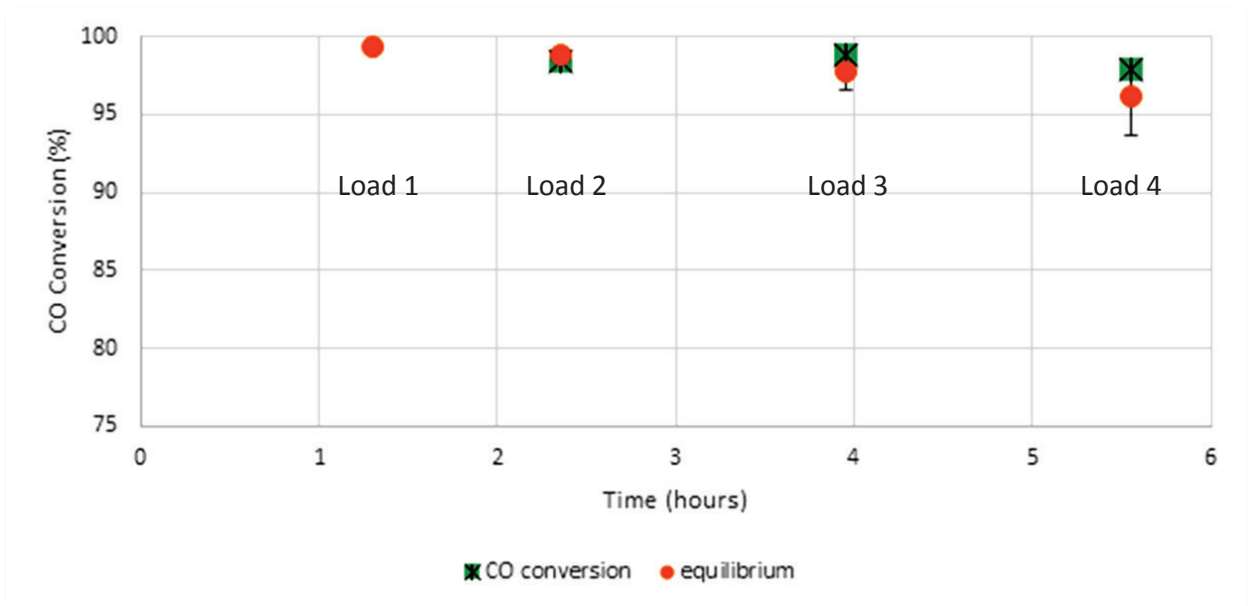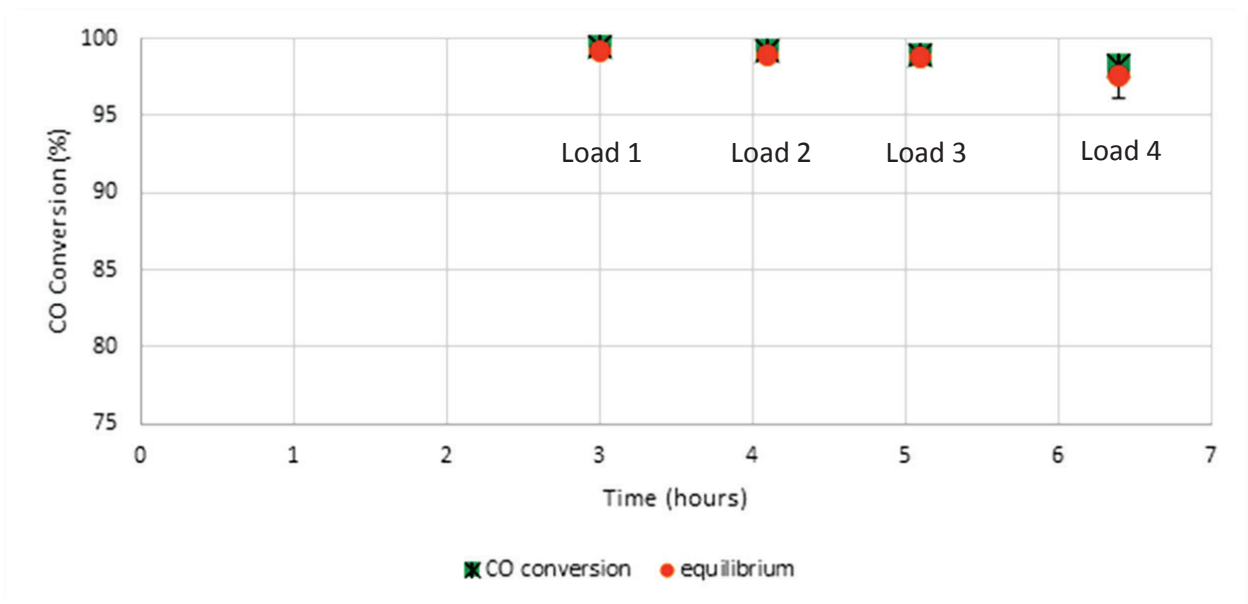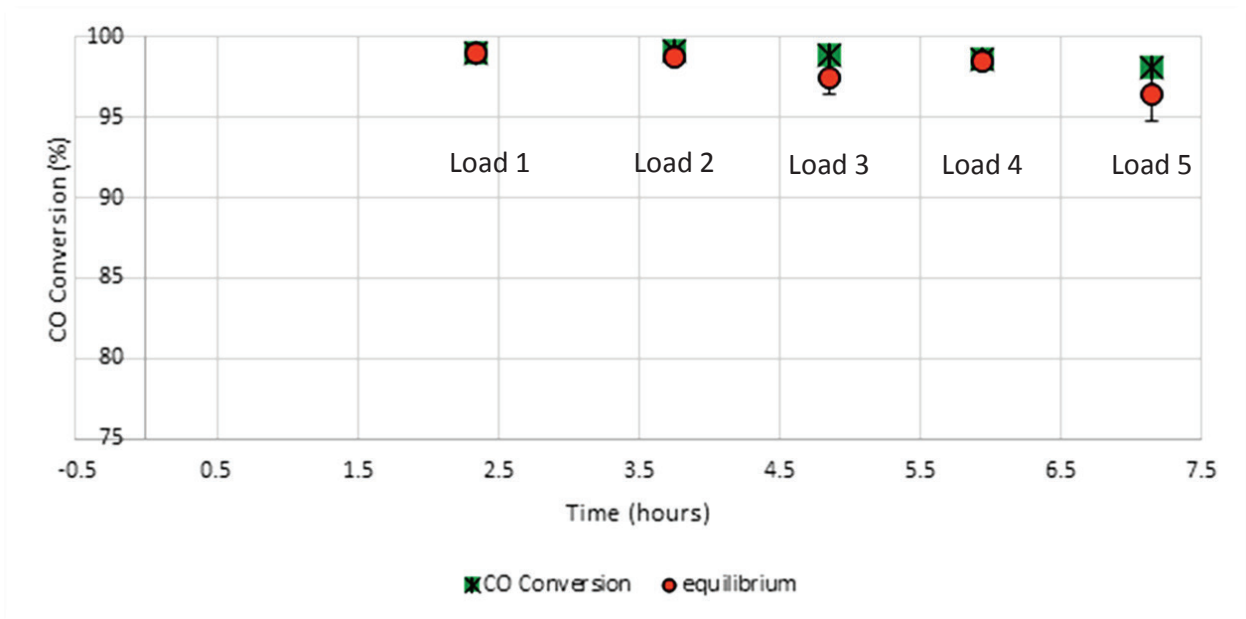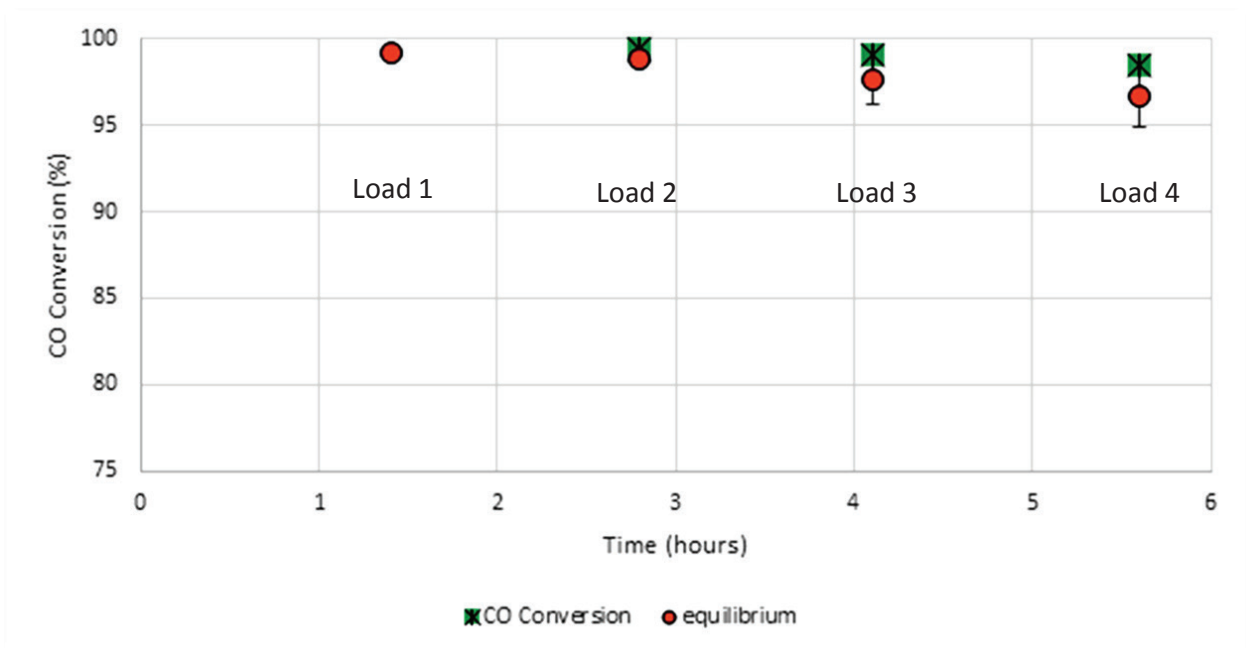

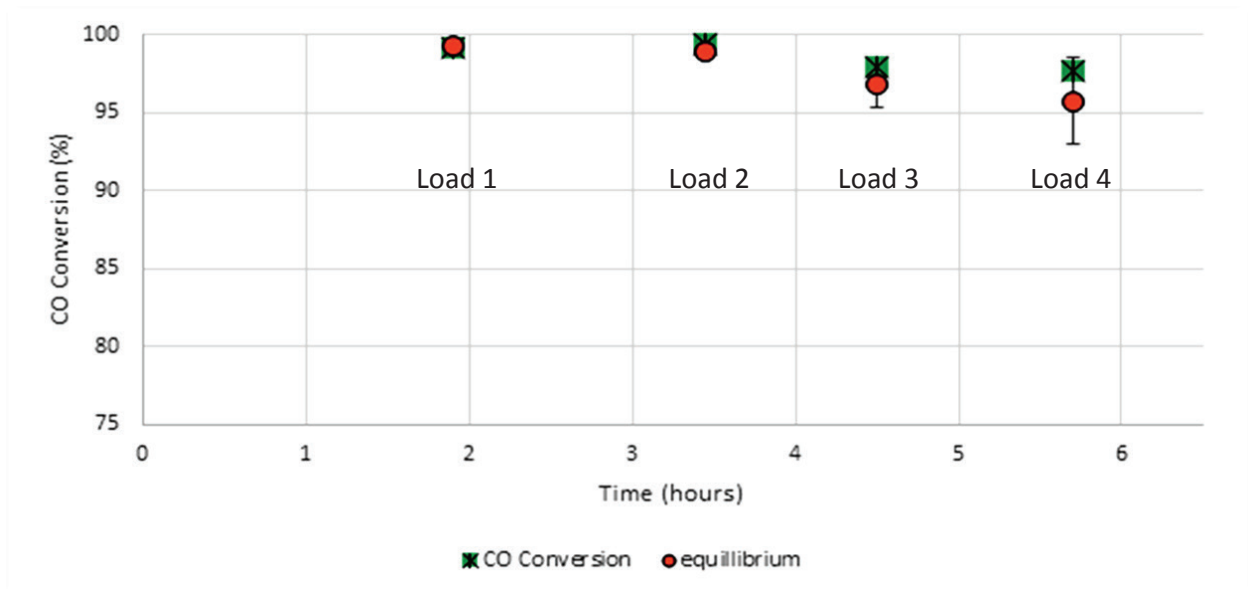**Figure 6-5** Methane conversion achieved in the reforming stage relative to thermodynamic equilibrium conversion for run 5.
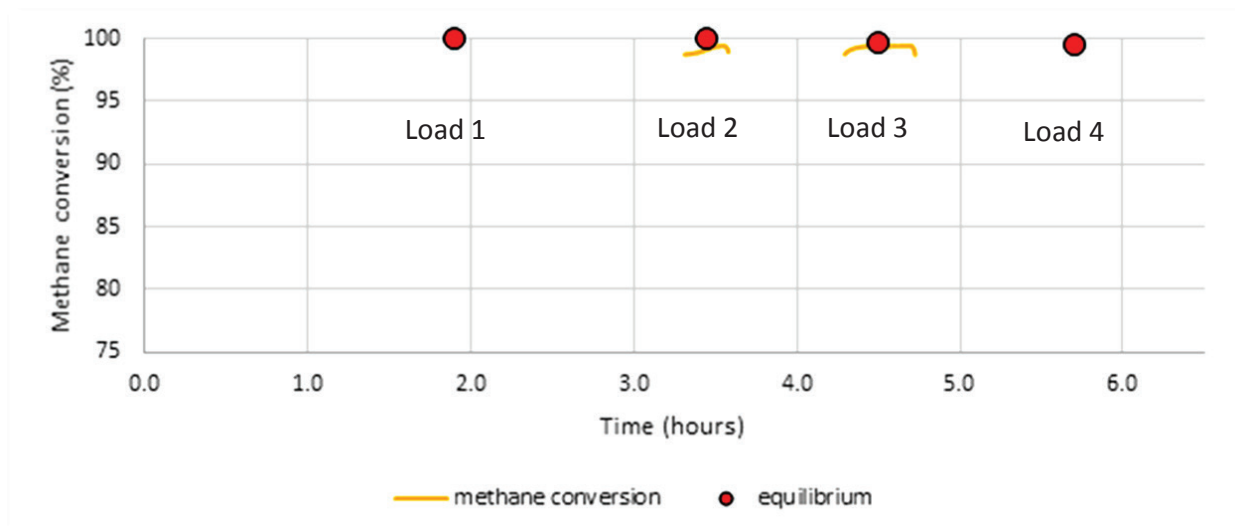
Figure 6-6 Methane conversion achieved in the reforming stage relative to thermodynamic
equilibrium conversion for run 6.

From figure 6.1 to 6.6 it can be seen that actual conversions obtained were found to be approximately the same as thermodynamic equilibrium conversions for steam reforming at the set flow conditions. It can thus be assumed that an excess of catalyst was used in the *FLOX Reformer* to ensure that this was indeed the case. This is unsurprising as the *FLOX Reformer* is guaranteed by the manufacturer to exhibit a minimum lifetime of 5000 hours – usually this is achievable though an excess of catalyst.

For runs at 800 and 840°C it is clear that conversions are always above 98% with the reaction going to virtual completion as the reforming temperature is above 700°C. The excessive S/C ratio also promotes the reaction to virtual completion.

Runs performed at 750°C (run 1 and 4) show a significant decrease in equilibrium conversion with increasing load since reforming temperatures are less than 700°C and a relatively low S/C ratio. Methane conversions of approximately 90 - 95% are achievable under this test condition, with methane content of approximately 1% on a dry gas basis in the reformer outlet stream predicted. The actual methane conversion obtained is found to decrease, but not to the extent of the predicted equilibrium conversion – probably due to incorrect positioning of the thermocouple measuring point as there are large temperature differences across the catalyst bed compared to runs at higher temperatures. Slight errors as expected from flue gas analysis and microGC analysis could also be the cause for this slight deviation.

6.4.2 Water gas shift

Figure 6.7 – 6.12 shows the actual conversions obtained in the water gas shift reaction stage compared to equilibrium conversions for the set flow conditions. Again both WGS inlet and outlet temperatures were used for equilibrium conversions and the range shown by error bars. Water gas shift inlet conditions were approximated by using Aspen simulation software using the actual methane conversion achieved in the reforming stage as determined by chromatography and infrared analysis. This allowed for the approximation of the CO content prior to the WGS stage and thus allowed for the determination of CO conversion.

As for steam reforming, actual CO conversions observed in the water gas shift outlet are nearly identical to thermodynamic equilibrium conditions for the runs performed. In all cases both the equilibrium and actual conversions are seen to be above 95% as the reaction is driven to completion through the high S/C ratio. Both equilibrium and actual conversion is seen to drop slowly as the load is increased due to a less favourable S/C, with the equilibrium range increasing due to a large increase in the outlet temperature compared to inlet temperature.

In all cases CO content exiting the WGS stage is found to be less than 0.3%, which is in agreement with results of industrial LTS. It can again be assumed that a large excess of commercial (CuZnO) catalyst was used within the *FLOX Reformer* as the reaction always exhibits thermodynamic equilibrium conversions.

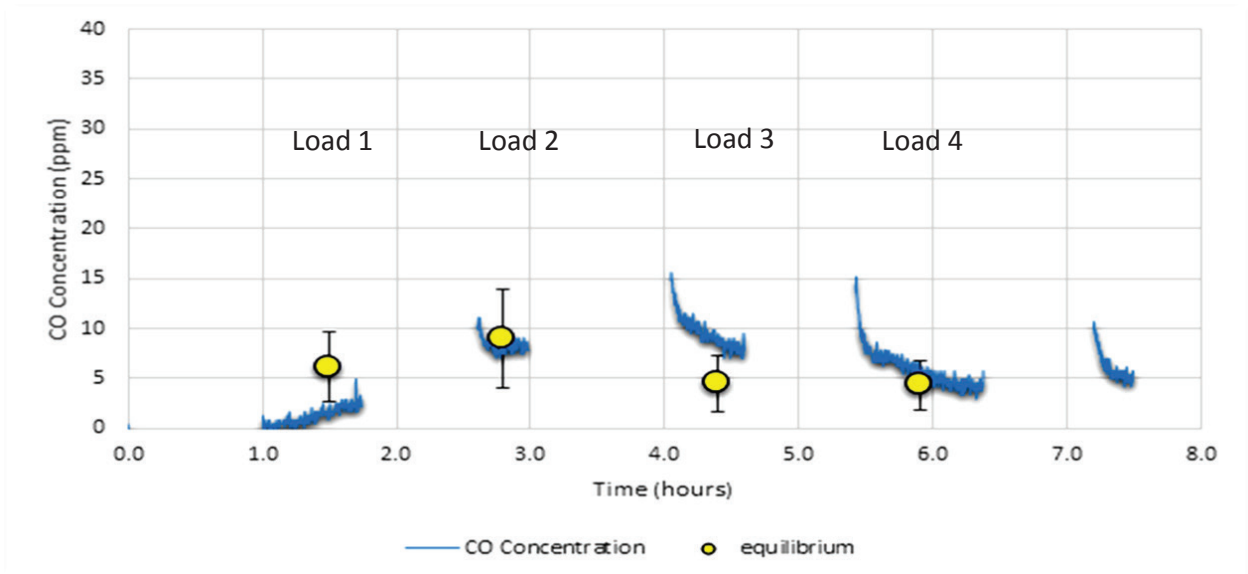**Figure 6-7** CO conversion achieved in the WGS stage relative to thermodynamic equilibrium conversion for run 1.

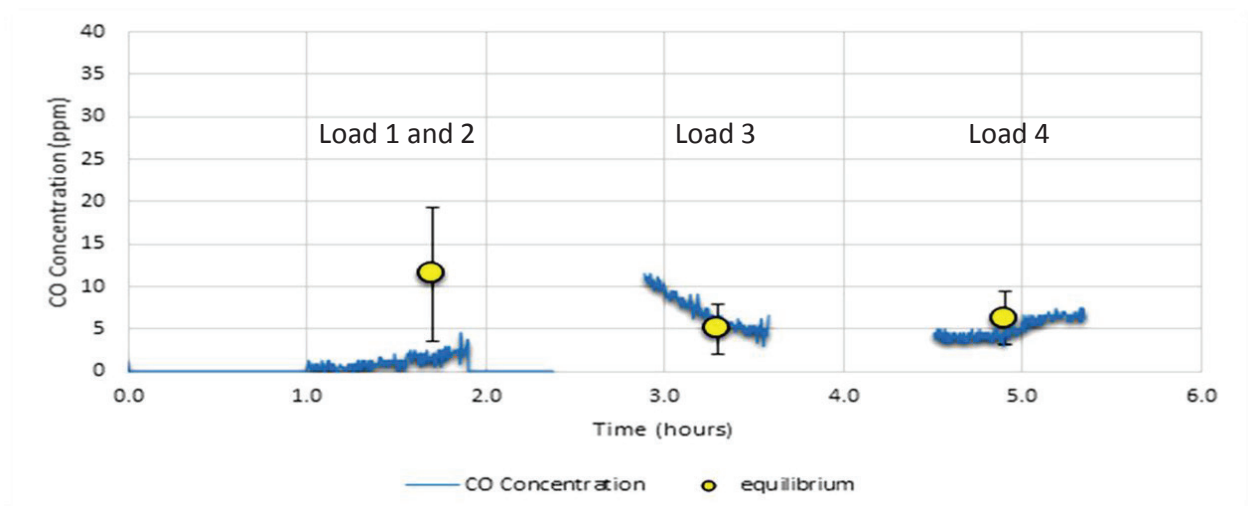**Figure 6-8** CO conversion achieved in the WGS stage relative to thermodynamic equilibrium conversion for run 2.

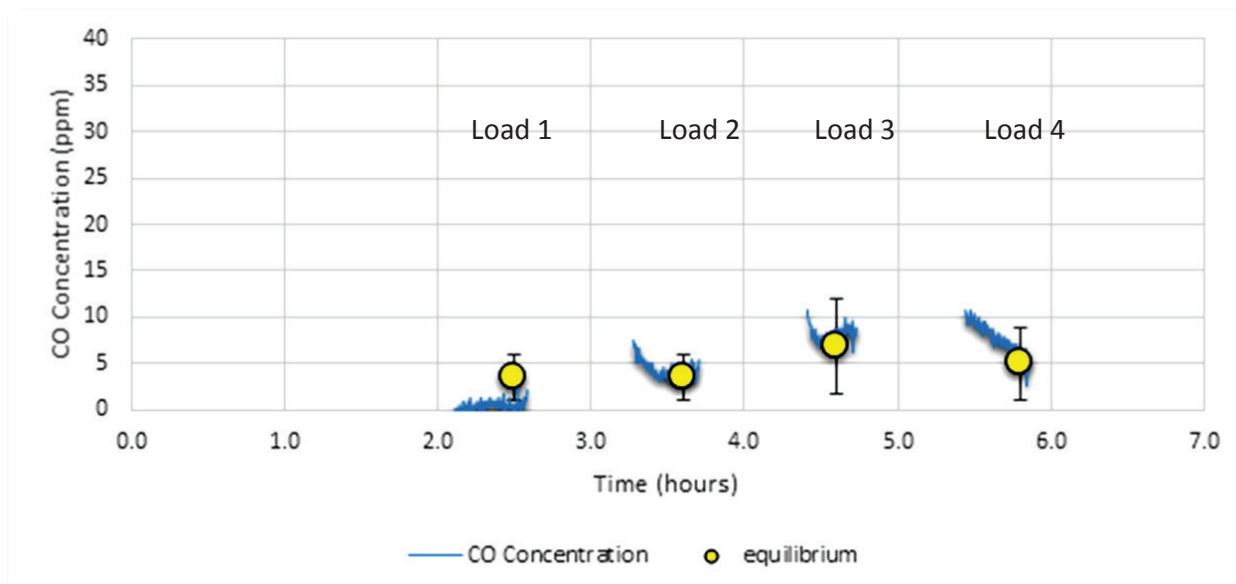**Figure 6-9** CO conversion achieved in the WGS stage relative to thermodynamic equilibrium conversion for run 3.

Figure 6-10 CO conversion achieved in the WGS stage relative to thermodynamic equilibrium conversion for run 4.

Figure 6-11 CO conversion achieved in the WGS stage relative to thermodynamic equilibrium conversion for run 5.

Figure 6-12 CO conversion achieved in the WGS stage relative to thermodynamic equilibrium conversion for run 6.

6.4.3 Selective methanation

Figure 6.13 – 6.18 illustrates the actual CO concentrations achieved in the SMET stage versus equilibrium concentrations as calculated by Aspen simulation software. The actual wet gas inlet composition to the SMET stage was calculated by means of the actual obtained reforming and WGS conversions as shown previously using Aspen.

In all cases the equilibrium conversion was found to be above 99% due to the large hydrogen excess driving the reaction to virtual completion. Again the inlet and outlet temperatures for SMET were used in equilibrium calculations, but in this case the deviation in equilibrium conversion versus temperature was found to be negligible. Actual equilibrium concentrations generally being 10 ppm or below.
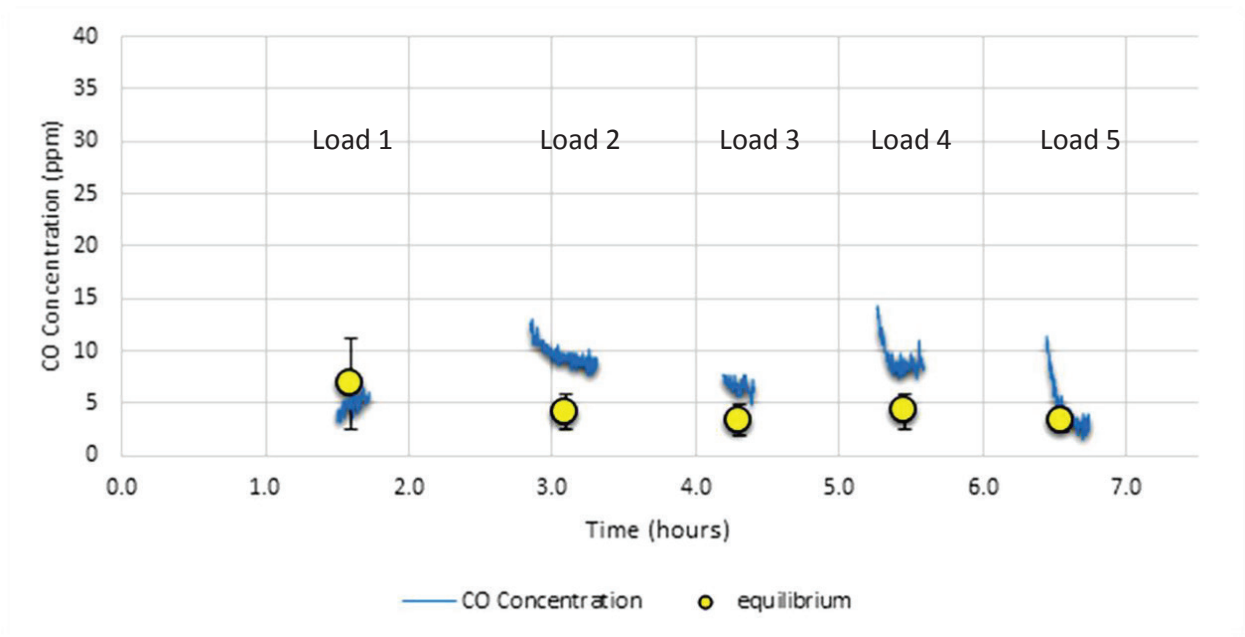
Figure 6-13 CO concentration achieved in the SMET stage relative to thermodynamic equilibrium concentration for run 1.
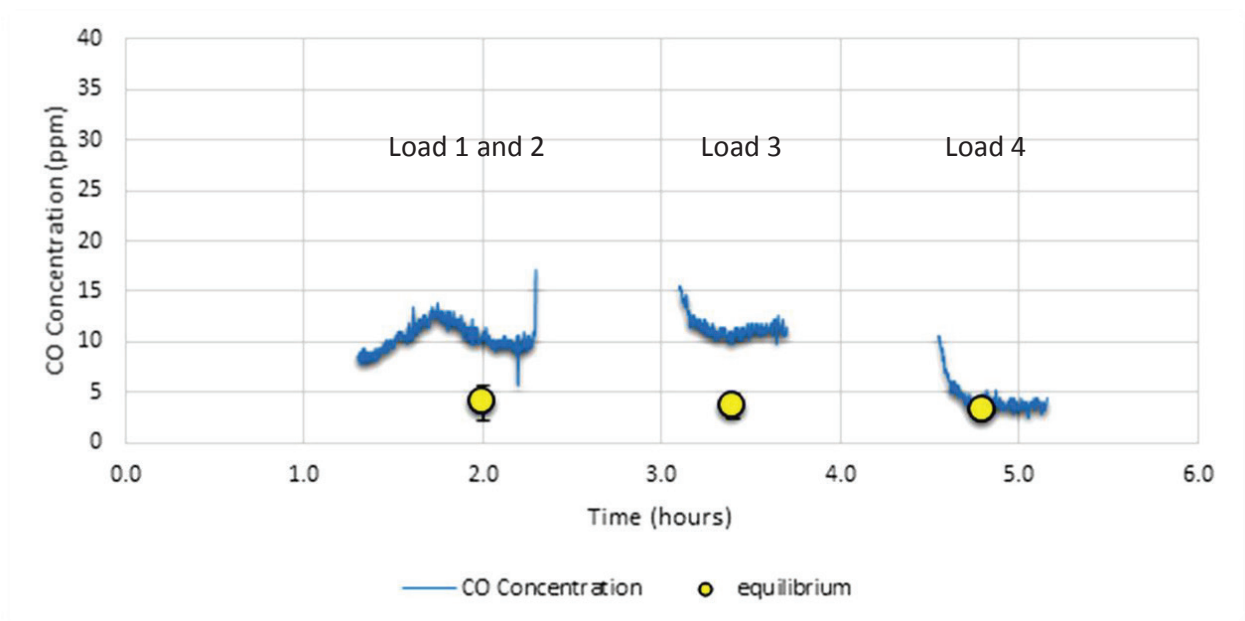

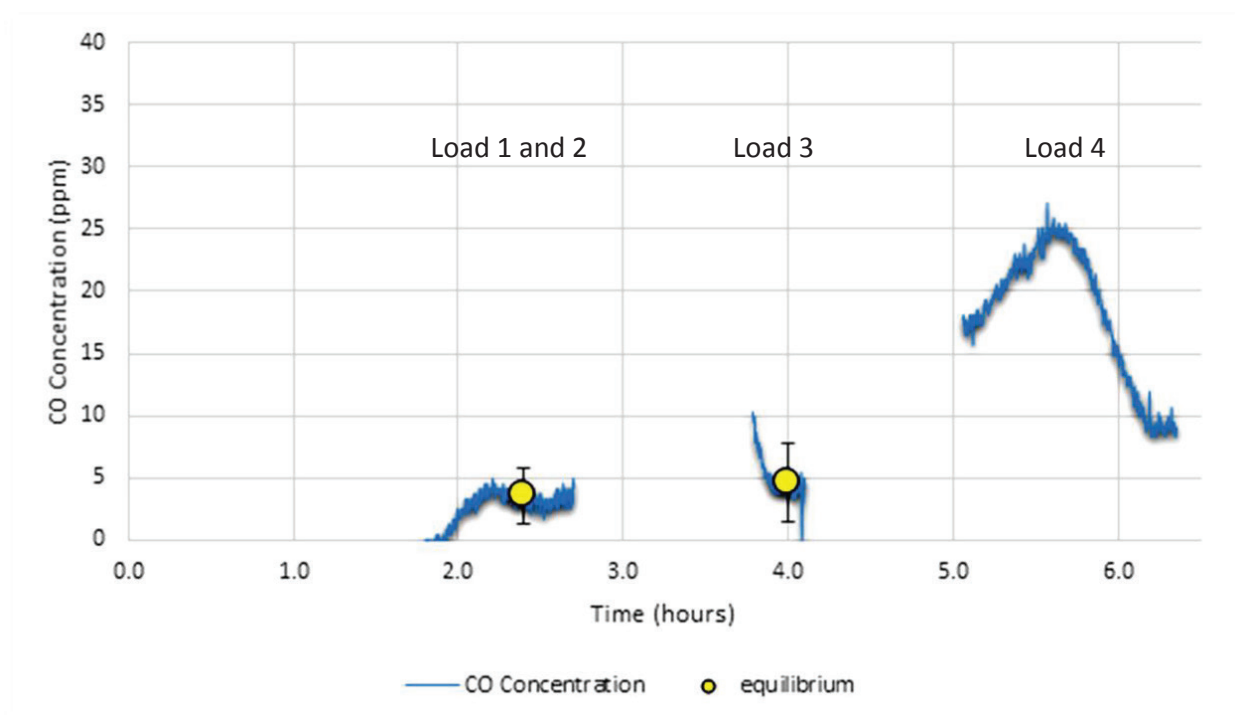**Figure 6-14** CO concentration achieved in the SMET stage relative to thermodynamic equilibrium concentration for run 2.

Figure 6-15 CO concentration achieved in the SMET stage relative to thermodynamic equilibrium concentration for run 3.

Actual CO concentrations were found to be close to equilibrium concentrations for most cases as can be seen in figure 6.13 – 6.18, with a few exceptions (notably in run 4 and run 5). The temperatures for SMET of 200 – 230°C used in all performance testing is within the manufacturer-specified temperature range, although somewhat on the higher end of the acceptable 150 – 250°C range for selective methanation. At these temperatures, reverse WGS reaction cannot necessarily be discounted and can potentially be the cause for CO content slightly higher than expected.

The CO content was found to be below the 10 ppm acceptable limit as required by a low temperature PEM fuel cell for all tests when both the temperature of the WGS and SMET stages were in the range of 190 – 230°C, with the exception of load 4 of run 6, where the temperatures in both stages were found to be above this range due to unexpected flame/FLOX cycling. In this particular case, CO content was observed to spike above 20 ppm, clearly visible in figure 6.18 at load 4.

It should also be noted that a 1% variance and detection limit on the 0 – 400 ppm flue gas analysis cell limited accurate readings below 4 ppm, with the drift of the cell in the low CO content range also leading to potential inaccuracies, which in turn could affect the actual conversion obtained.

Figure 6-16 CO concentration achieved in the SMET stage relative to thermodynamic equilibrium concentration for run 4.

Figure 6-17 CO concentration achieved in the SMET stage relative to thermodynamic equilibrium concentration for run 5.

Although the manufacturer specified a SMET temperature operating window of 190 – 230°C, this studies seems to suggest that temperatures over 210°C should be avoided as CO content increases to the 10ppm level and above. Lowering the SMET temperature is easily achievable by the increase in excess water so as to ensure an adequate drop in temperature. At temperatures above 200°C there is further potential of increased (non-selective) CO_2

98

methanation occurring, which will both negatively affect CO conversion levels and the reformer thermal efficiency.

Figure 6-18 CO concentration achieved in the SMET stage relative to thermodynamic equilibrium concentration for run 6.

Conversion of carbon dioxide by methanation as found during the 6 runs is given in table 6.3 showing that at the SMET temperatures investigated in this study substantial amounts of carbon dioxide conversion to methane occurred. Actual carbon monoxide conversions and selectivities are also presented.

Table 6-3 Carbon monoxide and dioxide methanation conversions observed for after the SMET stage including the corresponding CO methanation selectivity.

Run	Load	CO methanation conversion (%)	CO_2 methanation conversion (%)	CO methanation selectivity (%)
1	1	99.7	9.7	4.5
	2	99.4	9.6	6.3
	3	99.4	7.6	8.0
	4	99.4	6.9	15.2
2	1	N/A	N/A	–
	2	99.8	9.4	4.6
	3	99.3	6.5	6.8
	4	99.6	8.4	10.0
3	1	99.7	9.7	1.7
	2	99.4	9.4	4.0
	3	99.3	9.9	5.6
	4	99.6	7.2	12.0
4	1	98.0	3.0	4.5
	2	97.8	4.2	4.7
	3	99.2	5.4	7.2
	4	99.3	8.0	7.0
	5	99.7	5.3	14.5
5	1	N/A	N/A	–
	2	96.5	2.5	5.5
	3	98.3	5.0	6.4
	4	99.6	3.7	14.5
6	1	N/A	N/A	–
	2	99.7	7.0	4.0
	3	99.3	9.6	11.0
	4	N/A	N/A	–

From table 6.3 it can be observed that CO_2 conversion levels up to 10% occurred which although on first glance may be considered low, is substantial due to the large amount of carbon dioxide (20%) compared to carbon monoxide (0.1 – 0.3%) in the dry gas outlet. It can be noted that carbon monoxide selectivity is always below 20% which confirms this. This is detrimental as hydrogen is consumed through this reaction leading to a lower hydrogen production rate.

6.5 Thermal efficiency

Table 5.3 in the *Results* section presents the thermal efficiencies obtained for all 6 runs at the maximum load. The maximum theoretical efficiency is 80% and at this point 100% methane and CO conversion is assumed. Thermodynamic equilibrium, however, does not permit actual methane and CO conversions to these levels, although for all cases the actual conversions in reforming and WGS were found to be above 95%. SMET conversion was found to be in the same range.

This slight difference between 95 and 100% conversion leads to actual reformer efficiencies using flame combustion in the 71 – 77% range, which could be considered to be highly efficient and on par with most commercial fuel processors [30] . This efficiency obtained could be increased slightly if lower temperatures in the SMET stage was used as it could have greatly decreased carbon dioxide methanation.

A great amount of hydrogen is consumed in this process leading to lower hydrogen yields which negatively affects the efficiency. Some error could also be attached to the flue gas and microGC analysis readings as the hydrogen production is estimated from these readings and not directly measured.

Tests performed using FLOX combustion was found to be less thermally efficient and only in the 59 – 65% range. It was found from performance testing that, at an equivalent reformer load, significantly more methane was required in flameless combustion compared to flame combustion to keep the system temperature stable. This increase in fuel flowrate affects the efficiency as more methane is required to produce the same amount of hydrogen.

From this study it seems that the efficiency of FLOX combustion is lower than flame combustion as not all methane is combusted during the FLOX combustion process, although this was never confirmed and was not considered as part of the investigation.

7. Concluding Remarks

This study has succeeded in the objective of obtaining standardised benchmark data for the *FLOX Reformer*, the so-called "best-in-class" commercial fuel processor. The unit was successfully commissioned and integrated into an automated assembly with all the necessary balance of plant components required for automated control. The investigation included scoping of operating windows and reformate product compositions for the WS® FPM C1 *FLOX Reformer*.

Full scoping of both the SMET and WGS analysis streams were performed via flue gas and microGC analysis. The corresponding dry gas outlets were measured and conversions for all stages were obtained and found to be virtually identical to thermodynamic equilibrium throughout – an excess of catalyst in each stage has likely been included by the manufacturer to ensure long unit lifetime. This analysis was performed at various combustion flowrates, temperatures, reformer loads and steam-to-carbon ratios as found to be applicable to other commercial fuel processors and to the three individual stages of reforming, water gas shift and selective methanation in industry.

The *FLOX Reformer* was able to produce a CO outlet composition of 10 ppm or less, for all loads and temperatures, as is required with most PEM fuel cells and was able to produce more than 15 SCLM of hydrogen, enough to power a 1 kW fuel cell.

Start-up times were tested with two combustion flowrates and found to be on par with other 1 kW fuel processors available at the time and included a unique standby start-up which significantly cuts down start-up times from one hour to 30 minutes.

Full temperature profiles for all the relevant sections were obtained for all tests and the thermal efficiency of the reformer found to be above 70% using flame combustion whilst the supplier's unique *FLOX* combustion was lower (60%) due to lower combustion efficiency. The effect of carbon dioxide methanation which occurred at higher temperatures during the selective methanation phase also leads to slightly lower efficiencies.

The temperature control strategy although simple could be seen as a problem. The *FLOX Reformer* relies heavily on excess water to control the temperature in its CO clean-up stages through heat exchange with incoming water for steam generation. This excess is however difficult to predict and relies highly on the stability and consistency of the included water pump, which at times showed great fluctuations.

For future use it is recommended that the *Reformer* be run with a greater excess of water so as to negate carbon dioxide methanation through lower selective methanation and water gas shift temperatures. This will allow for greater thermal efficiencies and it is also recommended that a more controllable and quantifiable pump be used so as to obtain better temperature control throughout the system.

Lastly it is recommended that the reformer be used with flame combustion only if high thermal efficiency is required. Although stated as more environmentally friendly due to less CO_X, NO_X and SO_X emissions, FLOX combustion appears to be less efficient as not all methane is combusted and thus released into the atmosphere.

8. References

[1] K. Othmer, "Power Generation," in *Kirk Othmer Encyclopedia of chemical technology* , 4th ed., vol. 20, 1991, pp. 1-18.

[2] Barbir, "Future of hydrogen," in *PEM Fuel cell catalyst and MEA preparation and characterisation*, Cape Town, 2011.

[3] K. Othmer, "Hydrogen," in *Kirk Othmer Encyclopeadia of Chemical Technology*, 4th ed., vol. 13th, 1991, pp. 411-436.

[4] J. Muller, "Case study: Developing a market for a new technology," in *PEM fuel cell catalyst and MEA preperation and characterisation, University of Cape Town*, Cape Town, 2011.

[5] WS, *WS FLOX Reformer Product guide,* Stuttgart: WS, 2010.

[6] BP, "BP Statistical Review of world energy," 2015. [Online].

[7] G. Kolb, "Fuel processing for fuel cells," in *Fuel Cells*, 2008.

[8] J. Olivier and G. Janssens-Maenhout, "Trends in global CO2 emissions: Report," PBL Netherlands Environmental Assessment Agency, Amsterdam, 2013.

[9] K. Othmer, "Ammonia," in *Kirk Othmer Encyclopeadia of Chemical Technology*, 1991, pp. 335-361.

[10] S. Roberts, *Performance of gold catalysts for low temperature water gas shift,* University of Cape Town MSc Chemical Engineering: University of Cape Town, 2001.

[11] P. Schmidt, J. Michalski and C. Stiller, "Storage of renewable electricity through hydrogen production," in *World Renewable energy congress*, Sweden, 2011.

[12] K. Othmer, "Hydrogen energy," in *Kirk Othmer Encyclopeadia of Chemical Technology*, 1991, pp. 453-463.

[13] D. Bessarabov, "Electrocatalyst and MEA challenges in the fuel cell automotive industry," in *HySA*, Cape Town, 2011.

[14] P. c. inc., "Precision-Combustion," 2015. [Online]. Available: www.precision-combustion.com.

[15] I. inc., "innovatek," 2015. [Online]. Available: www.innovatek.com.

[16] H. Powertech, "h2powertech," 2015. [Online]. Available: www.h2powertech.com.

[17] WS, "FLOX," 2015. [Online]. Available: www.flox.com.

[18] helbio, "Helbio," 2015. [Online]. Available: www.helbio.com.

[19] WS, "WSReformer," 2011. [Online]. Available: www.wsreformer.de.

[20] WS, *WS FLOX REFORMER Documentation and Technical User manual,* Stuttgart: WS, 2010.

[21] J. Wunning, "Flameless Oxidation," in *HiTACG Symposium*, Germany, 2005.

[22] J. Wunning, "FLOX Flaameless Oxidation," in *Thermprocess symposium*, 2003.

[23] J. Wunning, "Compact steam reformer". United States Patent US2007/0006529A1, 11 January 2007.

[24] G. Austin, Shreve's Chemical Process Industries, 5th ed., New York: McGraw-Hill Book Co, 1984.

[25] P. Thevenin, Catalytic combustion of methane, Stockholm: KTH, 2002.

[26] J. Wunning, "Flameless combustion and it's applications," WS, Renningen, 2004.

[27] K. Othmer, "Carbon monoxide," in *Kirk Othmer Encyclopeadia of Chemical Technology*, 4th ed., vol. 5, 2004, pp. 52-61.

[28] S. Tada, R. Kikuchi, W. Katsuya and K. Osada, "Long-term durability of Ni/TiO2 and RueNi/TiO2 catalysts for selective CO methanation," *Journal of Power Sources,* vol. 264, pp. 59-66, 2014.

[29] H. Schmid and J. Wunning, "FLOX Steam reforming for PEM Fuel Cells," WS - Fuel Cells, Renningen, 2004.

[30] K. Pieniniemi, "Pilot Gasifier Producer Gas Analysis," in *HIGHBIO2- Centria University of Applied sciences*, 2011-2013.

[31] E. Calo, A. Giannini and G. Monteleone, "Small stationary reformers for H2 production from hydrocarbons," *International Journal of hydrogen energy,* vol. 35, pp. 9828-9835, 2010.

Appendix A

Raw calibration data for air blower, water pump and reforming mass flow controller.
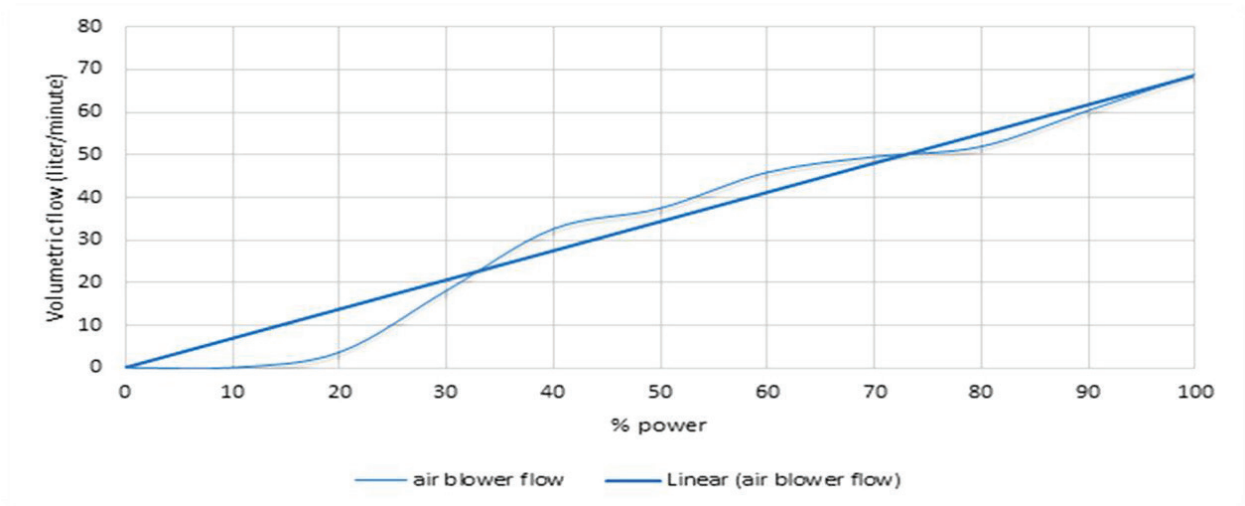
Figure A.1. Flow calibration chart for the attached air blower for the FLOX Reformer
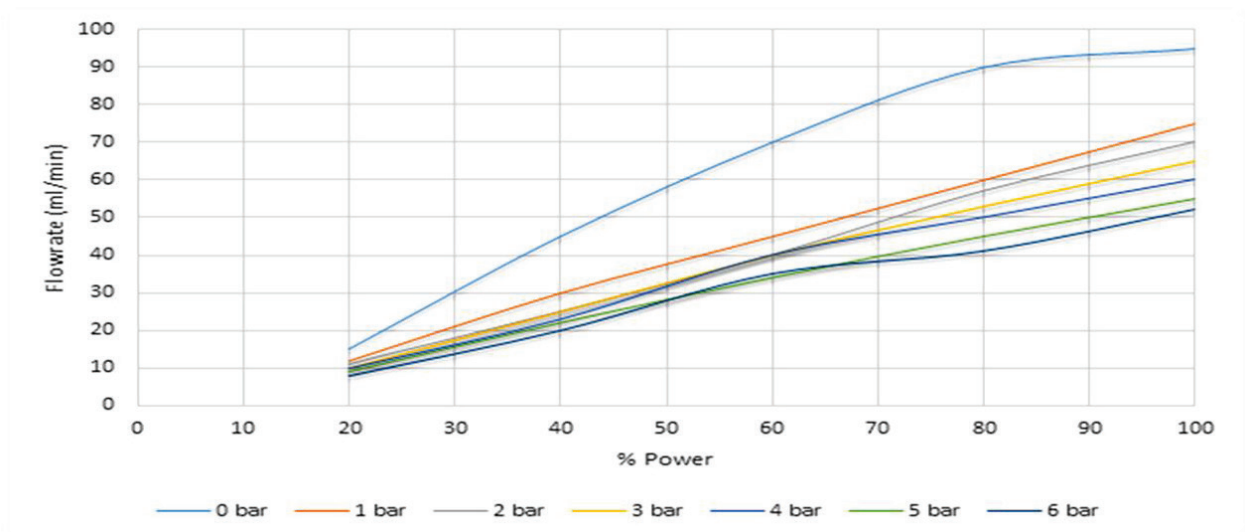
Figure A.2. Manufacturer supplied calibration chart for included water pump.
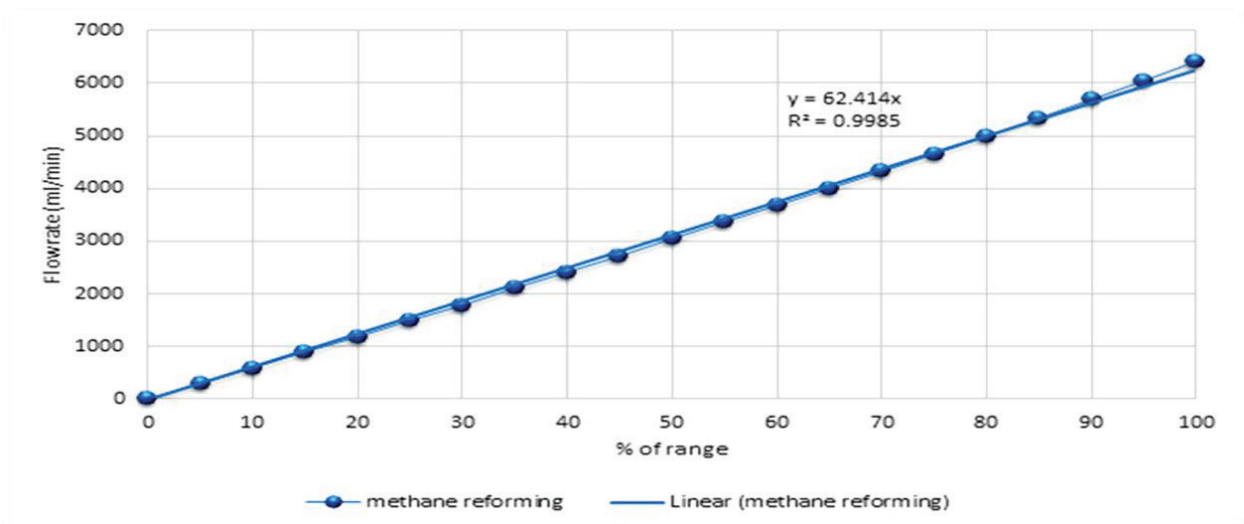
Figure A.3. Calibration chart for methane reforming mass flow controller

ii)   MicroGC calibration data for hydrogen, methane, carbon monoxide and carbon dioxide.
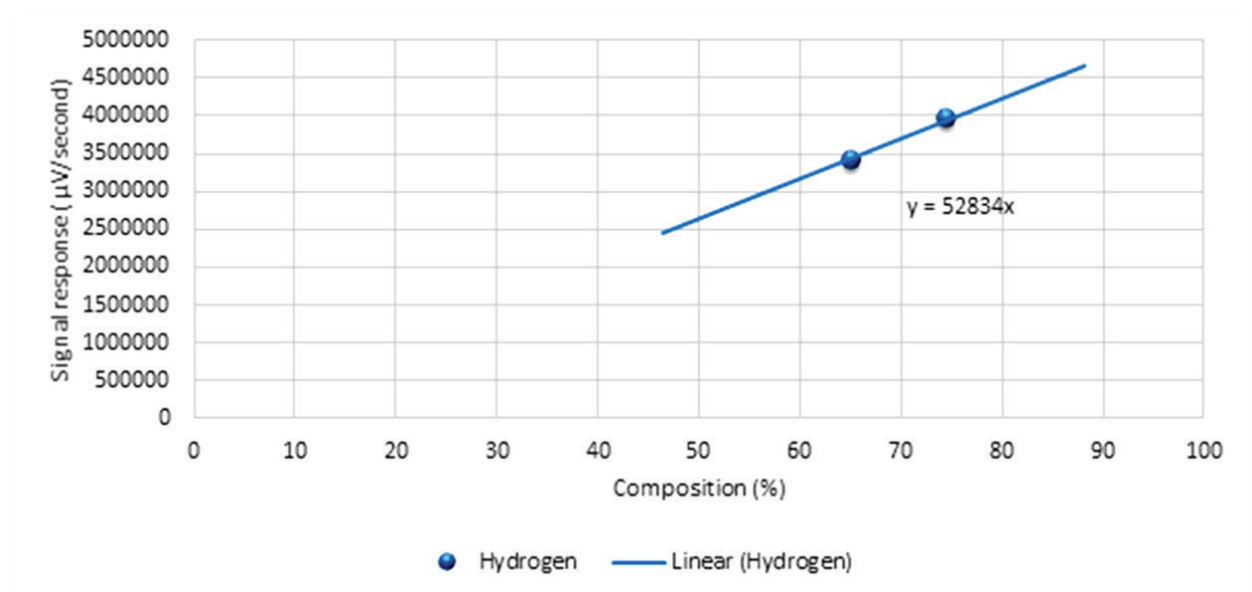
Figure A.4. Hydrogen calibration chart with included calibration factor.
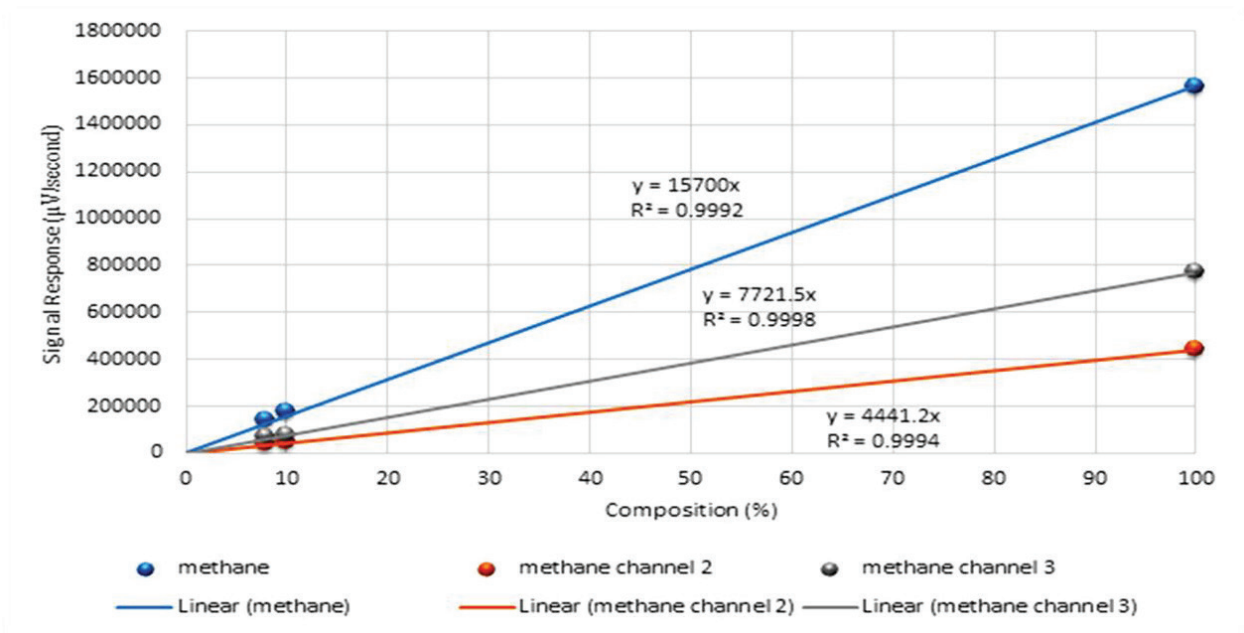
Figure A.5. Methane calibration chart with included calibration factor.
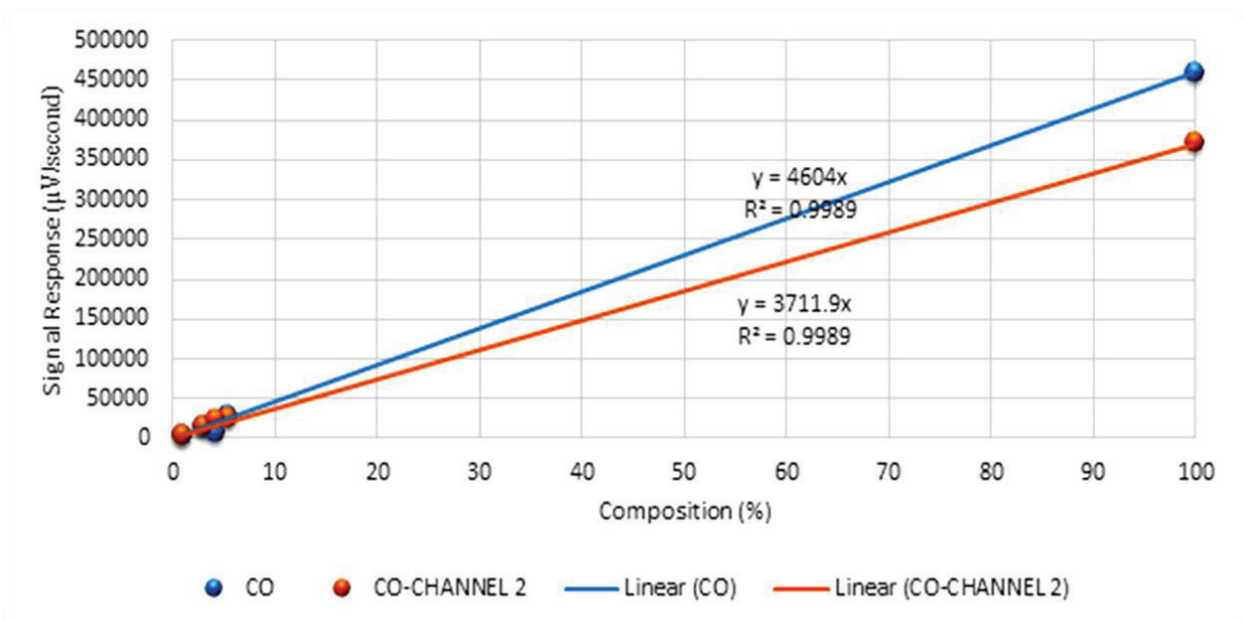
Figure A.6. Carbon monoxide calibration chart with included calibration factor.
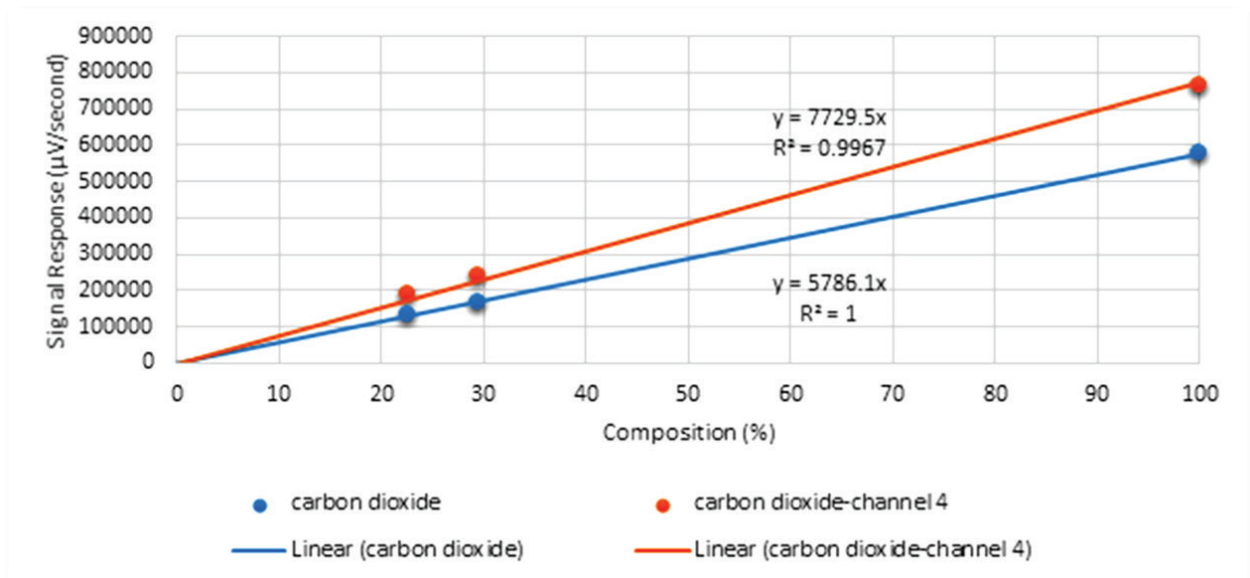
Figure A.7. Carbon monoxide calibration chart with included calibration factor.

Appendix B

System PLC user interface –
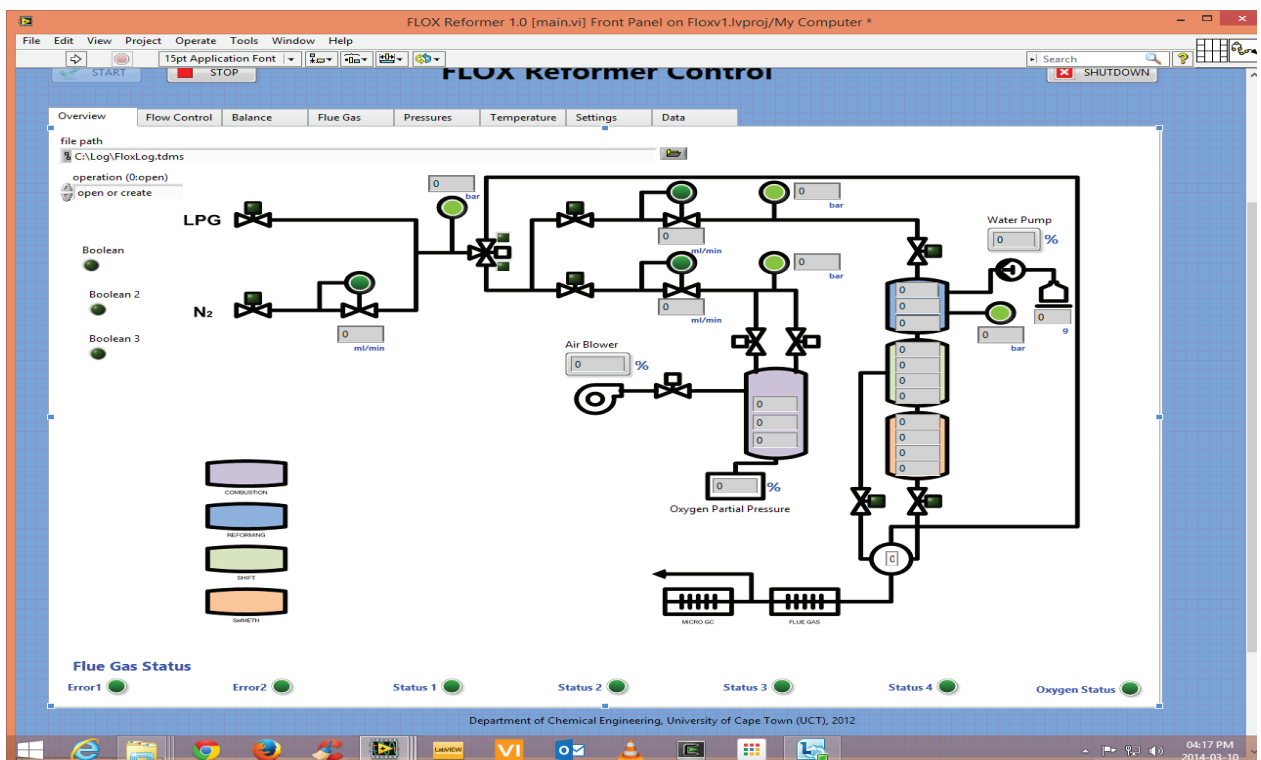
Figure B.1. Screenshot of system overview of PLC
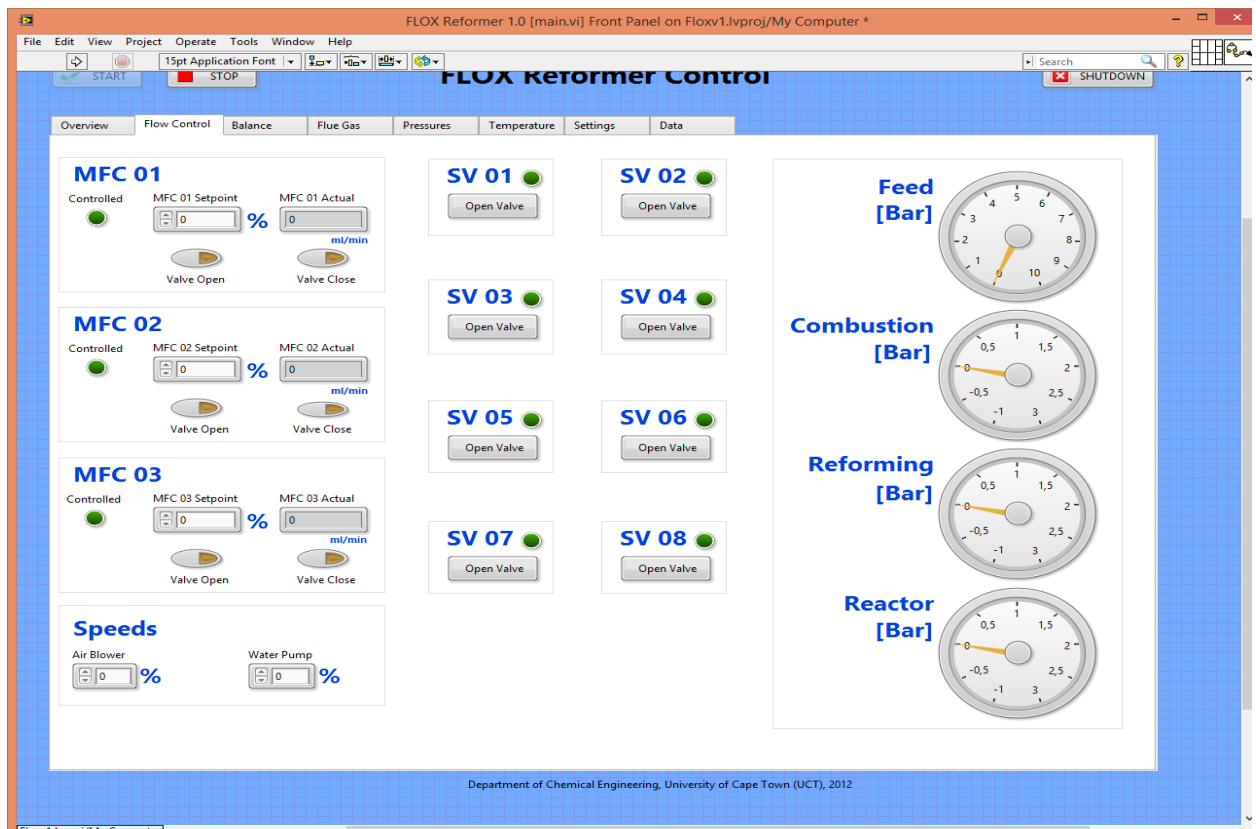
Figure B.2. Screenshot of system flow control of PLC
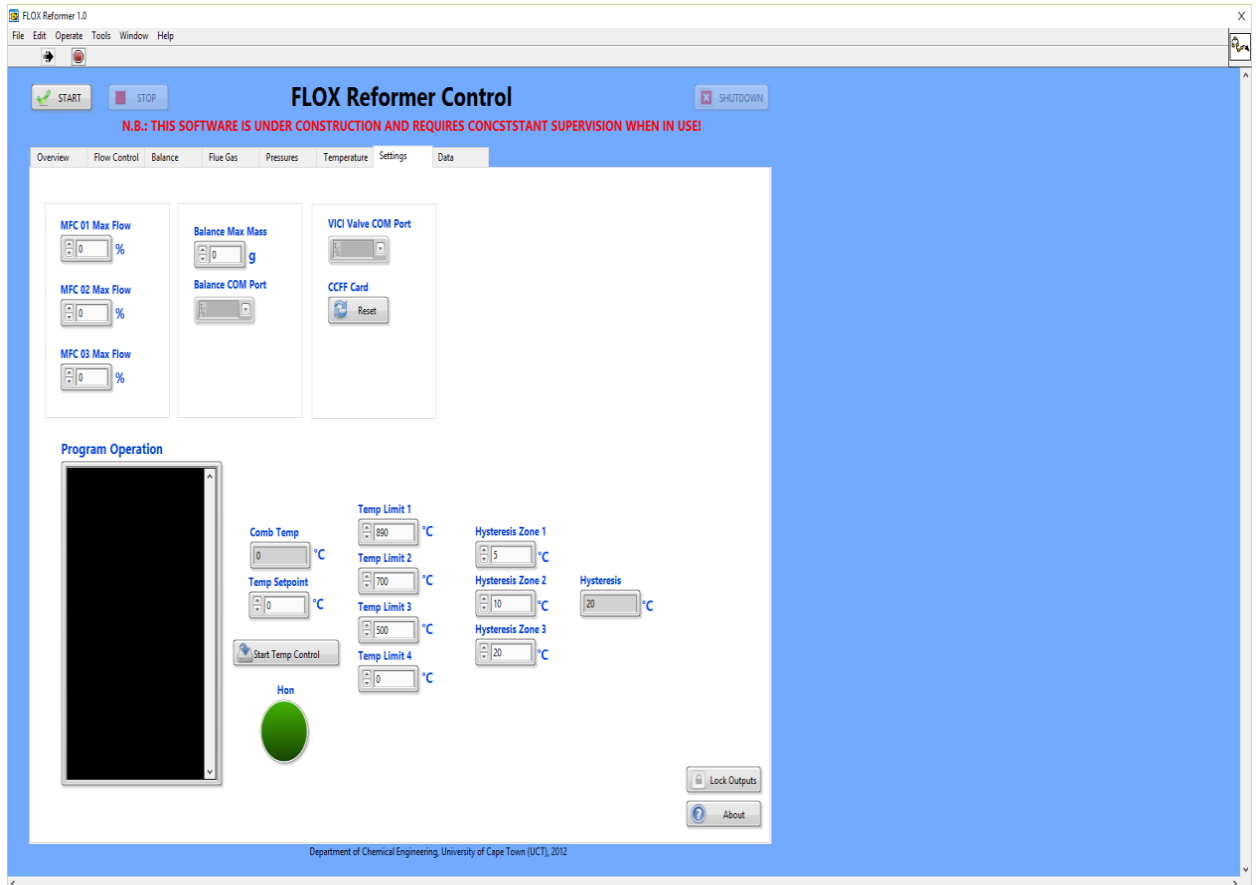
Figure B.3. Screenshot of system temperature control of PLC.
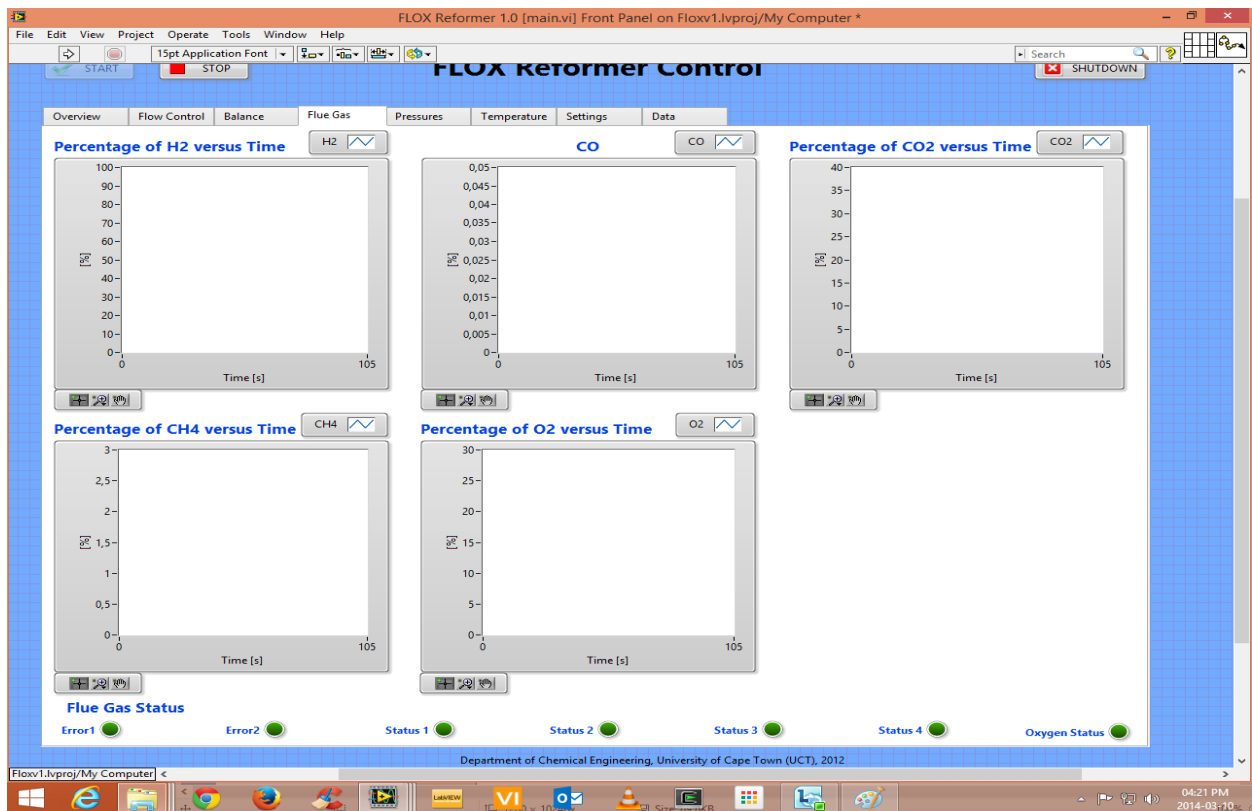
Figure B.4. Screenshot of system flue gas analysis of PLC.

Appendix C

MicroGC analysis data –

Table C.1. Averaged microGC analysis data for run 1.

Ref time	WGS time	Load	H_2 Ref	WGS	CO_2 Ref	WGS	CO Ref	WGS	CH_4 Ref	WGS
1.5	2.2	1	77.23	77.16	20.94	20.92	0	0.09	2.87	0.18
2.8	3.6	2	77.49	79.09	20.89	21.74	0	0.14	3.01	0.21
4.4	5.1	3	77.87	78.99	21.55	22.10	0	0.16	2.28	0.29
5.9	6.8	4	78.54	79.89	21.70	21.98	0	0.28	2.53	0.76
7.4		4	77.32		21.20		0		2.86	

Table C.2. Averaged microGC analysis data for run 2.

Ref time	WGS time	Load	H_2 Ref	WGS	CO_2 Ref	WGS	CO Ref	WGS	CH_4 Ref	WGS
1.3	1.3	1	78.16		19.87		0		1.71	
1.7	2.35	2	76.83	78.18	19.35	19.81	0	0.10	3.21	0.15
3.3	3.95	3	78.53	79.53	19.70	21.24	0	0.10	1.64	0.12
4.9	5.55	4	78.03	79.48	20.98	21.32	0	0.20	2.17	0.36

Table C.3. Averaged microGC analysis data for run 3.

Ref time	WGS time	Load	H_2 Ref	WGS	CO_2 Ref	WGS	CO Ref	WGS	CH_4 Ref	WGS
2.5	3	1	75.88	77.48	20.87	21.14	0	0.04	1.84	0.05
3.6	4.1	2	77.92	78.59	20.95	21.53	0	0.09	1.79	0.05
4.6	5.1	3	76.65	78.88	20.84	21.63	0	0.13	2.95	0.07
5.8	6.4	4	77.68	78.92	21.16	21.53	0	0.22	1.72	0.08

Table C.4. Averaged microGC analysis data for run 4.

Ref time	WGS time	Load	H_2 Ref	WGS	CO_2 Ref	WGS	CO Ref	WGS	CH_4 Ref	WGS
1.6	2.35	1	76.99	75.86	20.27	20.63	0	0.03	0.67	0.07
3.1	3.75	2	80.20	80.63	21.55	22.02	0	0.05	0.91	0.09
4.3	4.85	3	79.79	80.39	21.82	22.19	0	0.09	1.19	0.17
5.45	5.95	4	79.15	80.17	21.79	22.17	0	0.13	1.94	0.41
6.55	7.15	5	79.14	79.82	22.03	22.03	0	0.19	1.85	0.91

Table C.5. Averaged microGC analysis data for run 5.

Ref time	WGS time	Load	H_2 Ref	WGS	CO_2 Ref	WGS	CO Ref	WGS	CH_4 Ref	WGS
1.4	1.4	1	78.20		21.25		0		0.49	
2	2.8	2	79.33	74.98	21.75	20.80	0.00	0.03	0.55	0.07
3.4	4.1	3	78.88	79.56	21.96	22.23	0.00	0.07	0.88	0.07
4.8	5.6	4	78.94	79.27	22.08	22.23	0.00	0.14	0.80	0.22

Table C.6. Averaged microGC analysis data for run 6.

Ref time	WGS time	Load	H_2 Ref	WGS	CO_2 Ref	WGS	CO Ref	WGS	CH_4 Ref	WGS
1.9	1.9	1	76.81		18.34		0		1.33	
2.4	3.45	2	78.22	77.76	18.60	18.67	0	0.05	1.40	0.20
4	4.5	3	77.82	78.82	18.77	19.10	0	0.21	1.73	0.09
5.7	5.7	4	76.77		18.61		0		2.93	

Appendix D

Logging data graphs of system temperatures, balance readings and flue gas concentrations.

Run 1 – Raw data
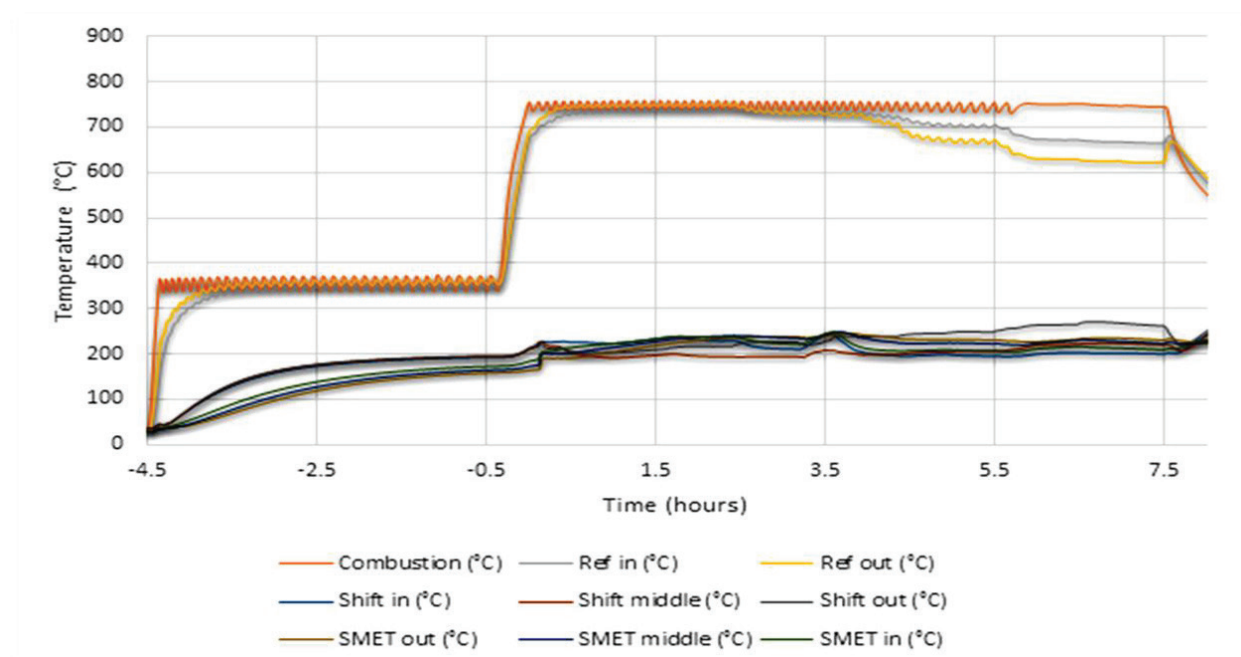
Figure D.1. Raw temperature graphs for run 1.
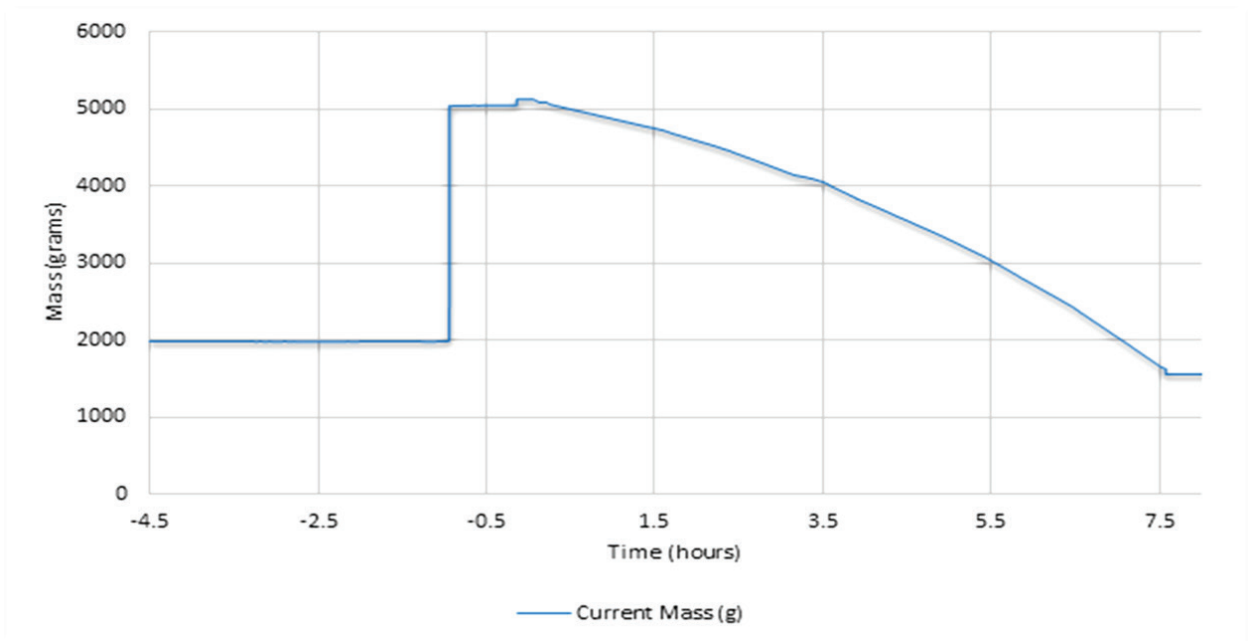
Figure D.2. Balance reading graph for run 1.
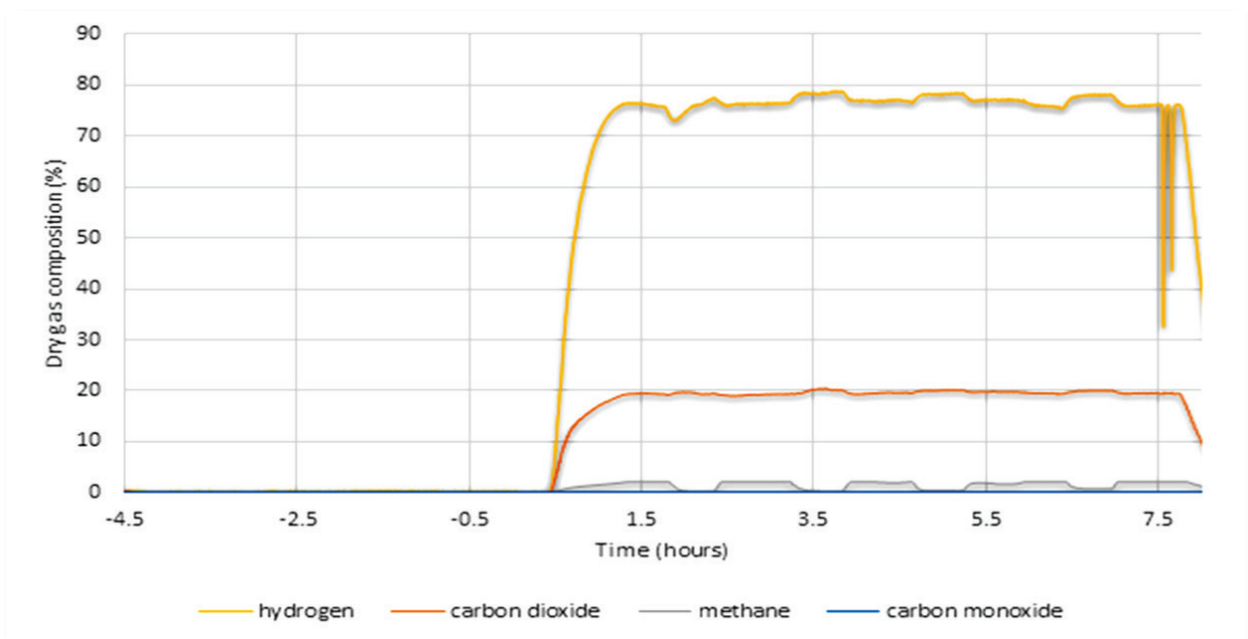
Figure D.3. Flue gas readouts graphs for run 1.

Run 2 – Raw data
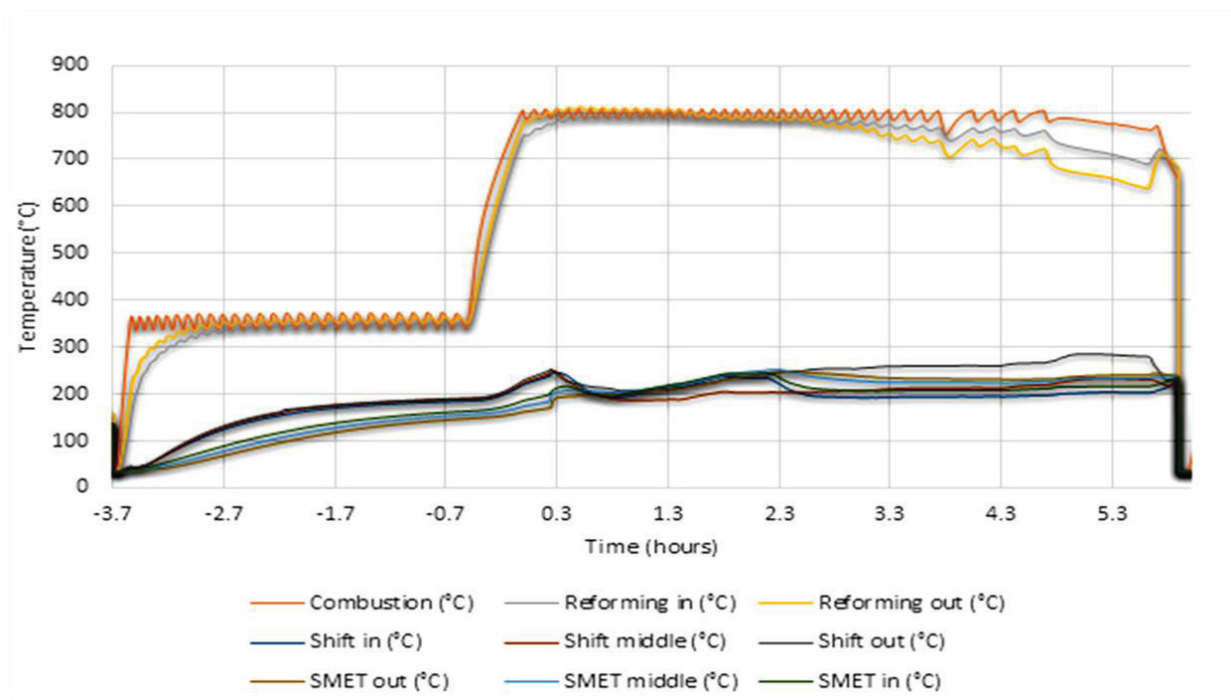
Figure D.4. Raw temperature graphs for run 2.
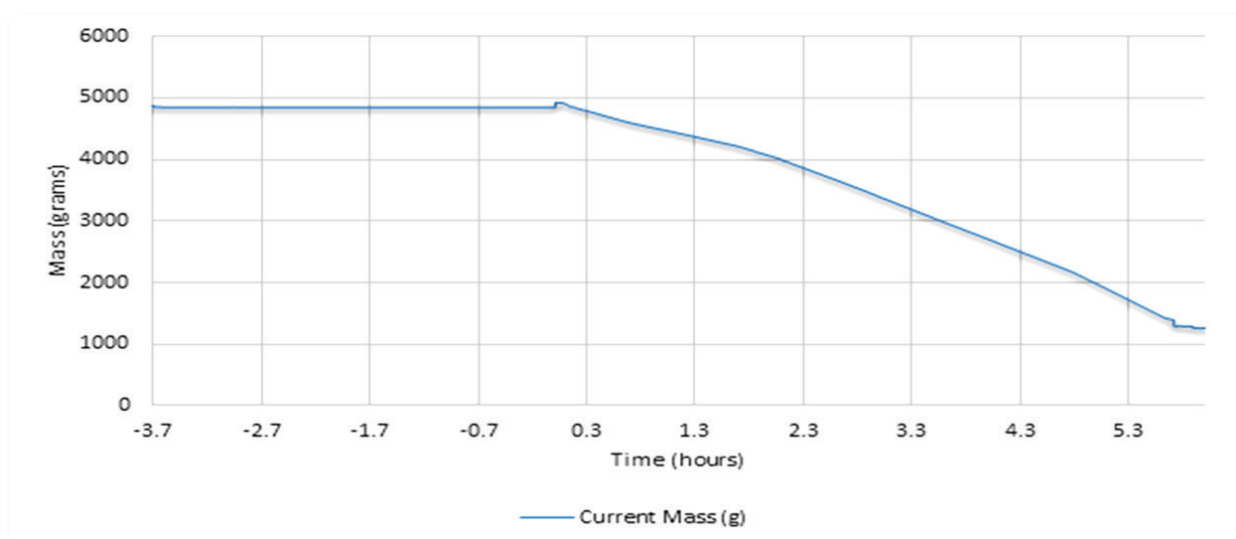
Figure D.5. Balance reading graph for run 2.
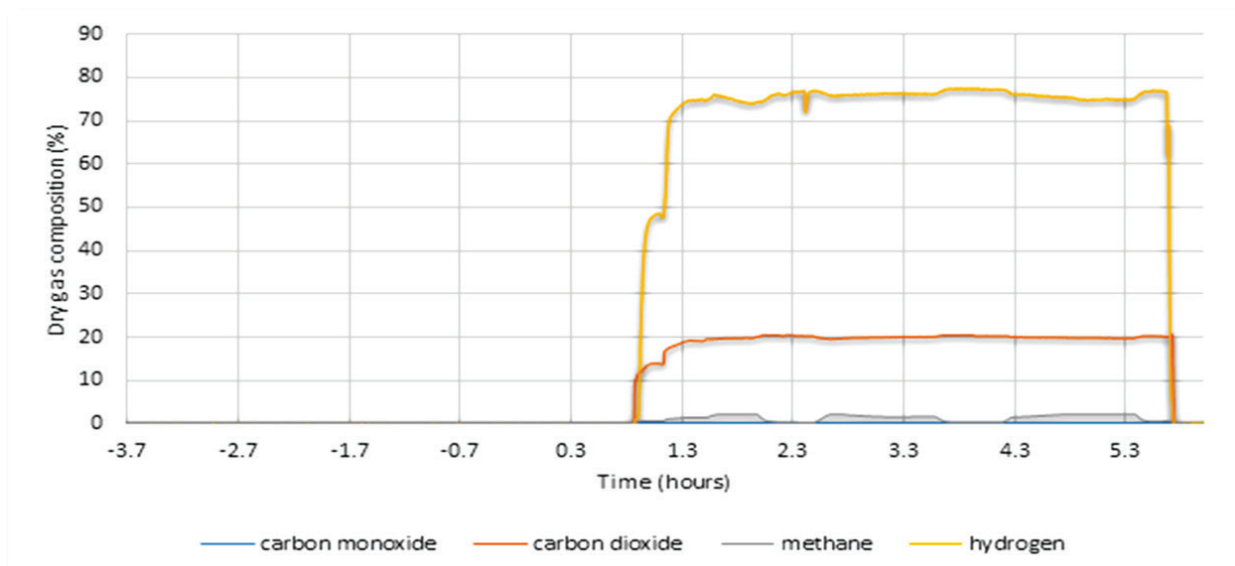
Figure D.6. Flue gas readouts graphs for run 2.

Run 3 – Raw data
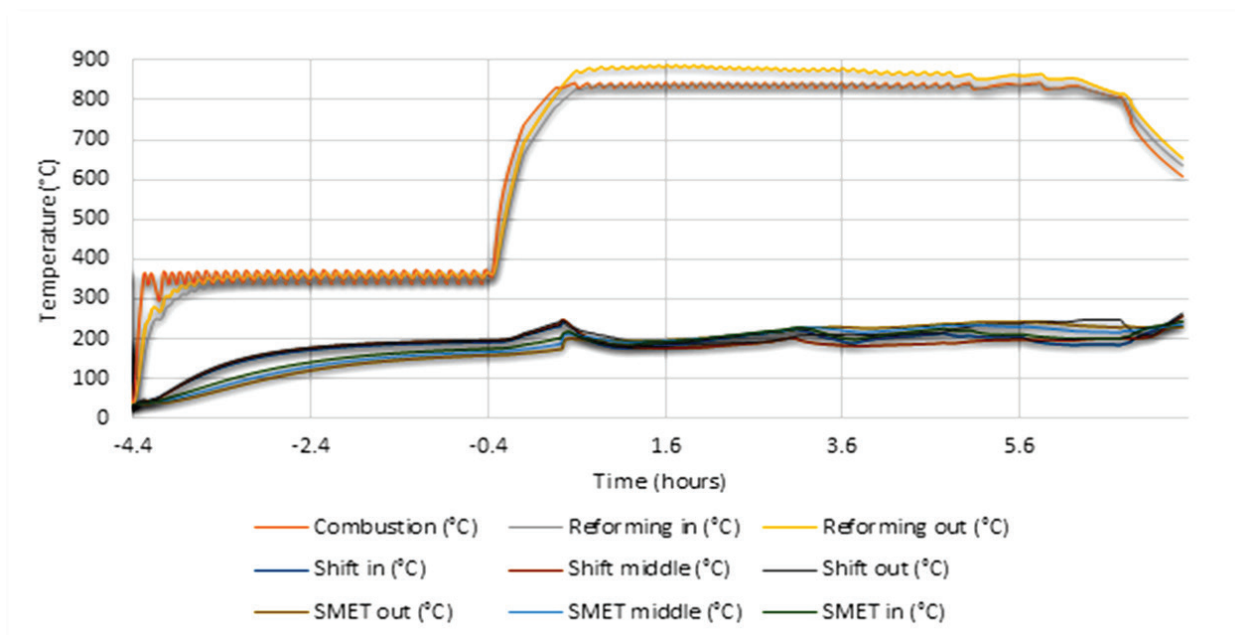
Figure D.7. Raw temperature graphs for run 3.
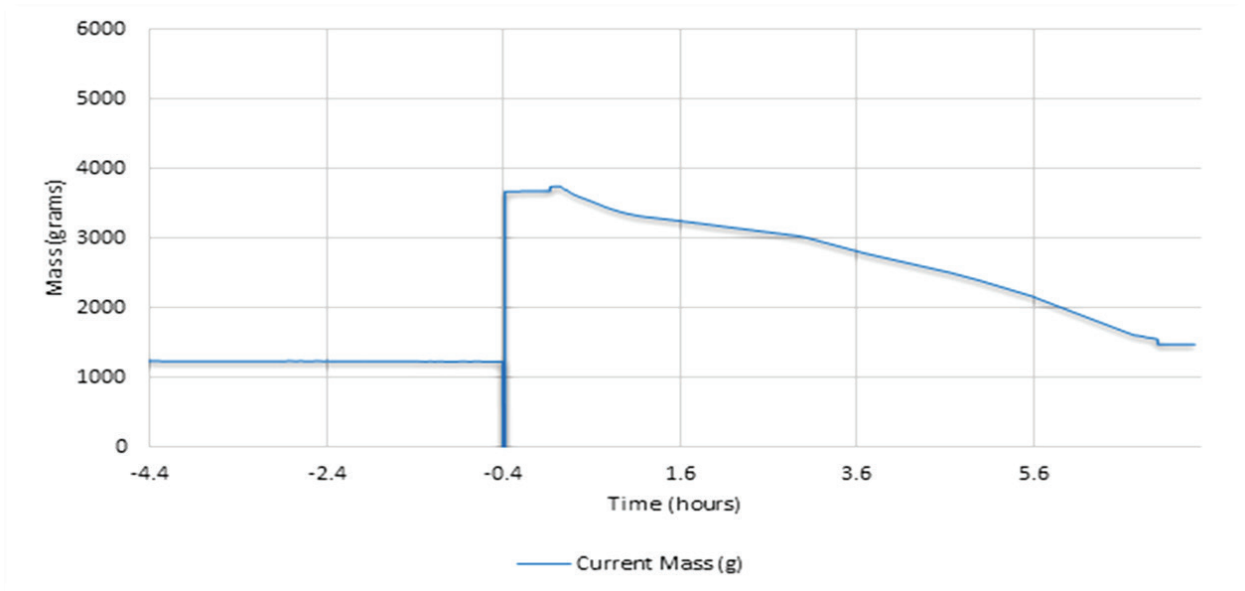
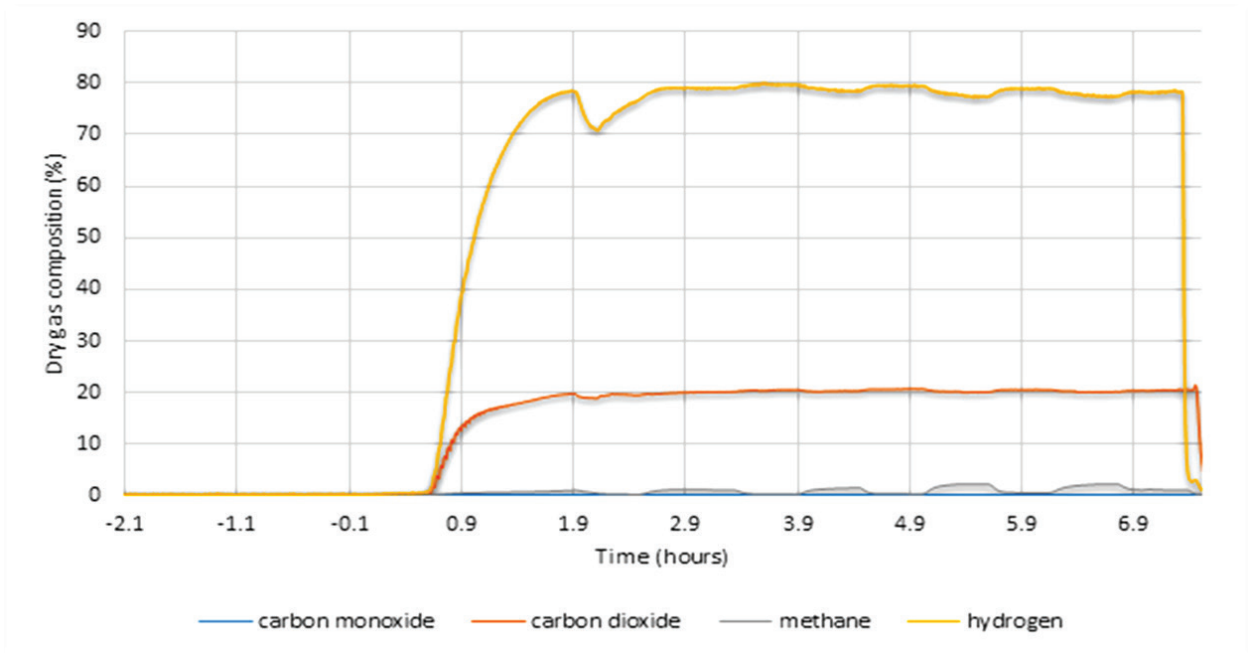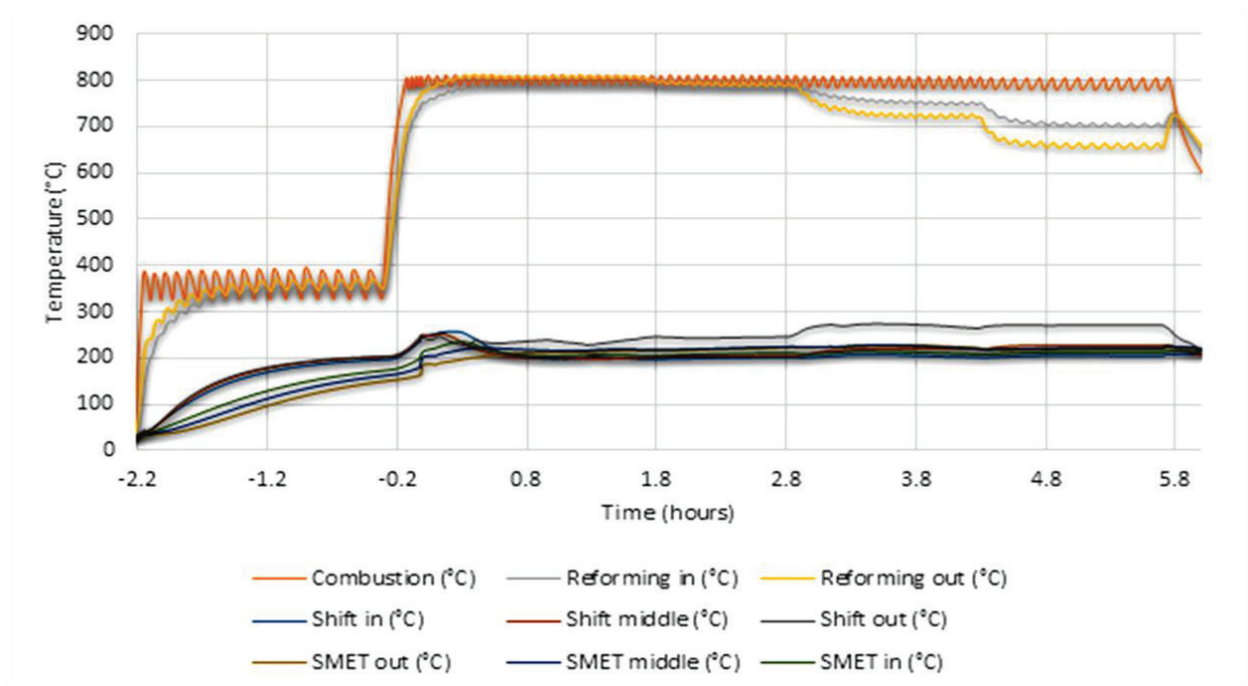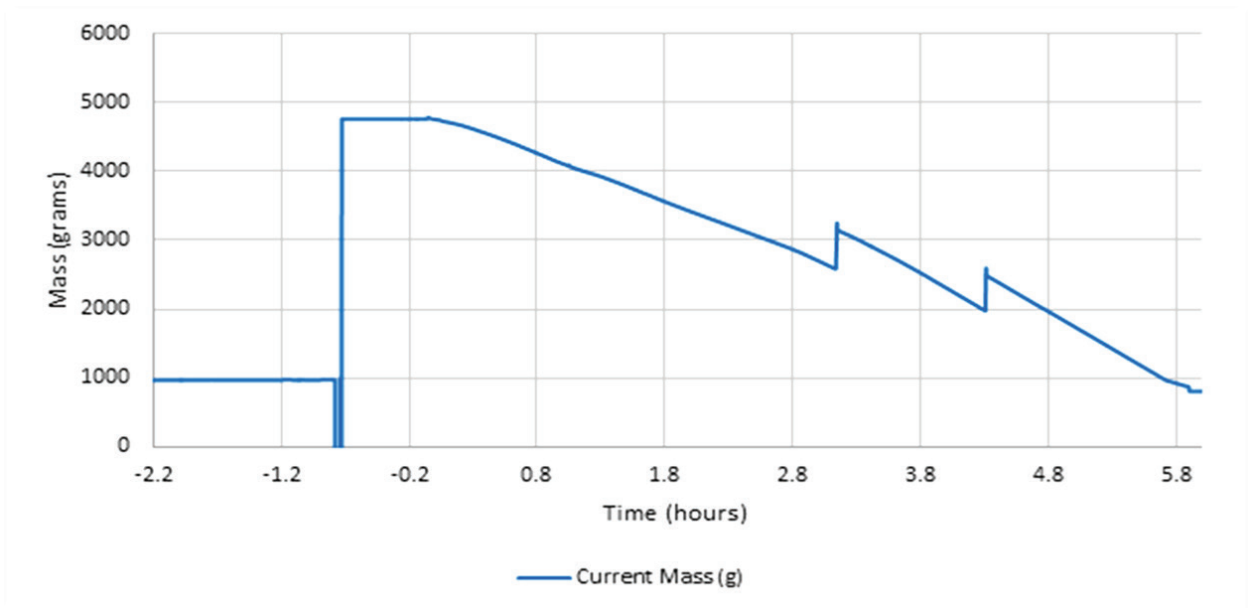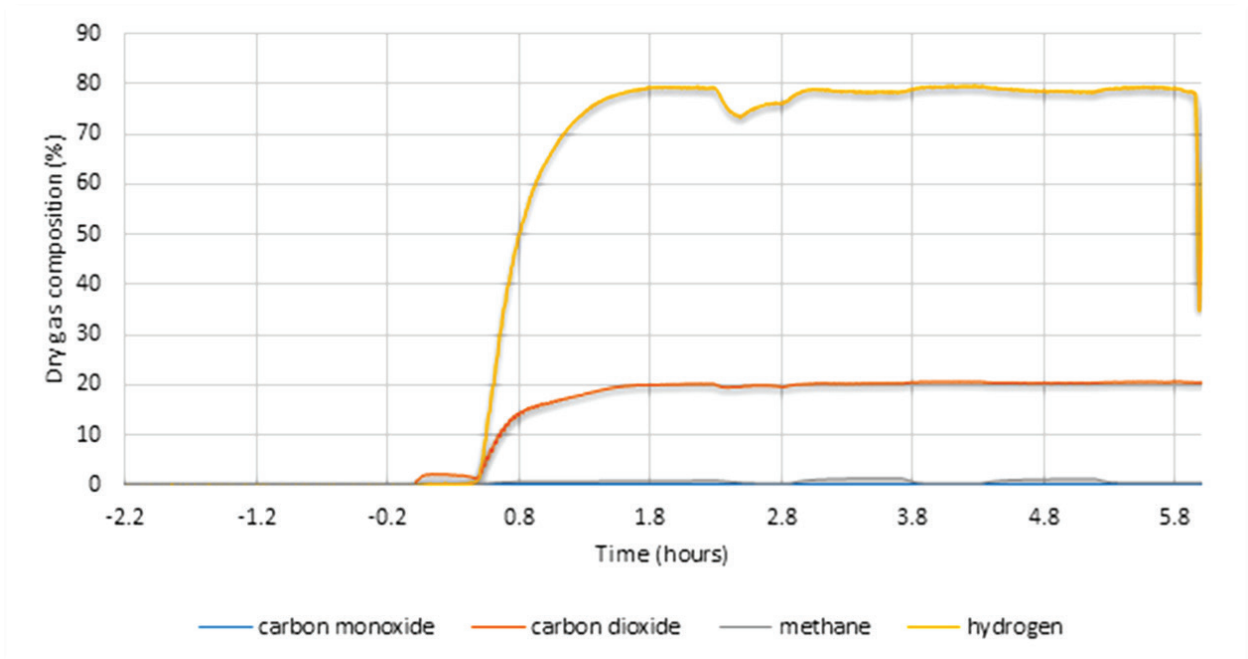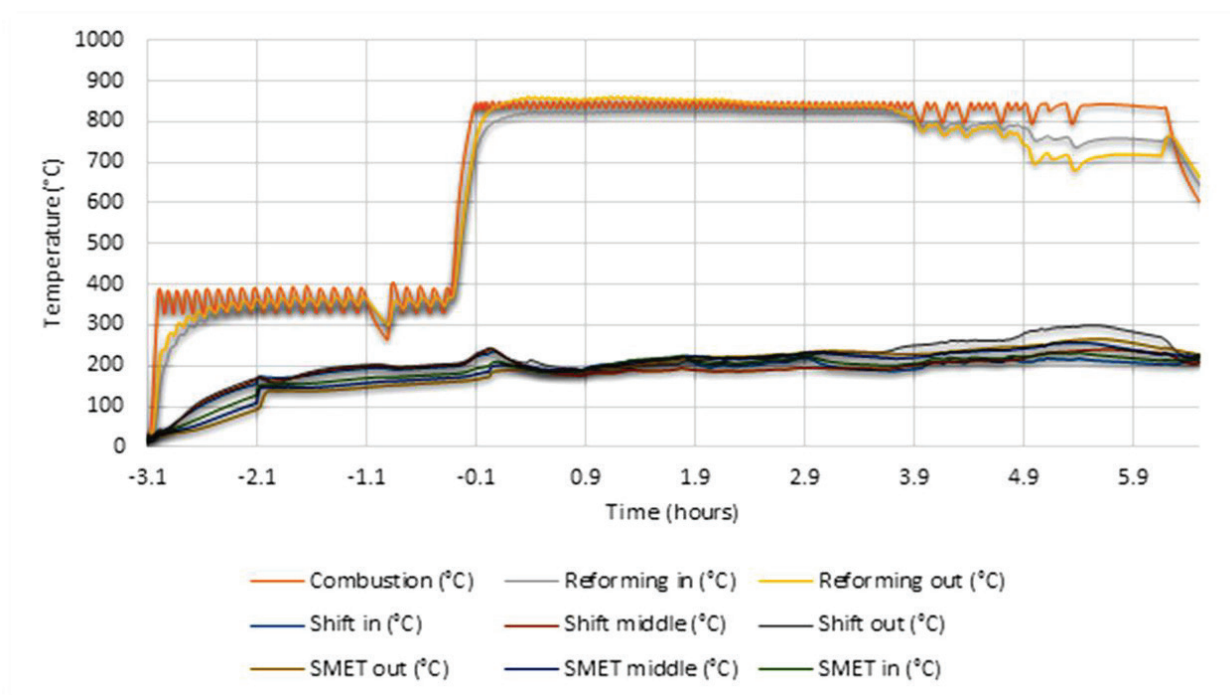**Figure D.8.** Balance reading graph for run 3.
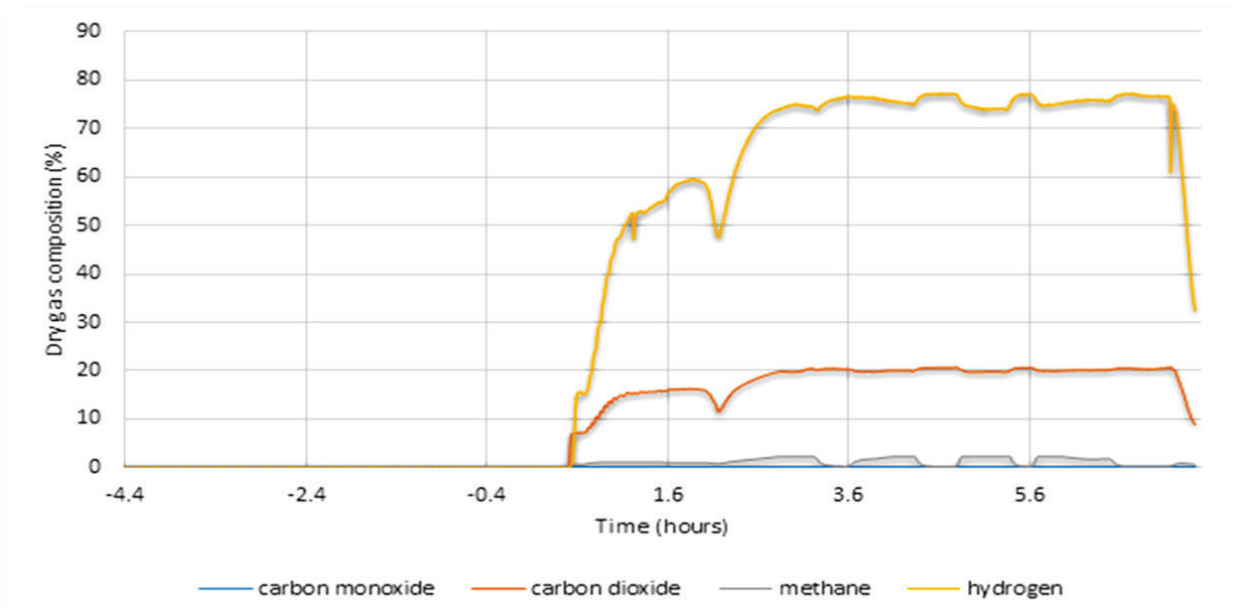
Figure D.9. Flue gas readouts graphs for run 3.

Run 4 – Raw data
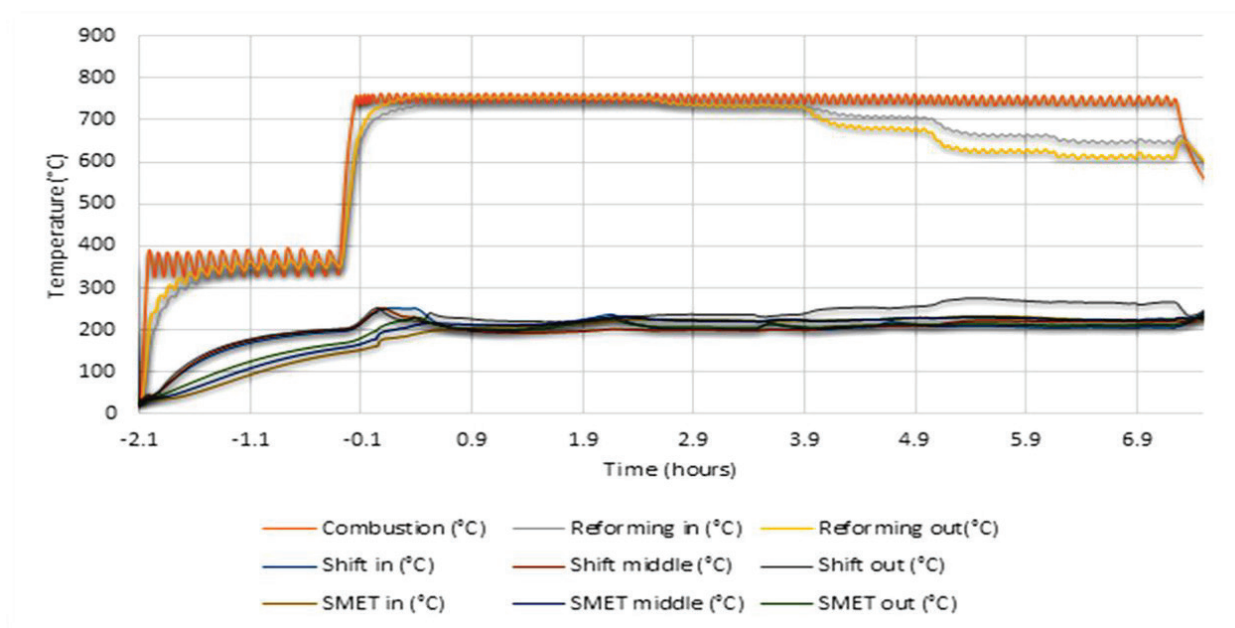
Figure D.10. Raw temperature graphs for run 4.
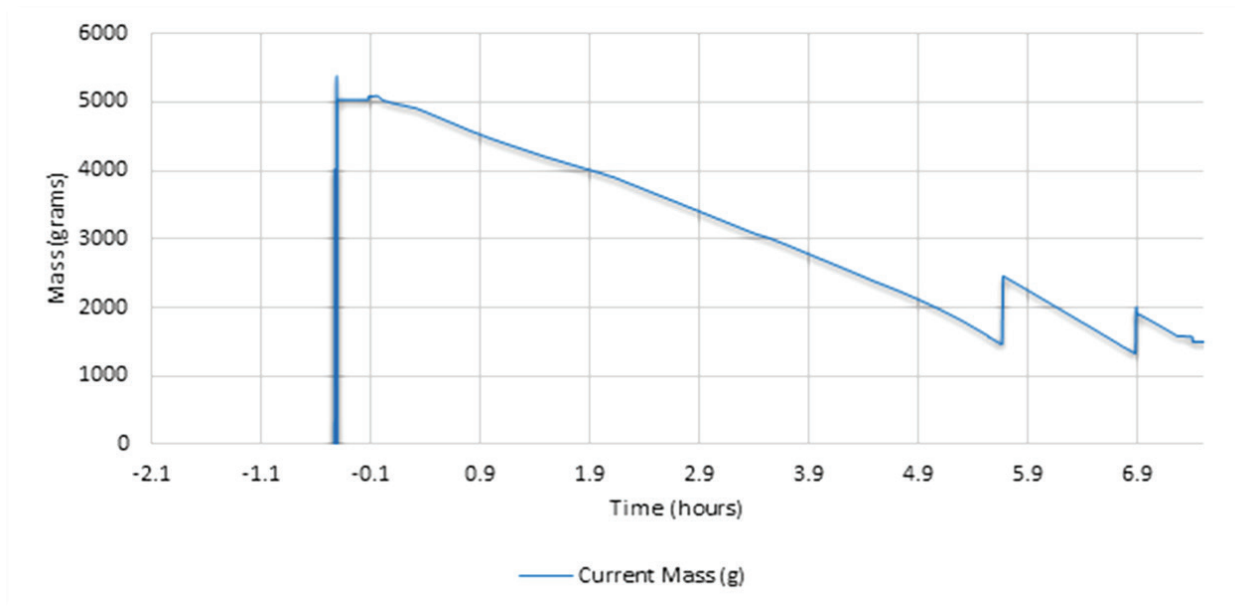
Figure D.11. Balance reading graph for run 4.

Figure D.12. Flue gas readouts graphs for run 4.

Run 5 – Raw data

Figure D.13. Raw temperature graphs for run 5.

Figure D.14. Balance reading graph for run 5.

Figure D.15. Flue gas readouts graphs for run 5.

Run 6 – Raw data

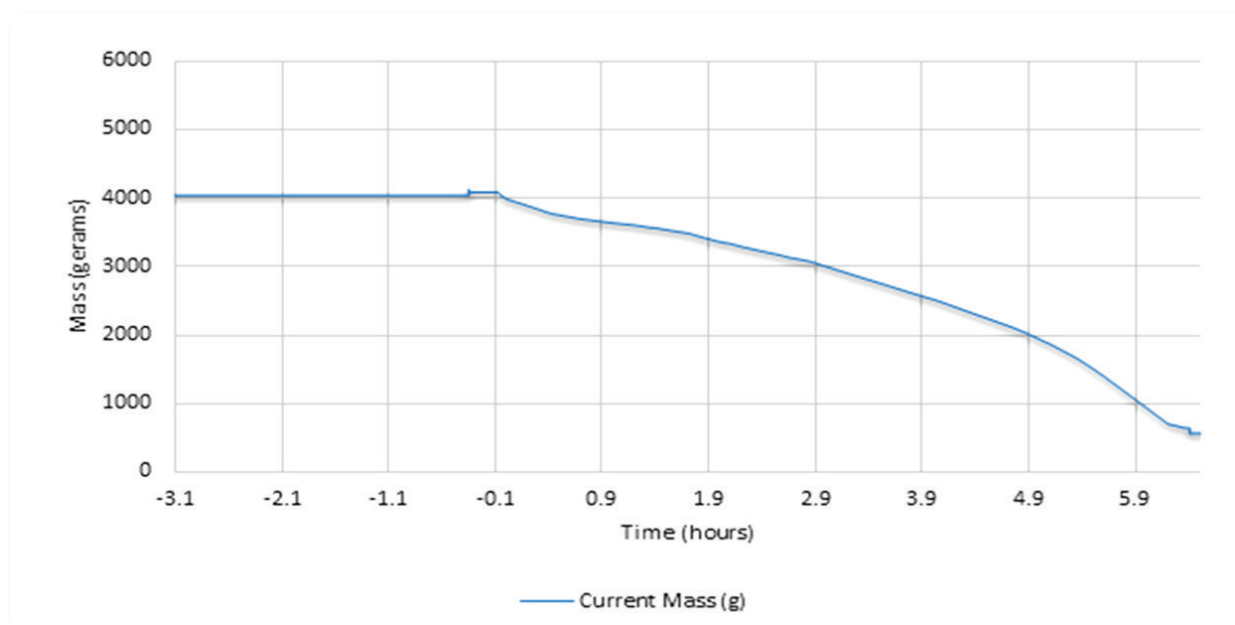**Figure D.16.** Raw temperature graphs for run 6.
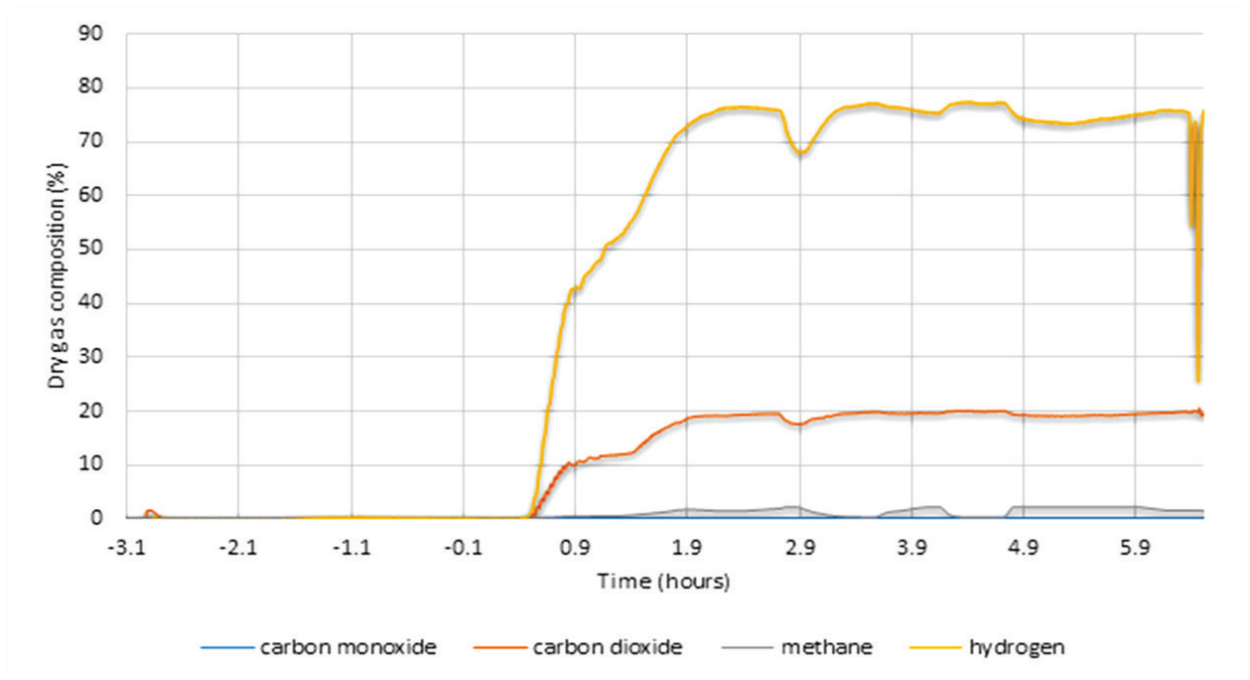

Figure D.17. Balance reading graph for run 6.

Figure D.18. Flue gas readouts graphs for run 6.